Faculty of Biological and Environmental Sciences
University of Helsinki
Helsinki, Finland

Unit of Systems Toxicology
Finnish Institute of Occupational Health
Helsinki, Finland

Nanosafety Research Centre
Finnish Institute of Occupational Health
Helsinki, Finland

Proteomic Characterization of Biological Effects Induced by Engineered Nanomaterials

Jukka Sund

Academic dissertation

To be presented for public examination with the permission of the Faculty of Biological and Environmental Sciences of the University of Helsinki in Haartman Institute, Lecture Hall 2, on April 4th 2014 at 12 noon.

Supervised by
Docent Anne Puustinen
Unit of Systems Toxicology / Nanosafety Research Centre
Finnish Institute of Occupational Health
Helsinki, Finland

Professor Harri Alenius
Unit of Systems Toxicology / Nanosafety Research Centre
Finnish Institute of Occupational Health
Helsinki, Finland

Reviewed by
Docent Tuula Nyman
Institute of Biotechnology
University of Helsinki
Helsinki, Finland

Professor Kirsi Vähäkangas
School of Pharmacy
University of Eastern Finland
Kuopio, Finland

Opponent
Docent Marc Baumann
Meilahti Clinical Proteomics Core Facility
University of Helsinki
Helsinki, Finland

ISBN 978-952-10-9808-6 (Paperback)
ISBN 978-952-10-9809-3 (PDF)
http://ethesis.helsinki.fi
Unigrafia
Helsinki, 2014

Football is a simple game; 22 men chase a ball for 90 minutes and at the end, the Germans win.
-Gary Lineker

TABLE OF CONTENTS

LIST OF ORIGINAL PUBLICATIONS

I. Sund J, Alenius H, Vippola M, Savolainen K, Puustinen A. Proteomic Characterization of Engineered Nanomaterial Protein Interactions in Relation to Surface Reactivity. ACS Nano 2011. 28 6:4300-9

II. Sund J, Palomäki J, Ahonen N, Savolainen K, Alenius H, Puustinen A. Phagocytosis of Nano-Sized Titanium Dioxide Triggers Changes in Protein Acetylation. Submitted to Journal of Proteomics

III. Palomäki J, Sund J, Vippola M, Kinaret P, Greco D, Savolainen K, Puustinen A, Alenius H. A Secretomics Analysis Reveals Major Differences in the Macrophage Responses towards Different Types of Carbon Nanotubes. Submitted to Nanotoxicology

Author's contributions to the publications

I. JS participated in the design of the study, performed the laboratory experiments and drafted the manuscript.

II. JS participated in the experimental design, performed the laboratory experiments and bioinformatic exercises, he also drafted the manuscript.

III. JS participated in the design of the study, helped to perform the cell exposures and proteomic analysis, excecuted the protein identifications and Western blot validation. He also helped to draft the manuscript.

ABBREVIATIONS

2AAA	Serine/threonine-protein phosphatase 2A 65 kDa regulatory subunit A alpha isoform
2D-DIGE	Two-dimensional difference gel electrophoresis
2DE	Two-dimensional gel electrophoresis
AFM	Atomic force microscope
ANXA1	Annexin A1
ANXA2	Annexin A2
APS	Aerodynamic particle sizer
BAL	Bronchoalveolar lavage
BET	Brunauer-Emmett-Teller method
CATB	Cathepsin B
CATD	Cathepsin D
CATH	Cathepsin H
CATS	Cathepsin S
CID	Collision-induced dissociation
CLIC1	Chloride intracellular channel protein 1
CME	Clathrin-mediated endocytosis
CNT	Carbon nanotube
CvME	Caveolin mediated endocytosis
CYTB	Cystatin-B
DPBS	Dulbecco's Phosphate-Buffered Saline
DLS	Dynamic light scattering
EDS	Energy dispersive spectroscopy
ENM	Engineered nanomaterial
ENP	Engineered nanoparticle
ESI	Electrospray ionization
FBS	Fetal bovine serum
FDR	False discovery rate
FPP	Fiber pathogenicity paradigm
GIT	Gastrointestinal tract
GM-CSF	Granulocyte-macrophage colony-stimulating factor
GO	Gene ontology

HSPB1	Heat shock protein beta-1
ICAT	Isotope coded affinity tag
ICR	Ion cyclotron resonance
IEF	Isoelectric focusing
IMAC	Immobilized metal ion affinity chromatography
IT	Intratracheal instillation
iTRAQ	Isobaric tags for relative and absolute quantitation
IV	Intravenous instillation
KEGG	Kyoto encyclopedia for genes and genomes
LC	Liquid chromatography
LDH	Lactate dehydrogenase
LEG1	Galectin-1
LPS	Lipopolysaccharide
m/z	Mass to charge ratio
MALDI	Matrix-assisted laser desorption ionization
MS	Mass spectrometry
MW	Molecular weight
PEST	Penicillin-Streptomycin
pI	Isoelectric point
PMF	Peptide mass fingerprint
PPIA	Peptidyl-prolyl cis-trans isomerase A
PRDX1	Peroxiredoxin-1
PRR	Pattern recognition receptor
PTM	Post translational modification
R CNT	Long rigid carbon nanotube
RES	Reticuloendothelial system
RME	Receptor mediated endocytosis
ROS	Reactive oxygen species
RPLC	Reversed-phase liquid chromatography
SCX	Strong cation exchange chromatography
SEC	Size exclusion chromatography
SEM	Scanning electron microscope
SILAC	Stable isotope labeling of cell culture
SMPS	Scanning mobility particle sizer
SODM	Superoxide dismutase 2
T CNT	Long tangled carbon nanotube

TEM	Transmission electron microscope
THIO	Thioredoxin
TiO_2	Titanium dioxide
TMT	Tandem mass tag
TOF	Time-of-flight
XRD	X-ray diffraction

ABSTRACT

Nanotechnology has been one of the major success stories of the early 21st century. The foundation for this success rests on the discovery that a small size confers completely new properties on materials. Nowadays, engineered nanomaterials (ENMs) are used in a plethora of applications such as paints, cosmetics, food products and electronics. These new properties, however, potentially make ENMs more reactive in biological systems than their large-scale counterparts. Already, asbestos-like effects have been described in mice after exposure to certain forms of carbon nanotubes (CNTs), while nano-sized titanium dioxide ($nTiO_2$) has been shown to evoke inflammation in mouse lung. Therefore, extensive nanosafety studies have to be performed to ensure that no adverse effects are suffered by either workers or end-users of ENM products. This thesis has investigated health effects of ENMs by proteomic methods, first by evaluating the uptake and interactions of ENMs with plasma and cellular proteins followed by an analysis of the effects of ENM exposure on the intracellular proteome and secretome of human primary macrophages.

The results revealed that ENM interactions with cellular proteins were governed by the surface reactivity of ENMs, whereas interactions with plasma proteins seemed to depend on the combination of both surface reactivity and active recognition, namely tagging of ENMs by opsonin proteins. The binding of cellular proteins to ENMs and subsequent interference with cellular processes might represent a novel cause of ENM toxicity, especially since transmission electron microscopy (TEM) micrographs indicated that several ENM species could be visualized free in the cytoplasm.

The cytoplasmic protein expression changes after exposure to silica coated and uncoated $nTiO_2$ revealed that silica coated TiO_2 induced stronger protein expression changes in the macrophages. Most of the proteins with altered expression were related to phagocytosis, oxidative stress and inflammation. These proteome changes indicate that macrophages are actively engulfing ENMs and processing them. Moreover, the up-regulation of oxidative stress related proteins might be an indication of oxidative burst. Finally, $nTiO_2$ treatment evoked acetylation of cytoplasmic proteins, a previously uncharacterized phenomenon in cells exposed to ENMs. The results from the macrophage secretome analysis showed that asbestos and long rigid carbon nanotubes (R CNTs) produced a similar response, while protein secretion profile of macrophages exposed to long tangled carbon nanotubes (T CNTs) exhibited a distinct profile. Bioinformatic analysis revealed that R CNTs evoked secretion of inflammation and apoptosis related proteins, possibly because of lysosomal damage. Functional assay confirmed that R CNT exposure triggered apoptosis in macrophages, while T CNTs and asbestos did not.

This thesis offers new knowledge concerning the biological effects of engineered nanomaterials. Proteomic methods proved to be useful in the ENM-protein interaction studies revealing that it would be beneficial to include the ENM-protein interaction experiments as part of the routine ENM characterization when assessing the health effects of ENMs. By employing quantitative proteomics, we obtained a global view of both cytoplasmic and secreted proteome changes of macrophages exposed to different ENMs.

1. INTRODUCTION

1.1. Engineered nanomaterials and nanotechnology

Engineered nanomaterials are intentionally produced materials having at least one dimension less than 100 nm. The small size brings out new physicochemical properties that differ substantially from the characteristics of the larger forms of the same material. For example, when the size of a molecule decreases, surface area grows in an inverse relationship, meaning that most of the atoms in a nanoparticle (NP) are located on the surface (Figure 1). ENMs are also easily modifiable, their solubility, shape, surface structure and charge can be changed. This explains why nanotechnology has been one of the success stories of 21st century, since it is these characteristics that are exploited in nanotechnology applications (Nel et al., 2006). Currently the global market value of nano-related technologies is estimated to be worth 200 billion € providing employment for 300 000 to 400 000 workers in the EU alone. By the year 2020, the market value of products utilizing nanotechnology has been predicted to reach 2 trillion € (EU, 2012).

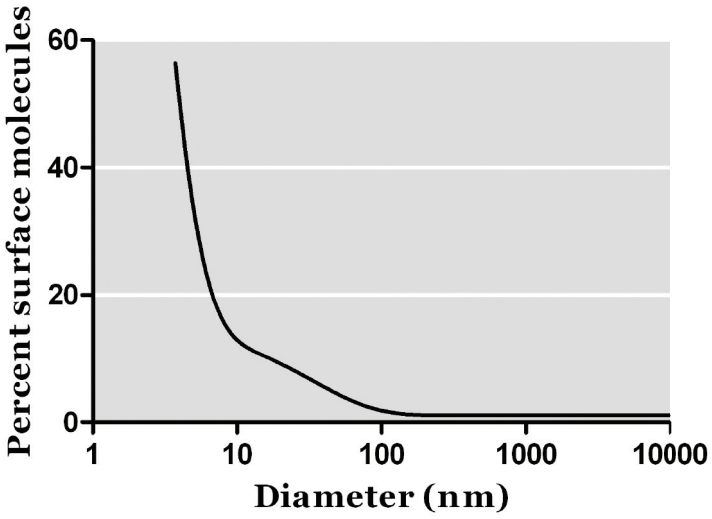

Figure 1. The relationship between particle diameter and percentage of surface molecules.
The percentage of molecules on the particle surface correlates inversely with the particle size. Modified from (Oberdörster et al., 2005)

1.1.1. Titanium dioxide

One of the most widely utilized nanomaterials is TiO_2 ($nTiO_2$), which has four major crystal structures: anatase, rutile, brookite and TiO_2. Anatase and rutile are the best known and utilized TiO_2 polymorphs in nanotechnology. Anatase

is the thermodynamically most stable phase when it is in 10-20 nm size-ranges, whereas rutile TiO_2 is most stable at sizes above 35 nm (Yin et al., 2013).

The high refractive index enables $nTiO_2$s to be used as pigments in personal care products, foods, paints and papers. TiO_2 nanoparticles are also exploited in water treatment, anti-bacterial applications, photovoltaics and electrochromic devices, due to their physicochemical properties which can be easily modified by doping and coatings (Yin et al., 2013; Weir et al., 2012; Robichaud et al., 2009). Their use in self-cleaning surfaces utilizing photocatalysis is another application for $nTiO_2$ particles, where organic particles are broken down chemically in the presence of light. In the future, $nTiO_2$ could be also utilized in green-energy technologies by taking advantage of $nTiO_2$ ability to efficiently split water to oxygen and hydrogen with the aid of UV excitation (Gupta and Tripathi, 2011).

As reviewed by Yin et al. (2013), TiO_2 nanoparticles have been widely studied in biomedical technologies. A significant portion of the medical applications under investigation involve photocatalysis, namely $nTiO_2$ mediated production of reactive oxygen species (ROS) after UV irradiation. In order for target cells to be killed by this method, called photodynamic therapy, TiO_2 NPs must be localized inside cells and tissues. This can be achieved by attaching specific antibodies to the NP surface, and these can target $nTiO_2$ to specific cells or to the cancer tissue. Similarly, targeting can be exploited in drug delivery systems utilizing TiO_2 NPs as vectors. Several shapes of $nTiO_2$s, such as whiskers and capsules, have been developed for drug delivery; therefore drugs can be attached to the surface of the pharmaceutical. Other emergent biomedical applications exploiting TiO_2 NPs are cell imaging, biosensors and genetic engineering.

1.1.2. Carbon nanomaterials

The primary building block, the basis of most carbon nanomaterials, is graphite, a hexagonal structure which is thermodynamically the most stable form of carbon at room temperature. Graphite honeycombs can form two-dimensional, single atom thick graphene layers, which can be further manipulated into carbon nanotubes (CNTs) or fullerenes – two of the most used carbon nanomaterials (Jariwala et al., 2013). Fullerene was the first synthetized carbon nanomaterial in the 1980s (Kroto et al., 1985). The first CNTs, by-products from fullerene synthesis, were reported in the following decade (Iijima, 1991), while graphene layers were successfully constructed only as late as 2004 (Novoselov et al., 2004).

CNTs are widely used in composites to increase conductivity and stiffness for example in plastics and sporting goods. CNTs are also added to fiber composites, which results in even stronger and stiffer, yet light-weight products, which are both advantages in wind turbine blades. Future applications include CNT-

metal composites with high strength and low density, which could be used in the automotive industry and CNT-plastics with flame retardant abilities. In addition to composites CNTs are used in coatings. They can be utilized to make transparent, conductive films such as touch screens, but also in ship paints to reduce the attachment of algae and barnacles (De Volder et al., 2013).

Physical morphology enables CNTs to have small capacitance and increased carrier mobility – ideal properties for low-power, high-speed electronics such as the thin-film transistors utilized in displays. In addition, their good semiconducting properties mean that CNTs can be used in optoelectronics as light detectors and emitters. Other electronic applications where carbon nanomaterials and CNTs can be utilized are photovoltaics, where they help to convert sunlight into electricity and sensing applications such as gas, solvent and biomolecule sensors (Jariwala et al., 2013; De Volder et al., 2013).

CNTs and other carbon nanomaterials are being increasingly studied in medicine. CNTs have been reported to be efficient scaffolds for tissue engineering and implants. In addition, CNTs can be used as vectors for delivery of drugs, genes and functional RNA. Drugs can be attached to CNTs by two strategies: the hollow core of CNTs can be filled with the drug or then the drug can be attached either covalently or non-covalently to the outer walls of the CNT. Another medical application utilizes CNTs as such for cell killing by irradiating them with near-infrared (NIR) light. NIR causes heating of CNTs but not tissues, therefore only cells which have taken up CNTs will die. Since CNTs can be targeted to specific sites in the body and the release of the drug can be controlled, CNTs might have a major role in medicine in the future (Heister et al., 2013).

1.2. Health effects of engineered nanomaterials

The huge increases in the production volumes and the innumerable new nanotechnology applications being developed mean that human beings are coming into more and more contact with ENMs – both in occupational environments and in every-day life. As highlighted in the Krug and Wick (2011) review, ENMs are about the same size as proteins and DNA and possibly might interfere with cellular functions. Therefore, it can be postulated, that nanotechnology might end up being a double-edged sword: small size and new physicochemical properties of ENMs offer many opportunities and new possibilities but the same characteristics might represent serious threat to living organisms. This has necessitated the undertaking of extensive safety studies to clarify which ENMs pose problems and to determine how best to avoid or at least minimize the adverse effects. Although lagging behind with applied research seeking new nanotechnology discoveries, a large amount of toxicological research has already been conducted with ENMs (Table 1).

Table 1. ENM toxicity studies

Example references	Objective	Method
(Cedervall et al., 2007; Dutta et al., 2007; Ge et al., 2011; Göppert and Müller, 2005; Lundqvist et al., 2011; Lynch and Dawson, 2008; Monopoli et al., 2011; Safi et al., 2011; Tenzer et al., 2011; Tenzer et al., 2013; Treuel et al., 2014; Walkey et al., 2014; Wang et al., 2011)	ENM-protein interactions	Protein corona studies
(Gonçalves et al., 2010; Haniu et al., 2006; Pfaller et al., 2009; Simon-Deckers et al., 2008; Movia et al., 2011; Xia et al., 2013)	Toxicity screening	Cell models
(Dostert et al., 2008; Liu et al., 2011; Lohcharoenkal et al., 2013; Lunov et al., 2011; Palomäki et al., 2011; Park et al., 2008; Sharma et al., 2007; Tahara et al., 2012; Tilton et al., 2013; Yazdi 2010)	Toxicity mechanisms	Cell models
(Ryman-Rasmussen et al., 2009; Bermudez et al., 2004; Li et al., 2007; Lindberg et al., 2012; Mangum et al., 2006; Poland et al., 2008; Rossi et al., 2010b; Sager et al., 2008)	Acute and sub-chronic effects, genotoxicity, inflammation, carcinogenesis	Animal models
(Kolosnjaj-Tabi et al., 2010; Nemmar et al., 2001; Poland et al., 2008; Rossi et al., 2010b; Shvedova et al., 2005; Rancan et al., 2012)	Assessment of exposure routes and strategies	Animal models
(George et al., 2011; Lin et al., 2013; Liu et al., 2012)	High throughput toxicity screening	Zebra fish models
(Aschberger et al., 2011; Gottschalk et al., 2009; Gottschalk et al., 2011; Wang et al., 2013)	Environmental effects	Algae, microbe, fresh water invertebrate models, modelling
(Brouwer, 2012; Grieger et al., 2010; Liao et al., 2008; Nel et al., 2013; Van Duuren-Stuurman et al., 2012; Zuin et al., 2011)	Risk assessment and reduction	Predictive toxicology paradigms, modelling

1.2.1. Exposure routes

The most probable entry routes of ENMs into the human body are via the respiratory system, through the skin or by ingestion. The most vulnerable route is the lung, since it has been claimed that ENMs might be able to cross air-blood barrier (Oberdörster et al., 2005). The airways have three main defense mechanisms: epithelium, mucus and cellular defense. Downwards from the nose, the epithelium of respiratory tract is mostly ciliated. The epithelium functions as a barrier preventing the entry of pathogens and foreign molecules into the body. In addition, the epithelial cells participate in inflammatory reactions by recognizing pathogens and activating the immune cells. The mucus secreted by goblet cells and serous and mucosal glands in the airway epithelium acts in concert with the cilia to form the mucociliary escalator, which transports particles and pathogens deposited in the mucus away from the airways into the pharynx, where the foreign objects are swallowed. Mucus also contains many antimicrobial proteins such as lysozyme, lactoferrin, peroxidase and defensins. In addition, immunoglobulins and opsonins are secreted into the mucosa. The cellular defense consists of non-specific defense cells, such as alveolar macrophages and polymorphonuclear leukocytes - both professional phagocytes, and specific cellular defense cells, T and B cells, located in the lamina propria and Waldeyer's ring (Fokkens and Scheeren, 2000).

Whereas larger particles usually become stuck in the mucus layer in the upper part of the respiratory system, the nano-sized particles, due to their small aerodynamic diameter, are able to pass deeper into the alveoli and this pulmonary region is not protected by a mucus layer. Here, alveolar macrophages and epithelial cells are responsible for the defense and therefore, can be considered to be targets of inhaled ENMs (Oberdörster et al., 2005; Donaldson et al., 2013).

ENMs such as TiO_2 and zinc oxide (ZnO) are widely used in sunscreens, thus coming into contact with the skin. Normal, healthy skin is an efficient barrier preventing entry of bacteria, viruses and foreign molecules to the body. However, hair follicles might provide an entry route and if the skin has a wound or contains lesions, the ENMs present in sunscreen might be able to pass through the skin. Some reports have postulated that ENMs are able to be taken up in the gut, which is alarming because nowadays many food products contain nanomaterials. For example, Lycopene which is a synthetic form of tomato carotenoid is used in soft drinks as a colorant (Elsaesser and Howard, 2012; Chaudry et al., 2008).

1.2.2. Protein corona

Regardless of whether ENMs enter the body via the respiratory system, blood or through the skin, they are immediately coated and covered by biomolecules such as proteins, lipids and sugars, thus forming a so-called corona around the ENM. The nanoparticle-corona complex is perhaps the most important factor influencing the fate of ENMs inside the body. Moreover the corona has an effect on several other ENM properties e.g. agglomeration, uptake and toxicity. The corona, together with materials' so called synthetic identity consisting of size, shape and surface chemistry, make up the biological identity of ENMs (Figure 2). Therefore, the biological identity of a given ENM will be different in blood than it is in the lung. ENMs can also retain their protein-corona when passing through different biological environments, meaning that a particle entering the body through the lung is likely to exhibit a fingerprint of the lung proteome even though it is being analyzed in the blood (Monopoli et al., 2011; Walkey and Chan, 2012).

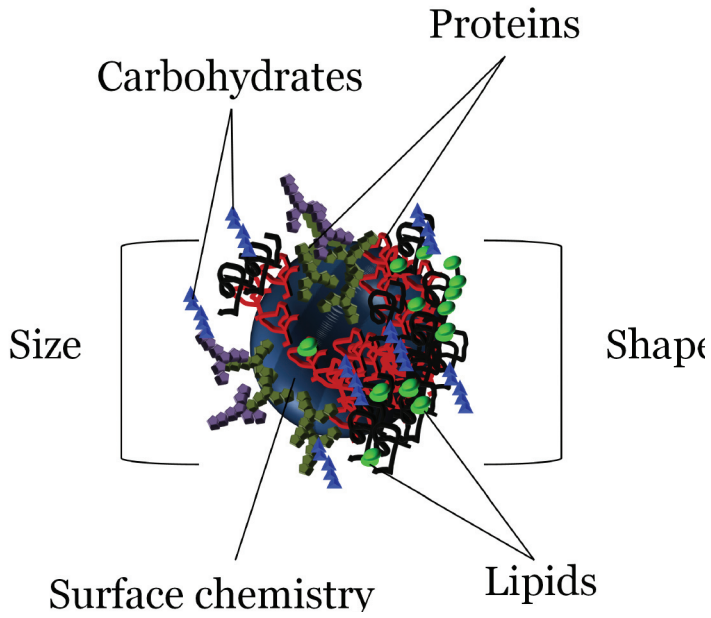

Figure 2. Biological identity of ENMs.
Figure illustrating the biological identity, consisting of synthetic identity and biomolecule corona, of a given ENM in a biological environment. Synthetic identity consists of the size, shape and surface chemistry of the ENM.

The ENM surface has a high free energy, which invites adherence of biomolecules. Proteins bind to ENMs via weak physical forces such as Van der Waals and electrostatic interactions in thermodynamically favorable conditions. Proteins adhere to ENMs with different binding energies, determining which proteins form the corona. Moreover, many proteins may interact simultaneously with the material and other proteins having an effect on the corona formation and resulting in multiple protein layers. This means that the corona, at least the plasma protein corona, can be relatively thick, perhaps as much as 54 nm (Monopoli et al., 2011; Walkey and Chan, 2012).

ENMs interact with proteins differently depending on their material characteristics. Previously, hydrophobic and, more importantly, charged ENMs were thought to bind proteins better. Surface curvature was another property thought to influence protein binding, after it was found that smaller particles bound fewer proteins than their larger counterparts - i.e. the smaller the particle the higher the surface curvature, therefore the area for interaction with proteins is smaller (Monopoli et al., 2011; Walkey and Chan, 2012). Recently, however, Tenzer et al. (2013) showed that none of the ENM properties alone were enough to be a governing factor in protein corona formation in plasma. Only the exposure time could be singled out as having an effect on corona size. Furthermore, all the materials, irrespective of surface charge, seemed to acquire a negative charged corona in biological (pH ~7) environments, meaning that the majority of adhering proteins had an isoelectric point (pI) less than 7.

ENMs have been claimed to acquire two different coronas in plasma: a hard corona and a soft corona (Lynch et al., 2007; Tenzer et al., 2011) although the existence of soft corona is still somewhat controversial. The proteins with strong binding energies are believed to form the hard corona, interacting directly with the material. The hard corona is highly stable consisting of less than 100 different proteins that cannot easily be removed from the ENM. The soft corona, on the other hand, is made up of either proteins interacting with proteins of the hard corona, or as some studies suggest, proteins adhering to ENMs with weaker binding energies. The soft corona is never at equilibrium; the interacting proteins are constantly changing. The hard and soft coronas are considered to evolve over the course of time by the Vroman effect where the most abundant proteins bind the ENMs first and are gradually replaced with lower abundance proteins with higher affinities towards ENMs (Monopoli et al., 2011; Walkey and Chan, 2012). However, Tenzer and collaborators (2013) postulated that the change of proteins over time is not qualitative but only quantitative, as most of the proteins forming the final corona were already adhering with ENMs after 30 seconds. Moreover the same study claimed that the complete protein-corona is formed much faster and is more complex than previously thought, including almost 300 different proteins.

ENM-protein interactions can be spontaneous or involve specific biological recognition. Epitopes or the surface curvature of ENMs can be recognized by proteins leading to highly regulated biological processing and possibly to immunological reactions, whereas spontaneous binding can have other outcomes in biological systems. For example, carbon nanotubes can interact directly with cell surface proteins to evoke cytotoxicity. The attached proteins themselves might also mediate toxic outcomes by undergoing conformational changes and exposing new epitopes, which could then become targets of the cells of the reticuloendothelial system (RES) as non-self, initiating immune reactions. As such, the adherence of plasma proteins to ENMs has been described to facilitate material uptake and

stronger immunological reactions. These reactions are mediated by opsonins, such as immunoglobulins, complement proteins or fibrinogen, which facilitate immune responses by tagging exogenous molecules and thus help phagocytic cells to recognize harmful molecules. In addition, the biokinetics and fate of ENMs inside the body can completely change depending on the proteins with which the material interacts, for example the attachment of apolipoproteins might help materials pass through barriers such as the blood-brain barrier (Monopoli et al., 2011; Walkey and Chan, 2012). Clearly, more studies are needed to understand how the protein corona affects ENM safety and biodistribution.

1.2.3. Uptake, biodistribution and degradation

ENM toxicity largely depends on the material's ability to enter cells. Entry is affected by many factors, for example size, shape, surface charge and reactivity, agglomeration state, cell type and protein corona. Whether ENMs are taken into cells only actively or both actively and passively is still unresolved. It has to be also taken into account that a portion of the nanomaterials is likely to be aggregated in physiological environments. Therefore the immunological effects can be mediated by a mixture of aggregated and individual particles (Heister et al., 2013; Tenzer et al., 2013; Canton and Battaglia, 2012; Kettiger et al., 2013).

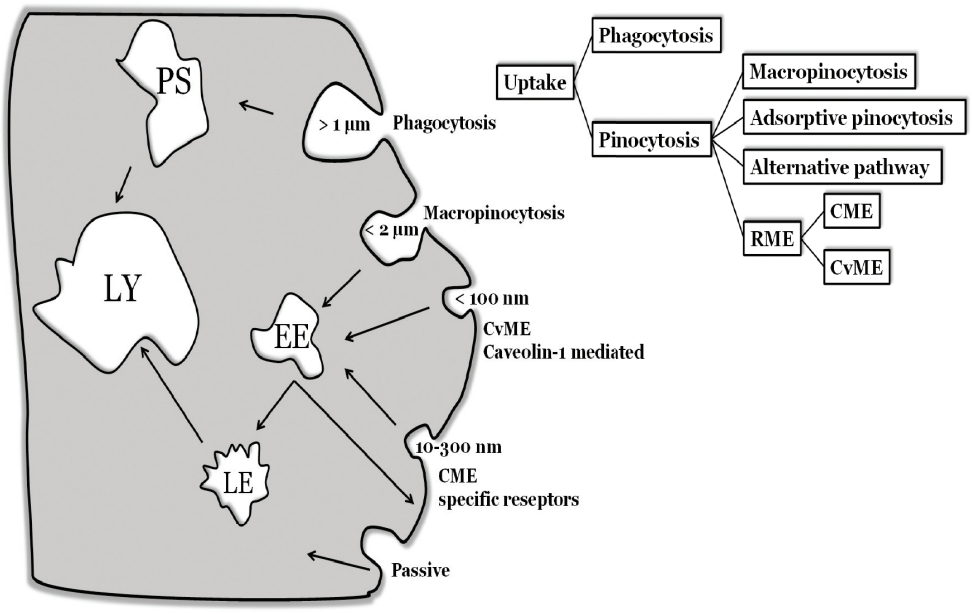

Figure 3. Uptake pathways. *Figure illustrating the most common pathways involved in ENM uptake. PS phagosome, LY lysosome, EE early endosome, LE late endosome, RME receptor mediated endocytosis, CME clathrin-mediated endocytosis CvME caveolin mediated endocytosis*

The small size and ability to interact with biomolecules, makes it possible for the ENMs to utilize endogenous cellular uptake mechanisms (Figure 3) and possibly to exert an effect on cellular processes (Monopoli et al., 2011). Phagocytosis is an active process normally conducted by the professional phagocytes of the immune system, such as macrophages and neutrophils. Large, > 1 μm particles and agglomerates are taken up by phagocytosis, a process which utilizes Fc, immunoglobulin and complement receptors located on the cell membrane. Another active process is pinocytosis, which can be divided into macropinocytosis, adsorptive pinocytosis, receptor mediated endocytosis (RME) and alternative pathway. Similarly to phagocytosis, macropinocytosis is one way to allow the cells to take up large, < 2 μm particles but also nano-sized particles can be ingested. This process is non-specific and also the surrounding fluid is externalized. In contrast, RME occurs via ENM-receptor interactions. The two best characterized RME pathways are clathrin-mediated endocytosis (CME) and caveolin mediated endocytosis (CvME). In CME, ENMs in the size range of 10-300 nm are internalized in clathrin-coated vesicles utilizing highly specific receptors. CME can also occur non-specifically when cationic particles bind to the negatively charged cell surface. CvMe, on the other hand, is mediated by caveolin-1 proteins which coat a small, 50-80 nm, invagination in cell membrane called caveola. The CvME system means that cells are able to ingest large particles, ENMs up to 100 nm in size (Canton and Battaglia, 2012; Kettiger et al., 2013).

In their review Kettinger et al. (2013) considered that the optimal size for efficient uptake is 50 nm. In contrast, Canton et al. (Canton and Battaglia, 2012) proposed the best size to be 20-30 nm. Nevertheless, particles larger than 50 nm or smaller than 20 nm can be taken up, although more slowly and inefficiently. Positively charged particles tend to be ingested more effectively, especially via adsorptive pinocytosis, whereas negatively charged ENMs are taken up by alternative uptake routes, adhering to proteoglycans in cell surface. Furthermore, spherical particles seem to be more readily ingested than rod-shaped or materials with higher aspect ratio, whereas a high surface area also disturbs the rate of uptake. Heister et al. (2013) reviewed the uptake of high aspect ratio CNTs and concluded that CNT bundles are taken in by phagocytosis, while individual fibers shorter than 400 nm can enter cells passively. Similarly CNTs have been reported to penetrate through the cell membrane and to inflict mechanical damage to cells. Should this occur, CNTs are able to reside free in the cytoplasm (Canton and Battaglia, 2012; Kettiger et al., 2013; Dumortier, 2013). CNTs are thought to enter cells by a tip-first mechanism, which could explain the toxicological effects and frustrated phagocytosis encountered in CNT exposed cells (Shi et al., 2011).

After entry, ENMs are transferred inside vesicles into the subcellular compartments depending on uptake mechanism. If ENMs are internalized via phagocytosis, they are trafficked inside phagosomes directly to lysosomes, where under normal conditions, the cargo is degraded by proteases at low pH. In

contrast, the other uptake mechanisms use early endosomes to sort out whether the cargo should be directed to lysosomes for degradation or recycled back to the plasma membrane. If the cargo is destined for degradation, it is placed into large vesicles which form multi-vesicular bodies that mature into late endosomes and finally into lysosomes (Figure 3) (Canton and Battaglia, 2012). Kettinger et al. 2013) reviewed that some ENMs, especially the positively charged ones, are able to escape from lysosomes by a 'proton sponge effect'. In addition, CNTs might be able to puncture vesicle membrane. Should they escape from lysosomes, then ENMs might be free to interact with other cell organelles.

Once inside the body, the critical question is where do the ENMs end up? In the lung alveoli, ENMs can be endocytized by alveolar epithelial cells and gain access to blood circulation. ENMs can also end up in the blood circulation after inhalation – or even to central nervous system via the olfactory bulb. Once in the blood circulation, ENMs are most likely taken up by cells of the reticuloendothelial system and, therefore, are transported to the liver or spleen, while the smallest, < 10 nm, ENMs are eliminated through the kidneys. If ENMs are not recognized by defense mechanisms of the blood, they might cross air-blood or blood-brain barrier, and become deposited in the brain or heart (Elsaesser and Howard, 2012; Kettiger et al., 2013). The body is able to degrade and excrete safely many ENMs such as porous silica nanoparticles and iron oxide nanoparticles, even oxidized CNTs can be destroyed by peroxidase and myeloperoxidase, expressed in neutrophils. However, it is possible that some ENMs can accumulate in organs and cause damage. Moreover, they can remain at the site of entry, like high aspect ratio CNTs, which have been found to persist in the pleural space causing fibrosis and asbestos-like effects (Donaldson et al., 2013; Kettiger et al., 2013; Dumortier, 2013).

1.2.4. Health effects of nano-sized titanium dioxide

While fine-sized TiO_2 has been generally considered as an inert material, the same cannot be said about $nTiO_2$. Shi and collaborators (2013) stated that inhaled $nTiO_2$ particles induced acute local and systemic effects in mice, causing pulmonary inflammation and accumulation of the particles into liver, spleen and kidneys. Short term *in vitro* studies have also suggested that $nTiO_2$s are able to cause erythrocyte hemolysis. Furthermore, dermal exposure studies have revealed that $nTiO_2$ particles are not able to penetrate isolated pig skin in a 24 hour experiment. However, further *in vivo* experiments show that, when applied to the ears of domestic pigs, the same particles enter the deep layer of epidermis after 30 days. In addition, an experiment with 60 day exposure revealed that $nTiO_2$ could penetrate through the skin of hairless mice completely and subsequently

particles were found in many organs and tissues. In an oral exposure study, rats fed with $nTiO_2$ containing diet developed a slight injury to the liver and heart which was probably caused by disturbed gut microflora and disturbed energy and amino acid metabolism.

The results of genotoxicity studies are more conflicting. Some groups have reported clastogenic and genotoxic effects *in vivo* after intratracheal instillation, while other groups have detected no effects whatsoever. Similarly, many *in vitro* experiments have shown clear genotoxicity, whereas other studies have postulated that $nTiO_2$s are incapable of causing mutations. These conflicting results might be attributable to the heterogeneous selection of $nTiO_2$ particles used in the exposures, the different metrics used in the experiments or the use of different cell types. Importantly, the number of studies showing DNA damage is far greater than of those indicating that $nTiO_2$s are not genotoxic, which means that $nTiO_2$s are potentially hazardous and must be treated accordingly until more definitive studies have been conducted (Shi et al., 2013).

The main mechanisms by which $nTiO_2$ particles cause toxicity are triggering the formation of reactive oxygen species and by inducing inflammation. Because of their large surface area, nanoparticles are especially potent generators of ROS. Oxidative stress and inflammation go hand-in-hand with accumulation of $nTiO_2$ particles lead to chronic inflammation which induces ROS formation, similarly, intracellular radical formation after particle uptake can result in the initiation of inflammatory signaling. Sustained ROS production can then lead to mutations in critical genes and tumor formation. Inflammatory reactions are meditated by cytokines released from cells and tissues encountering $nTiO_2$s. Another marker of inflammation, the influx of neutrophils to the surrounding tissue, has been reported in many studies after $nTiO_2$ treatment (Shi et al., 2013; Shvedova et al., 2012).

The relatively short history of $nTiO_2$ production means that epidemiological data is not yet available. The occupational carcinogenicity studies with workers exposed to TiO_2 dust, containing mainly large TiO_2 particles and possibly agglomerates and aggregates of $nTiO_2$ particles, have not detected any increased risk of cancer or other lung diseases. However, because of the paucity of epidemiological data of occupational $nTiO_2$ exposures and numerous *in vivo* studies claiming that $nTiO_2$ is carcinogenic and poses a health risk, the recommendation is that exposure to nano-sized TiO_2 should be minimized in occupational environments (Shi et al., 2013).

1.2.5. Health effects of carbon nanotubes

The fibrous morphology - i.e. high aspect ratio - of carbon nanotubes has raised concerns that CNTs might cause asbestos-like effects. Some CNTs can be included in the fiber pathogenicity paradigm (FPP), where the main reason for the toxicity of a given material is its morphology, i.e. it has to be thin, long and biopersistent (Figure 4), whereas its chemical composition plays a lesser role (Donaldson et al., 2013). Indeed, reports have been published, where CNTs have caused toxic effects to cells (Palomäki et al., 2011) and to mice (Poland et al., 2008) in a manner similar to asbestos.

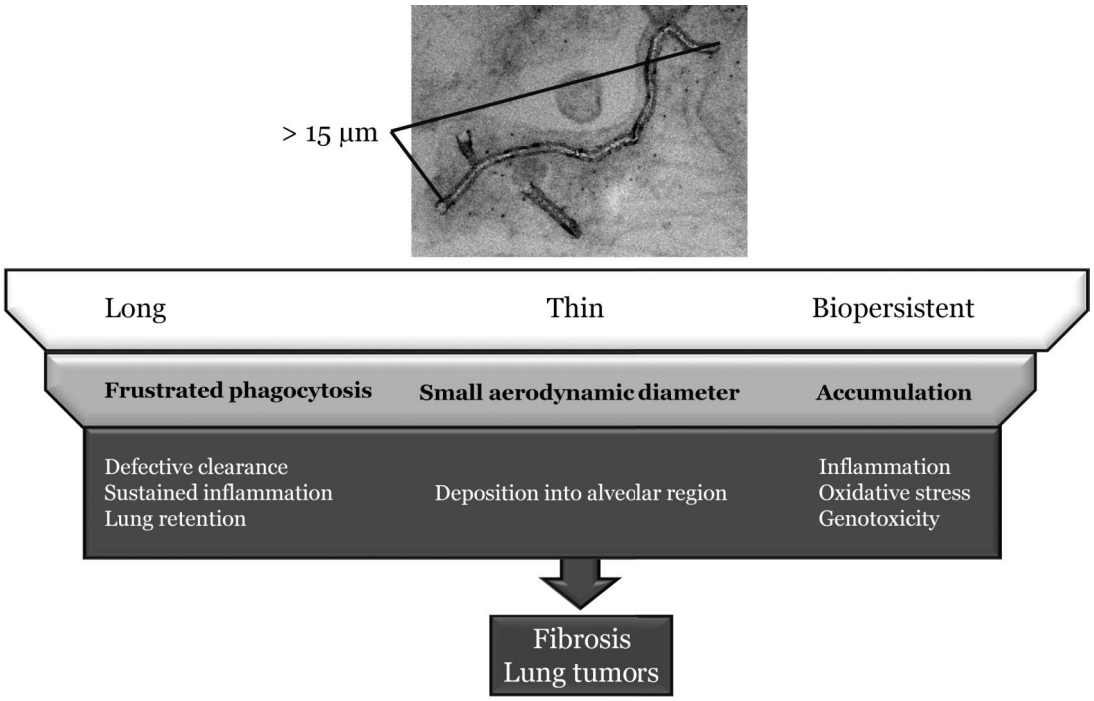

Figure 4. Fiber pathogenicity paradigm.
Diagram illustrating the adverse effects of high aspect ratio fibers.

In the case of airway exposure, alveolar professional phagocytes are the cells responsible for clearance of foreign material, bacteria and viruses. If a given fiber is longer than 15 µm, frustrated phagocytosis may result, where the fiber cannot be completely engulfed by phagocytic cells. Frustrated cells release chemotaxins that cause decreased migration of the fiber ingesting cells, which then reside in the lung rather than exiting the tissue normally along the mucociliary escalator. Cytokines and oxidants are also released, leading to stimulation of endothelial cells and recruitment of inflammatory cells. The persistent inflammation can then potentially lead to carcinogenesis in the lung. Frustrated phagocytosis has been characterized with some types of CNTs. Over 5 µm long fibers, such as CNTs, can also be retained in the pleura after inhalation exposure. The accumulation of

fibers causes inflammation, oxidative stress and genotoxicity and, if the fibers are biopersistent, the final outcome might be fibrosis or lung tumors (Donaldson et al., 2013). While length is a crucial factor in CNT toxicity, rigidity of the material is also important, since tangled CNTs are incapable of inducing equally serious effects (Palomäki et al., 2011).

Similarly to TiO_2, one of the most important reasons of CNT toxicity is oxidative stress. ROS may be generated either on the fiber surface by metal contaminants reacting with oxygen or indirectly via cellular processes (Donaldson et al., 2013). Direct outcomes of oxidative stress are peroxidation of proteins, DNA and lipids (Li et al., 2013). Selective peroxidation of mitochondrial lipids can result in caspase activation and apoptosis, which has been demonstrated after CNT exposure. Oxidative stress also has a role in the signaling cascades occurring in during inflammation. For example, ROS activate the NLRP3 inflammasome complex, which leads to secretion of pro-inflammatory cytokine Il-1β. Activation of NLRP3 inflammasome complex has been reported after CNT exposure, possibly because of activation of NADPH oxidase and ROS generation or due to lysosomal rupture and cathepsin release. Internalization of CNTs by phagocytes has been shown to cause the oxidative burst, another type of radical reaction, where large amounts of ROS are formed. This is normally used by professional phagocytes to cause disintegration of ingested pathogens. Similarly, it has been proposed that ROS formation could be one way for the cells to degrade CNTs in concert with peroxidase enzymes. The most reports have postulated, however, that when CNTs are ingested, the oxidative burst activates the lysosomal-mitochondrial axis, resulting in cell death (Shvedova et al., 2012).

CNTs can also cause actual physical damage to cells by puncturing the plasma membrane and thus interfering with normal cellular processes. Fibrous shape of CNTs can also inflict disruption of lysosomes and subsequent cathepsin release. Moreover, CNTs have been shown to interact with the centrosome structure resulting in DNA damage, while binding of CNTs to actin fibers has been reported to inhibit cell proliferation (Shvedova et al., 2012).

Even though no CNT induced lung tumors have been found *in vivo*, perhaps due to lack of long term studies, the results from numerous acute or sub-acute investigations, revealing adverse effects such as inflammation and fibrogenicity, have been interpreted to mean that CNTs might induce carcinogenesis in the long run (Donaldson et al., 2013). All in all, the nanosafety literature suggests that long and rigid CNTs share many common features of asbestos and, therefore, should be handled accordingly. Already, one company manufacturing carbon nanotubes, a CNT form not deemed especially hazardous, has set a very low 0.05 mg/m3, limit for occupational exposure (Pauluhn, 2010).

1.3. Methods and models used in ENM safety studies

1.3.1. Material characterization

One prerequisite for any ENM safety assessment is the extensive characterization of its physicochemical properties such as size, shape, surface area, solubility, aggregation/agglomeration, crystal structure and surface charge. Usually ENM samples contain a distribution of different sizes, which complicates the safety assessment for ENMs. ENMs can also be coated and their surface chemistry can be altered with doping, and this may well influence the toxic potential of the materials. Moreover, impurities such as catalyst residues and deficiencies in material morphology are often the reason for toxicity. Since currently no single method or machine is able to describe all these properties simultaneously, ENM characterization must be performed by using several methods, ant his makes the characterization both tedious and expensive (Table 2). By and large, because ENMs are an enormously heterogeneous group of materials, the scientific community has emphasized the importance of assessing safety of each ENM individually, and avoiding group-wide generalization (Heister et al., 2013; Park and Grassian, 2010; Johnston et al., 2013).

Table 2. ENM characterization methods

	Size	Shape	Surface area	Phase structure	Chemical composition	Surface charge (Z-potential)
BET			x (dry samples)[2]			
XRD	x			x	x	
DLS	x[1]		x (wet samples)[1]			x
SMPS	x[1]					
APS	x[1]					
TEM	x	x			x[3]	
SEM	x	x				
AFM	x	x				

BET Brunauer-Emmett-Teller method, XRD X-ray diffraction, DLS dynamic light scattering, SMPS scanning mobility particle sizer, APS aerodynamic particle sizer, TEM transmission electron microscope, SEM scanning electron microscope, AFM atomic force microscope, [1]Suitable for spherical materials, [2]Suitable for crystalline materials, [3]by EDS, energy dispersive spectroscopy attached to TEM

1.3.2. Exposure models

The respiratory system is regarded as the most important route for ENM exposure. Therefore, a large proportion of the ENM safety studies have utilized macrophages and epithelial cells in the *in vitro* studies and inhalation or intratracheal instillation exposures in the *in vivo* investigations. In addition, keratinocytes and *in vivo* dermal exposures have been used to study whether ENMs can enter body through the skin, while primary hepatocytes and liver cell lines are used to evaluate the effects of ENMs being deposited in liver from the blood circulation. Furthermore, some *in vivo* oral exposures have been performed to analyze whether ENMs are able to enter body from the gastrointestinal tract (GIT) (Johnston et al., 2013).

ENM exposure studies utilizing cells are cheap, reproducible and relatively rapid. *In vitro* assays can be performed with cell lines, primary cells and also by using 2D or 3D co-cultures mimicking better complex tissue environments for example in the lung (Johnston et al., 2013). Cell lines can be obtained from nearly every tissue. However, cell lines do not always function normally, many processes are completely shut down or continuously activated, and therefore the response to exposure agents might not reflect true situations at all. In contrast, primary cells are more difficult to acquire and handle, not to mention more expensive but their reactions to stimuli reflect better the real-life situation. An example of the differences between immortalized cells and primary cells is the uptake of polystyrene nanoparticles - the primary macrophages and cells of promonocytic THP1 cell line were shown to ingest NPs by two completely different mechanisms (Lunov et al., 2011).

In vitro studies can be used for cytotoxicity, inflammation and genotoxicity assessments. Fast and reproducible cell studies are useful in cytotoxicity tests, as large numbers of different ENMs can be screened at different time-points. The most widely used methods include trypan blue, lactate dehydrogenase (LDH) and MTT assays, which all reflect distinct mechanisms, while being straightforward and relatively cheap. Moreover, genotoxicity screening of ENMs is easily conducted with cells, utilizing robust methods such as micronucleus and chromosome aberration assays and single cell gel electrophoresis (SCGE or Comet), a technique used to study DNA strand breaks. However, genotoxicity studies must always be verified with *in vivo* tests if they are to be used in setting-up occupational exposure limits. Inflammatory cells such as macrophages can be used to study inflammation for example by measuring the amounts of different cytokines after ENM treatment or by studying inflammasome activation (Fadeel et al., 2012; Palomäki et al., 2011; Lindberg et al., 2009; Palomäki et al., 2010).

Macrophages are professional phagocytes acting at the borderline between innate and adaptive immunity. Because of their presence in key locations such as the brain, liver, lung, blood and skin, macrophages are often the first cells

to encounter foreign molecules or pathogens. According to their functions, macrophages can be divided into classically activated (M1), alternatively activated (M2), regulatory, tumor-associated (TAM) and myeloid-derived suppressor cells (MDSCs). Of these, M1s are the classical macrophages recognizing and killing bacteria, viruses and protozoa, while M2s function in wound healing and inhibit inflammation. The activation state of the macrophages depends on the local environment and switching between activation states is not uncommon (Murray and Wynn, 2011).

Under normal conditions, macrophages are anti-inflammatory, since they secrete interleukin-10 (IL-10), a potent anti-inflammatory cytokine. Macrophage activation occurs when the cells encounter pathogens, foreign molecules or damaged self-tissue. After activation, macrophages start secreting pro-inflammatory cytokines such as tumor necrosis factor (TNF), IL-1 and the inflammation promoting nitric oxide (NO). These further boost the local inflammation response. IL-12 and IL-23 are also secreted leading to polarization of T_H1 and T_H17 cells, which are critical cells that intensify immune responses. Therefore, macrophages not only phagocytize foreign material or pathogens but also enhance the local inflammation response by alerting and activating other immune cells (Murray and Wynn, 2011).

The main function of airway epithelial cells (ECs) is to act as a barrier between the organism and its surrounding environment, preventing entry of foreign molecules, bacteria and gases to the body. Furthermore, they have a major role in immunological cascades. ECs recognize foreign molecules, pathogens and damaged self-proteins by pattern recognition receptors (PRRs) which are present in large numbers at the EC surface. Activation of these receptors leads to secretion of pro-inflammatory cytokines and chemokines which recruit and activate immune cells such as macrophages, dendritic cells and T-cells (Lambrecht and Hammad, 2012). Recently, Juncadella and collaborators (2013) reported that ECs were also able to phagocytize apoptotic cells and thus to participate in airway clearance. Moreover, they postulated that ECs participated in controlling the cytokine environment of the lung.

The effects observed in *in vitro* studies are difficult to extrapolate with confidence into responses in tissues not to mention responses in human beings (Johnston et al., 2013). Therefore, when assessing nanosafety, *in vivo* studies are still compulsory. The two widely used methods to study the effects of inhaled ENM are inhalation exposure and intratracheal instillation (IT) (Johnston et al., 2013). The more laborious and expensive of the two is the inhalation exposure. This is a whole-body exposure method, where mice are placed in an exposure chamber and allowed to inhale aerosolized ENMs, which can be produced in situ with a particle generator or a solid particle dispenser (Rossi et al., 2010b). IT experiments do not require such specialized equipment and considerably less material is needed.

In IT, a suspension containing the ENMs is administered directly to the trachea of the mice via catheter. Generally, IT experiments have been reported to inflict stronger effects than inhalation exposures, this being speculated to be due to the fact that after IT, most of the particles are deposited directly onto the alveoli, while in inhalation exposure, particles deposit more evenly throughout the whole respiratory system, better reflecting real-life situation (Johnston et al., 2013).

Intravenous (IV) instillations and oral exposures can be used to study the distribution of ENMs inside the body. Biodistribution studies provide knowledge about the deposition sites of ENMs, therefore giving information on secondary targets of the materials. Some materials may cause no effects in the primary exposure site, such as the lung or GIT, but once reaching a secondary target organ like spleen or liver, then adverse effects are elicited (Johnston et al., 2013). Furthermore, IV exposures offer indispensable knowledge about how the ENMs used as drug vectors are cleared and how the material surface modifications affect clearance and biodistibution (Luo et al., 2013). ENMs can be also injected into the peritoneal cavity of mice, which is used to mimic the pleura. In this way, the material's ability to cause fibrosis and lung cancer can be assessed (Poland et al., 2008). *In vivo* dermal studies are also utilized to investigate the skin penetration abilities of ENMs. This is especially interesting because of the use of ENMs in many cosmetics, mainly in sunscreens (Elsaesser and Howard, 2012).

Since many of the individuals exposed to ENMs also suffer from underlying diseases such as asthma, cardiovascular diseases or skin disorders, it is possible that the exposure to ENMs could aggravate the disease. Therefore, ENM safety studies have been conducted, utilizing knock-out mice that have been developed to mimic many diseases and disorders, further emphasizing the usefulness of *in vivo* studies (Johnston et al., 2013; Rossi et al., 2010a).

In vivo studies can be used to assess acute, sub-acute, sub-chronic and chronic effects of ENMs. Moreover, they can be used to study a multitude of end-points. For example, lung inflammation can be detected classically by measuring neutrophil influx into the lung or by quantifying the expression of inflammation linked cytokines from lung tissue or from bronchoalveolar lavage (BAL). The genotoxic studies such as micronucleus, chromosome aberration and Comet assays used in *in vitro* tests function also in *in vivo* examinations. The results of these studies may then be used for carcinogenicity assessments. Arguably the most important *in vivo* studies regarding ENMs are toxicokinetics studies, which are intended to reveal absorption, distribution, metabolism and excretion of ENMs. These results can then be widely used in toxicity studies, in risk assessment and in the regulation of ENMs (Fadeel et al., 2012).

1.4. Proteins and proteomics

While DNA is the information library of life, containing all the knowledge about how cells, tissues and organisms are constructed and function, the biomolecules that make life possible are proteins. In order for a given gene to be expressed as a protein, it has to be first transcribed into mRNA and then translated into protein in a cascade where every step is tightly controlled. After transcription, mRNA can be degraded or otherwise processed thus having an effect on the translation. The resulting protein can then be degraded if not needed or if incorrectly folded. Proteins are also modified by post translational modifications (PTMs) profoundly affecting the function and activity of the protein and also its localization in the cell (Maier et al., 2009). Schwanhäusser and collaborators (2011) have postulated, that the correlation between detected levels of mRNA and its corresponding protein product is about 40%. They also proposed that the most important factor predicting the protein levels is the translation efficiency.

Proteomics investigates the entire protein content of a cell, tissue or organism; e.g. research into protein structure, localization, expression changes or interactions with other proteins. Since the term proteomics was first coined in 1995, the proteomic methods have evolved by leaps and bounds. In recent years, it has become possible not only to identify large amounts of proteins from a dilute biological sample but also to do it in a quantitative manner (Coombs, 2011). Proteome research adds a new information layer to functional genetics: whereas the latter is unable to state whether the genes or mRNAs really end up being functional proteins, proteomics detects only the proteins that are translated, which are, therefore, having an effect in the cell or tissue. Furthermore, proteomic methods are able to detect protein isoforms and PTMs, such as phosphorylation, glycosylation or acetylation (Phanstiel et al., 2011; Desaire, 2013; Choudhary et al., 2009). Figure 5 illustrates gel-based and MS-based proteomics workflows.

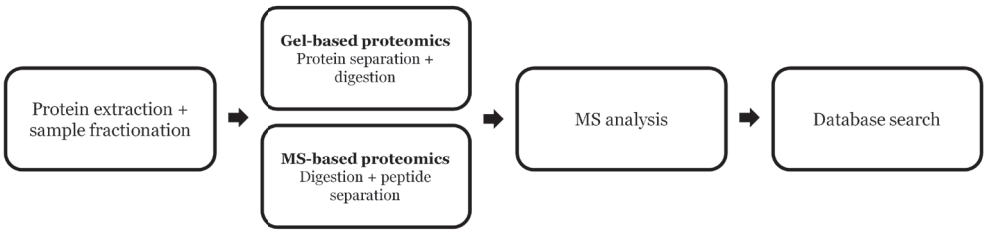

Figure 5. Proteomics workflow.

1.4.1. Protein and peptide separation

Even though not expressed simultaneously and in every cell and tissue, the human genome contains over 20 000 genes. The amount of proteins these genes encode is drastically larger, since mRNAs can be alternatively spliced and protein functions are controlled by PTMs (Smith et al., 2013). Therefore, in order to obtain maximal amount of identified proteins, protein fractionation is necessary. Already when extracting the proteins, the sample can be fractionated for example into membrane proteins (Thimiri Govinda Raj et al., 2011), cytoplasmic proteins (Hempel et al., 2011) and nuclear proteins (Lelong et al., 2012) in an attempt to reduce sample complexity. These procedures can be carried out with gradient centrifugation and different detergent treatments, or by utilizing commercial kits, which are becoming more and more available. Apart from making samples less complex, sample fractionation provides new information about protein the localization and proteomes of distinct cell compartments (Zhang et al., 2013).

Another problem encountered in many complex protein mixtures, especially in plasma, is the dynamic range, meaning that a few proteins dominate in terms of abundance, while the most interesting proteins are present only in minute concentrations. Therefore, also the detection of the less abundant protein is difficult (Wilson, 2013). To tackle this problem, the most abundant proteins can be depleted from the sample or the dynamic range can be selectively equalized. The problem with depletion is that the high abundant proteins might be adhering to other proteins, in the worst case scenario resulting in the depletion of the protein of interest. The selective equalization is based on ligand libraries containing millions of hexapeptides, which bind proteins. Only the proteins which bind to ligands are collected and analyzed. In this technique, the ligands of the most abundant proteins are quickly saturated and only a portion of them is taken to the analysis, while the rest are discarded. The down-side of equalization is that proteins must have an affinity for the ligands in order to be included in the analysis (Selvaraju et al., 2012).

After fractionation and possible equalization, proteins and peptides are usually further separated by their properties such as size, charge and hydrophobicity. The separations can be performed in tandem by different properties to achieve better resolution (Egas and Wirth, 2008). The most widely used technologies for protein and peptide separation are gel electrophoresis and chromatography techniques.

1.4.1.1. Gel-based

Gel electrophoresis can be one- (1DE) or two-dimensional (2DE). 1DE of proteins is a powerful separation method, where proteins are separated according to

their size inside polyacrylamide slab gels using electric current. After separation, proteins are visualized with different dyes such as Coomassie, silver staining or fluorescent dyes. After staining, protein bands or spots can be excised from the gel, digested in-gel and analyzed with MS (Graves, 2002).

1DE can resolve proteins in the molecular mass range of 10-300 kDa (Graves, 2002). In 1DE, proteins are usually denatured with SDS and heat treatment. Denaturation ensures that hydrophobicity has no effect on protein migration inside the gel, while SDS also confers a constant, negative charge on the proteins. Therefore, proteins are only separated according to their molecular weight. Separation by size is performed by gel sieving. The pore size of the gel can be used to control migration of proteins. In gels with small pores, the large proteins become stuck and therefore the smaller proteins are better separated. The optimal pore radius for separation of proteins between molecular weights from 10 to 200 kDa has been postulated to be 10 nm (Egas and Wirth, 2008).

Complex protein mixtures contain many proteins with the same molecular weight. Therefore, in many proteomic experiments, protein separation only by size is not adequate. In 2DE, proteins are first separated according to their isoelectric point (pI) in isoelectric focusing (IEF). This is followed by separation according to molecular weight. A routine 2DE experiment is able to resolve up to 2000 protein spots, revealing also protein isoforms and PTMs (Egas and Wirth, 2008; Gorg et al., 2004).

1.4.1.2. Chromatography-based

Since 2DE is relatively time consuming and offers low throughput, chromatography-based protein and peptide separation methods are being increasingly used. Mass spectrometry based proteomics usually utilizes liquid chromatography (LC) to separate peptides. Chromatography can be performed off-line or on-line coupled to a mass spectrometer. The most widely used method combining on-line LC and MS is reversed-phase liquid chromatography (RPLC), which separates peptides due to their hydrophobicities (Zhang et al., 2013).

Multiple off-line chromatography methods are available, to enhance peptide detection. Size-based separation can be achieved by applying size-exclusion chromatography (SEC). This method is well suited for MS, because no detergents are needed. Other methods include the use of strong cation exchange (SCX) to separate peptides by charge or the exploitation of immobilized metal ion affinity chromatography (IMAC) which can be used to identify proteins carrying genetically engineered hexahistidine tags (Egas and Wirth, 2008). IMAC is also suited for PTM analysis, where it can be used to enrich phosphopeptides (Zhang et al., 2013).

One method taking advantage of the best parts of gel-based and mass spectrometry based proteomics is 1DE coupled to LC-MS (GeLCMS). In GeLCMS, proteins are separated in 1DE and the resulting protein lanes are cut into 10-20 pieces, which are digested and analyzed with LC-MS. The 1DE step is fast, robust and reproducible, removing impurities and reducing sample complexity, while splice isoforms and degraded proteins are also better differentiated (Lundby and Olsen, 2013).

1.4.2. Mass spectrometry and protein identification

The main driver of proteomics progression has been the evolution of mass spectrometry. The introduction of soft ionization methods, electrospray ionization (ESI) (Yamashita and Fenn, 1984) and matrix-assisted laser desorption ionization (MALDI) (Karas et al., 1985), which do not cause degradation of proteins and peptides, have made possible protein identification. The developers of ESI and MALDI were awarded the Nobel Prize in Chemistry in 2002, highlighting the importance of soft ionization methods for proteomics and for biological macromolecule analysis.

The basic components of nearly all mass spectrometers are as follows: ion source, mass analyzer and the detector (Van Oudenhove et al., 2013). In the ion source, such as ESI or MALDI, the peptides are ionized. ESI is usually coupled to LC, because it is able to ionize peptides from liquids. Peptides or proteins are ionized using high voltage between the outlet of the LC and the inlet of the mass spectrometer. In MALDI, the ionization is performed by applying laser energy into peptides or proteins which are immobilized in a special matrix. Heat from the laser desorbs the matrix from the samples and $[M + H]^+$ ions from the sample are released into the gas phase. While MALDI not as compatible to LC coupling as ESI, MALDI is a good method for the analysis of intact proteins. The mass analyzer is used to store and separate the ions according to their mass to charge ratio (m/z). Most mass analyzers use either scanning, ion-beam or trapping to analyze ions. While ion sources and mass analyzers can be combined in different configurations, the most common are MALDI coupled to TOF and ESI coupled to trapping or ion-beam devices. In addition, many mass analyzers can be used in the same instrument, such as three quadrupoles in tandem (triple quadrupole, TQ), ion trap and orbitrap or TQ and ICR. These hybrid instruments provide even better resolution and mass accuracy (Table 3) (Yates et al., 2009).

Table 3. Different mass analyzers and their properties. *Data from Yates et al., 2009 and Zhang et al., 2013*

Mass analyzer	Benefits	Drawbacks
Quadrupole (Q)	high dynamic range	medium scan rate, low resolution, low mass accuracy
Ion trap	fast scan rate	medium dynamic range, low resolution, low mass accuracy
Time-of –flight (TOF)	fast scan rate, high mass accuracy, high dynamic range	medium resolution
Orbitrap	high mass accuracy, high resolution	medium scan rate, medium dynamic range
Fourier transform ion cyclotron resonance (FTICR)	extremely high mass accuracy, high resolution	medium dynamic range, slow scan rate

Proteins are enzymatically digested into peptides to facilitate protein identification. Digestion can be performed in-gel or in-solution using a variety of different enzymes. The most widely used enzyme is trypsin, which cleaves proteins at the C-terminal to residues Lys and Arg. Trypsin is also resistant to auto-cleavage and is able to produce peptides with an average length of 14 amino acids carrying at least two positive charges (Switzar et al., 2013). In order to identify the peptides, the obtained peptide masses obtained from mass spectrometry are compared with sequence databases. The identifications can be made based on peptide masses, called peptide mass fingerprints (PMFs), or based on fragmented peptides, called tandem mass spectra (MS/MS). In PMF, the comparison methods utilize molecular weights of peptides; the key is to use specific proteases which cleave proteins site-specifically (Sadygov et al., 2004). In contrast, MS/MS based peptide identification compares observed MS/MS spectra to theoretical fragment ion spectra (Deutsch et al., 2008).

Modern mass spectrometers produce a huge amount of data in large-scale proteomics exercises that manual interpretation of spectra for protein identifications is impossible. Consequently, many automated programs employing algorithms for matching MS/MS spectra to sequences in vast libraries have been developed. The two widely used algorithms are Mascot (Perkins et al., 1999) and SEQUEST (Eng et al., 1994). Mascot calculates the likelihood of an experimental MS/MS spectrum being able to match a theoretical MS/MS spectrum by chance: the end product is a probability score. Furthermore, a decoy search can be performed by matching MS/MS spectra to reversed or scrambled peptide sequences giving the false discovery rate (FDR) for the match (Choi et al., 2008). SEQUEST algorithm uses two calculations for the identification. The

first one is called XCorr and it provides a statistical value of the correlation of between experimental and the calculated spectra. The algorithm then calculates ΔCN which is the difference between the best and second best spectrum match (Sadygov et al., 2004). However, it should be kept in mind that the algorithms are not perfect, manual validation of the spectra is still needed, at least for the identifications with the lowest scores (Zhang et al., 2013).

1.4.3. Quantitative proteomics

Quantitative proteomics can be gel-based or MS-based. The gel-based most often utilizes 2DE and the actual quantitation of proteins is performed analyzing intensities of the stained protein spots in the gel. MS-based quantitation, on the other hand, relies on a combination of reproducible liquid chromatography, mass spectrometry and bioinformatics.

1.4.3.1. Gel-based quantitation

In 2DE, treated and untreated samples are run in different gels, proteins are visualized by silver staining, Coomassie or fluorescent stains and image analysis software is used to detect differences in spot intensities. Differently expressed protein spots are then excised, in-gel digested and analyzed by MS (Görg et al., 2004). Many successful studies have employed this protocol ranging from the characterization of viral infection (Öhman et al., 2010) to evaluating the effects of TiO_2 on macrophages (Cha et al., January 2007). The main challenge in 2DE quantitation is to achieve reproducible gel separation. Inconsistent protein migration leads to difficulties in spot matching. Furthermore, incorrect spot matching increases the possibility of false positives and negatives. Moreover, the sensitivity and dynamic range of the used protein stains are still rather low, while also the analysis of hydrophobic proteins requires special methods (Rogowska-Wrzesinska et al., 2013).

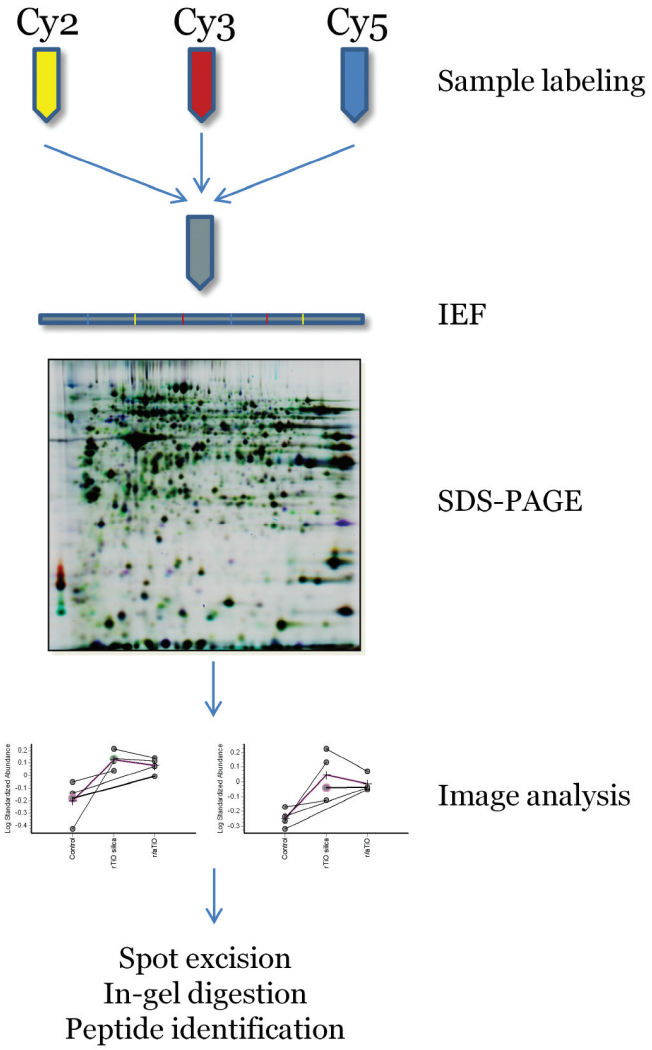

Figure 6. 2D-DIGE workflow. *Samples are labeled with fluorescent tags (Cy3 or Cy5) prior to IEF. The internal standard containing an identical amount of all samples is labeled with Cy2. Samples are then combined and 2DE is performed. Image analysis software is used to quantify protein expression via their spot intensities. Differentially expressed protein spots are excised, in-gel digested and identified by MS and database searches. IEF isoelectric focusing*

The invention of the DIGE method (Figure 6) has provided better spot matching, sensitivity and reproducibility of the gel electrophoresis (Ünlü et al., 1997). In DIGE, proteins are labeled with fluorescent dyes prior to IEF. The dyes, called CyDyes, are incorporated into the proteins via an N-hydroxysuccinimide (NHS) ester reactive moiety which binds to the ε-amino groups of lysine residues. Three different CyDyes are available for DIGE, each emitting light at different wavelengths; Cy2 at 506 nm, Cy3 at 565 nm and Cy5 at 680 nm. CyDyes coupled with NHS have identical pIs and MW and thus they do not to distort IEF or gel electrophoresis. In a typical DIGE experiment, treated and untreated proteins are stained with Cy3 and Cy5. In addition, an internal standard, containing an identical amount of all samples is labeled with Cy2. The three samples are then combined and 2DE is performed. Subsequently software such as DeCyder from GE Healthcare is used to quantify spot intensity. The main advantage of DIGE

compared to classic 2DE is that treated and untreated samples can be analyzed in the same gel together with the internal standard. This greatly reduces gel-to-gel variation, while the presence internal standard facilitates spot matching and can be used to standardize protein expression changes. These characteristics have made DIGE the gold-standard of gel-based quantitation (Coombs, 2011). DIGE has been utilized successfully in numerous proteomic studies such as secretome analysis (Garcia-Lorenzo et al., 2012), oxidative stress studies (Aparicio-Bautista et al., 2013) and in biomarker research (Rostila et al., 2012; Mustafa et al., 2013; Hamelin et al., 2011).

1.4.3.2. MS-based quantitation

The invention of better software algorithms and protein labels together with the evolution of MS equipment and increased genome information have enabled mass spectrometry based protein quantitation. Novel MS-based proteome analyses surpass the gel-based versions by being more high-throughput and resulting in more protein identifications but, at the same time, they offer quantitation of the identified proteins and they possess a much improved dynamic range. The two main classes of mass spectrometry based quantitation are stable isotope labeling and label-free quantitation. Stable isotope labeling is then further subdivided into absolute quantitation and relative quantitation (Coombs et al., 2011).

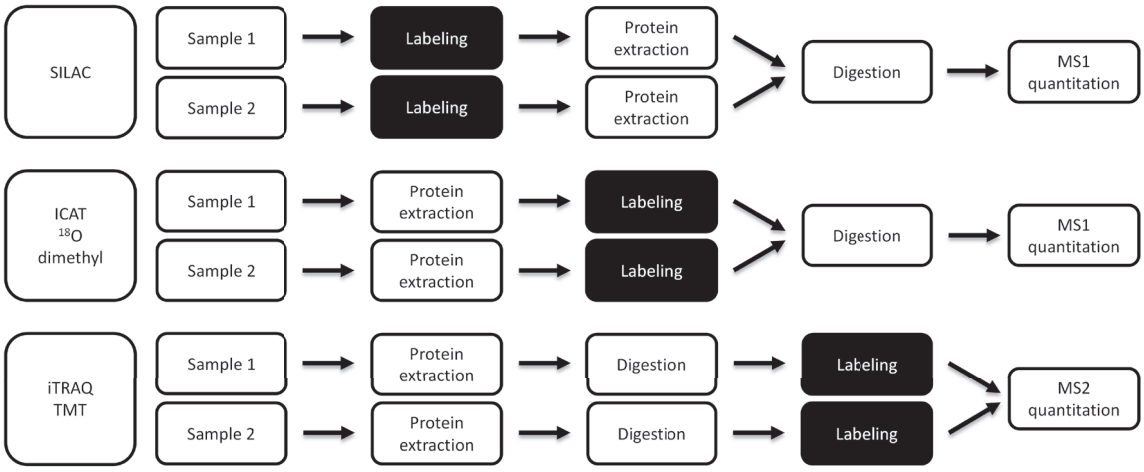

Figure 7. Stable isotope labeling. *The figure illustrates work-flows of MS-based quantitative proteomics taking advantage of stable isotope labeling. MS mass spectrometry, SILAC stable isotope labeling of cell culture, ICAT isotope coded affinity tag, iTRAQ isobaric tags for relative and absolute quantitation, TMT tandem mass tags*

Stable isotope labeling can be performed at the MS1 and MS2 levels (Figure 7). Most of the stable isotope labeling techniques, such as isotope coded affinity tag (ICAT) (Gygi et al., 1999), dimethyl labeling (Hsu et al., 2003) and ^{18}O (Reynolds et al., 2002), rely on MS1 level quantitation. In these methods, isotopes are incorporated to proteins prior to digestion. Many of these labels, however, induce a shift in the retention time and this makes data analysis more complicated. The use of metabolic labels such as stable isotope labeling of cell culture (SILAC), which is based on incorporation of labeled essential amino acids in whole cells, can simplify data analysis because all of the samples can be run in the same LC-MS analysis. In SILAC, cells are grown either in normal media or media containing heavy amino acids such as $^{13}C6$-arginine and $^{13}C6$-lysine. Labeled and unlabeled protein samples are mixed after extraction, and the peptides containing light and heavy isotopes can then be distinguished and quantitated at the MS1 level (Ong, 2012). Two major techniques utilizing quantitation of fragmented peptides at the MS2 level are isobaric tags for relative and absolute quantitation (iTRAQ) (Ross et al., 2004) and tandem mass tags (TMT) (Dayon et al.,2008). The main advantage of using isobaric tags is the possibility for multiplexing (up to 8), since in MS1 based quantitation, the analysis is restricted to two or three experimental conditions. The isobaric tags, consisting of a mass reporter, a cleavable linker which balances the mass and an amine reactive group, are incorporated into digested peptides. MS2 level quantitation is based on the intensity of the mass reporter, which is released when the linker is fragmented in the mass spectrometer. Labeling digested peptides achieve better labeling efficiency when using metabolic labeling, since in SILAC, the labeling efficiency depends on cell divisions. The major drawback of MS2 level quantitation occurs when the target peptide is fragmented simultaneously with a coeluting peptide. This results in a mixture of fragment ions from both the target peptide and peptides with similar m/z, thus the reporter ion intensities originate from a mixture of peptides, not only from the target. This problem is not an issue when using MS1 based quantitation (Zhang et al., 2013).

Two main lineages of label free quantitation exist: spectrum counting (Liu et al., 2004) and ion intensity based quantitation (Bondarenko et al., 2002). Spectral counting is based on the number of observed spectra from peptides of a given protein – abundant proteins are counted more often than scarce proteins. In contrast, ion intensity based quantitation relies on the chromatographic peak area of the peptides. The area is proportional to the ion intensity of a peptide. Both of these methods have their strengths and weaknesses: spectral counting fails to quantify low abundant proteins, while ion intensity based quantitation relies on the reproducibility of LC-MS/MS runs. Label free protein quantitation offers even greater analytical depth and a better dynamic range than methods based on labeling. In addition, label free techniques are not affected by incomplete tag incorporation and are inexpensive. However, they do require more instrument

time, highly reproducible LC separation and advanced data analysis (Schulze and Usadel, 2010).

While MS-based quantitative proteomics clearly outperforms gel-based in the number of identified proteins and quantitation efficiency (Coombs, 2011), the gel-based methods still offer robust and effective protein quantitation. One of the advantages of gel-based methods over MS-based is the analysis of protein PTMs. The PTM changes can be readily seen in the 2D gels as shifts in the pI of protein spots, whereas the detection of PTMs by mass spectrometry is much more laborious. Moreover, gel-based quantitation can be used to detect protein modifications, such as carbonylation and thiol oxidation, that cannot be enriched for MS-based methods (Rogowska-Wrzesinska et al., 2013).

1.4.4. Data analysis

Proteomics experiments produce data in the form of protein identification lists and quantification information. Single protein identification and a change in its expression after a given stimulus is not sufficient to be used as a starting point for hypothesis. Furthermore, the large number of identifications obtained from proteomics exercises makes data analysis time-consuming. Thus, several tools and databases have been constructed which assist in the in-depth analysis of protein expression changes and thus correct interpretation of the results becomes possible (Malik et al., 2010).

Gene ontology (GO) (Ashburner et al., 2000) is the most basic step in screening proteomic data. It is used to characterize proteins by a given number of terms. Since the number of terms is limited, the ambiguity of protein terminology is reduced, thus facilitating automated analyses. The GO is a hierarchical structure. On top of the hierarchy are three main GO-categories: 'biological process', 'molecular function' and 'cellular component'. Each GO-entry is given a GO-identifier in a number format and a term belonging into one of GO-categories. The terms represent nodes in the hierarchy and they can have one or more child nodes. In addition, one child node can have numerous parent nodes which means that there are several information layers available in the protein function description. A given protein can be afforded one or several terms in all GO-categories (Malik et al., 2010). GO information can be used in downstream processing to detect enriched GO annotations in the proteomic data set. Especially in large data-sets, enriched terms can provide valuable information about activated and deactivated processes in different conditions. One example of a widely used enrichment tool is DAVID (Malik et al., 2010).

The next steps in data interpretation are pathway analysis and protein interactions. Pathway analysis describes physical and functional interactions

between proteins, which makes pathway analysis a useful method for investigating signal transduction, metabolic processes and cell cycle progression. The data in pathway analysis databases is manually curated and more detailed than that obtained in protein interaction databases. A plethora of free and commercial pathway analysis tools exist, the most popular being Kyoto encyclopedia for genes and genomes (KEGG) (Ogata et al., 1999), Reactome and Ingenuity pathway analysis (IPA). Enrichment tools such as DAVID offer additional value in highlighting over-represented pathways in proteomic data sets. Since most of the cellular processes are performed by protein complexes rather than single proteins, additional information on protein functions can be obtained from protein-protein interaction (PPI) databases. PPI resources such as Human protein reference database (HPRD) and IntAct contain information on physical and functional interactions assembled from experimental and computational data (Malik et al., 2010).

1.4.5. ENM health effect studies utilizing proteomics

Proteomics has been so far utilized sparingly in ENM safety research (Table 4). Mostly studies have utilized proteomics for protein corona investigations (Tenzer et al., 2013; Cedervall et al., 2007; Jedlovszky-Hajdu et al., 2012) and only a few *in vivo* studies with proteomics methods have been published. One study found high-sensitivity inflammation marker proteins from mice lung after the animals were exposed to swCNTs two times per week for three weeks by pharyngeal aspiration (Teeguarden et al., 2011). Another study compared the effects of inhaled silver nanoparticles (AgNPs) in allergic and healthy mice. Here the mice inhaled AgNPs on 7 days for six hours per day and the proteomes of plasma and BAL were analyzed, revealing immunotoxic markers in BAL in both healthy and asthmatic mice (Su et al., 2013). In addition, Gao and collaborators (2011) characterized an early response in lymph nodes 24 hours after intradermal injection of $nTiO_2$s. All of the *in vivo* ENM proteomics studies have utilized mass spectrometry based proteome analysis.

Table 4. Nanosafety studies utilizing proteomics

Reference	Exposure route / Cell line	Material	Method	Main conclusions
In vivo				
(Teeguarden et al., 2011)	Pharyngeal aspiration	swCNT, asbestos, carbon black	LC-MSMS, label-free quantitation	Inflammation, Oxidative stress
(Su et al., 2013)	Inhalation	AgNP	LC-MSMS, qualitative	Immune responses
(Gao et al., 2011)	Intradermal injection	TiO_2	LC-MSMS, isotope labeling	Early response in lymph nodes
In vitro				
(Ge et al., 2011)	BEAS-2B	TiO_2	2D-DIGE-MSMS	Oxidative stress
(Gonçalves et al., 2010)	Primary neutrophils	TiO_2	Protein array	Neutrophil activation
(Haniu et al., 2006)	U937	mwCNT	2DE-MSMS	Response to stress
(Yuan et al., 2011)	HepG2	swCNT	LC-MSMS, iTRAQ quantitation	Oxidative stress
(Tilton et al., 2013)	3D culture (THP-1, Caco-2/HT29-MTX)	TiO_2 nanobelts, swCNT	LC-MSMS, label-free quantitation	Cell proliferation

Proteomics has been exploited more in *in vitro* studies. In these, $nTiO_2$ has been shown to cause expression changes in defense-related and cell-activating proteins and also to inflict oxidative stress to BEAS-2B cells (immortalized bronchial epithelial cell line) (Ge et al., 2011) and to activate primary human neutrophils (Gonçalves et al., 2010). In these experiments, Ge and collaborators (2011) utilized two-dimensional difference gel electrophoresis (2D-DIGE). The human neutrophil study took advantage of a more unconventional proteomic method, the namely protein array. The safety of CNTs *in vitro* has been analyzed with both gel-based proteomics and with mass spectrometry based proteomics. Haniu and collaborators (2006) used 2DE to detect proteome changes in U937 human monoblastic leukemia cell line after treatment with two different mwCNTs, finding similarly activated signaling cascades such as the response to stress and cell death, while some proteins changes were unique to mwCNT type. In another study, Yan and others (2011) studied the effects of swCNTs on human hepatoma cells (HepG2) by using iTRAQ coupled with LC-MS/MS; they found oxidative stress and interference with protein synthesis.

In a more complex study design, the effects of TiO_2 nanobelts and mwCNTs were compared in SAE (primary small airway epithelial) and THP-1 cells and in Caco-2/HT29-MTX (intestinal epithelial cell line/goblet cell line) co-cultures in low and high concentrations for 1 and 24 hours using transcriptomics and

quantitative MS-based proteomics. The results indicated that at early time-points the cells reacted to ENMs similarly by a displaying generic response to an insult, however, after a longer exposure period, mwCNTs activated the cell through a distinct mechanism by activating cell proliferation, anti-apoptotic and DNA repair mechanisms (Tilton et al., 2013).

The available proteomic methods and instruments offer one tool for the nanosafety research field, where high throughput approaches are needed. Moreover, proteomic exercises can be included in large scale systems biology studies, which produce data that can be used to distinguish safe ENMs from dangerous.

2. AIMS OF THE STUDY

The novel physical and chemical properties of engineered nanomaterials have made nanotechnology one of the major successes of 21st century. However, some ENMs have been shown to inflict adverse effects *in vitro* and *in vivo*. Thus far, very few studies investigating the health effects of ENMs by proteomic techniques have been performed. Here, our goal was to analyze the crucial first steps after ENMs come into contact with biological systems by utilizing proteomic methods. The specific aims were:

- To study the interactions of ENMs with plasma and cellular proteins and to determine whether all ENMs are taken up by relevant cells of the respiratory system; human primary macrophages and lung epithelial cells (I).

- To elucidate the cytoplasmic proteome changes after exposure to silica coated and uncoated titanium dioxide in macrophages and to evaluate the effects of ENM coating to particle toxicity (II).

- To investigate and compare the effects induced by two types of long carbon nanotubes and asbestos on macrophage protein secretion and to analyze the impact of CNT morphology to toxic effects (III).

3. MATERIALS AND METHODS

3.1. Materials used

The used ENMs are listed in Table 5. The composition of the materials was determined by energy dispersive spectroscopy (EDS; ThermoNoran Vantage, Thermo Scientific, Breda, The Netherlands) attached to transmission electron microscope. The crystallinity and phase structure of nanopowders were characterized with X-ray diffractometer (Siemens D-500, Siemens AG, Karlsruhe, Germany) and specific surface area of the used nanomaterials was measured by adsorption, using the Brunauer-Emmett-Teller (BET) method (Coulter Omnisorp 100CX, Florida, USA). The morphology of the materials was determined with a scanning electron microscope SEM (Zeiss ULTRAplus FEG-SEM, Carl Zeiss NTS GmbH, Oberkochen, Germany). Surface charge of the materials was analyzed with Zetasizer Nano ZS (Malvern Instruments Inc, UK) instrument. The principle of the measurement has been described by (Jiang et al., 2009). SEM images of ENMs are shown in the Supporting information 7 (I) and Table 1 (III). ENMs were characterized both in the dry form and in dispersion.

Table 5. Materials used in the study.

Name	Vendor	Size	Publ.
rTiO_2 silica coated	Sigma-Aldrich	10 × 40 nm	I, II
rTiO_2 alumina coated	Kemira	~14 nm	I
rTiO_2 silicone coated	Kemira	~14 nm	I
r/aTiO_2	NanoAmor	30-40 nm	I, II
aTiO_2	Sigma-Aldrich	<25 nm	I
rTiO_2 coarse	Sigma-Aldrich	<5 µm	I, II
ZnO	Umicore	30-35 nm	I
SiO	NanoAmor	10 nm	I
m̂wCNT	SES Research	10-30 nm × 1-2 µm	I
swCNT	SES Research	<2 nm × 1-5 µm	I
Quartz sand	US Silica	<5 µm	I
Asbestos (Crocidolite)	Pneumoconiosis Research Centre	180 nm × 4.6 µm	III
Long tangled mwCNT	Cheaptubes Inc	8-15 nm × 10-50 µm	III
Long rigid mwCNT	Mitsui&Co, Ltd	<50 nm × ~13 µm	III

3.2. Cell culture

Human primary macrophages (I, II, III) were differentiated from the leukocyte-rich buffy coats of healthy blood-donors (Finnish Red Cross Blood Transfusion Service, Helsinki, Finland). The differentiation of macrophages was performed by isolating peripheral blood mononuclear cells from the buffy coats by Ficoll-Paque -gradient centrifugation after which the mononuclear cell layer was harvested. After washing the harvested cells three times with PBS (pH 7.4), the mononuclear cells were allowed to adhere onto six-well plates (1.4 million cells/well) for 50 minutes in RPMI 1640 medium supplemented with 2 mM L-glutamine and 1% PEST in +37°C 5% CO_2. The cells were then washed three times with PBS and after the last wash the adhered cells were given 0.5 ml Serum-Free Macrophage medium (Invitrogen, Carlsbad, CA, US) supplemented with 10 ng/ml granulocyte-macrophage colony-stimulating factor (GM-CSF, ImmunoTools GmbH, Germany) and 1% Penicillin-Streptomycin (PEST). The macrophage medium was changed every two days. Maturated macrophages were used for the exposure studies on the seventh day after the cell harvesting.

Human lung epithelial cells (I) (A549, ATCC, Manassas, VA, US) were cultured in RPMI 1640 medium (Invitrogen, Carlsbad, CA, US) supplemented with 10% of heat inactivated fetal bovine serum (FBS), 1% PEST antibiotics and 2 mM L-glutamine. All cells were grown in +37°C 5% CO_2.

Human monocytic leukemia cell line THP-1 (II) was obtained from the American Type Culture Collection (ATCC, US; cat. TIB-202) and grown in RPMI 1640 medium (Invitrogen, Carlsbad, CA, US) supplemented with 1% L-glutamine, 10% FBS (Gibco Life Sciences, Carlsbad, CA, US), 1% HEPES (Lonza, Basel, Switzerland), 1% PEST, 1% non-essential amino acids (Lonza, Basel, Switzerland) and 0.05 mM 2-mercaptoethanol (Lonza, Basel, Switzerland). Monocytes were differentiated to macrophages, by culturing the THP-1 cells for 48 h in the standard culture medium supplemented with 100 nM phorbol 12-myristate 13-acetate (PMA; Sigma-Aldrich, St. Louis, MO). In the ROS assays, the cells were seeded into 24-well plates in concentration of 2.5 × 105 / well

3.3. Cell Exposure Protocols

3.3.1. In vitro exposure conditions for TEM analysis (I)

Nanomaterials were sonicated for 15 minutes in an ultrasonic bath. Primary macrophages were exposed to either 5 or 300 μg/ml of nanomaterials in Serum-Free Macrophage medium supplemented with 10 ng/ml GM-CSF, 1% PEST and 1% bovine serum albumin (BSA, Sigma-Aldrich, St. Louis, MO, US) and incubated

24 hours in +37°C 5% CO_2. On the next day, the cells were washed two times with PBS (pH 7.4), fixed with 2.5% glutaraldehyde in 0.1 M phosphate buffer and removed from the plate by scraping.

Exposure to epithelial cells was carried out with 5 or 300 μg/ml of sonicated (15 minutes) ENMs in RPMI 16400 medium containing 10% of heat inactivated (FBS), 1% PEST antibiotics and 2 mM L-glutamine. The cells were exposed for 24 hours in +37°C 5% CO_2, washed two times with PBS and removed from the plate by trypsination and fixed with 2.5% glutaraldehyde in 0.1 M phosphate buffer.

After fixation, cells were post-fixed in 1% osmium tetroxide, dehydrated and embedded in epon. Thin sections were collected on uncoated copper grids, stained with uranyl acetate and lead citrate and then examined with a transmission electron microscope operating at an acceleration voltage of 80 KV (JEM-1220, Jeol Ltd., Tokyo, Japan).

3.3.2. Analysis of Cytoplasmic Proteins (II)

Prior to *in vitro* exposure, a stock suspension was made in glass tubes containing 900 μg/ml nanomaterials in Serum-Free Macrophage medium supplemented with 10 ng/ml granulocyte-macrophage colony-stimulating factor and 1% (V/V) PEST. Bovine serum albumin (BSA, Sigma-Aldrich, St. Louis, MO) was added to a final concentration of 0.6 mg/ml in order to reduce aggregate formation. The stock was sonicated for 20 minutes and diluted to a final concentration of 300 μg/ml in Serum-Free Macrophage medium supplemented with 10 ng/ml GM-CSF and 1% (V/V) PEST for the exposures. Cells were exposed for 24 h in 6-well plates in +37°C 5% CO_2. Serum-Free Macrophage medium supplemented with 10 ng/ml GM-CSF and 1% (V/V) PEST was used as a negative control. After treatment, cells were washed three times with warm DPBS (Dulbecco's Phosphate-Buffered Saline, Gibco Life Sciences, Carlsbad, CA, US) and removed from the plates by trypsination and scraping. The cytoplasmic proteins were enriched with QProteome Mitochondria Isolation Kit (Qiagen, Valencia, CA, US).

3.3.3. Analysis of Secreted proteins (III)

Fiber suspensions for experiments were prepared by weighing the materials into glass tubes and diluting them to 1 000 μg/ml stock solution with 2% fetal bovine serum in phosphate buffered saline (FBS/PBS) which was sonicated for 20 minutes at +30°C in a water-bath. The stock solution was further serially diluted to a final concentration of 100 μg/ml in Serum-Free Macrophage medium and again sonicated for 20 minutes at 30°C just before cell exposures.

Old media was carefully removed and replaced with new media containing 100 μg/ml fibers. Macrophages were allowed to ingest materials for two hours. The cells were washed twice with DPBS and incubated for 4 h with RPMI-1640 with supplemental 1% PEST and L-glutamine before supernatant collection. Each macrophage sample represented a pool of separately stimulated cells from three different blood donors. Four independent repeat experiments were performed.

3.4. Determination of Radical Production (II)

The effect of r/aTiO_2 and rTiO_2 silica nanoparticles on ROS generation was assessed both in THP-1 cells and in the cell-free environment. 2',7'-Dichlorofluorescein diacetate (DCFH-DA, Calbiochem, Germany) was used to detect intracellular ROS production. After DCFH-DA crosses cell membrane, it is de-esterified to non-fluorescent 2',7'-dichloridihydrofluorescin (DCFH), which is unable to pass cell membranes and therefore stays in the cells. DCFH is oxidized to intracellular, fluorescent 2',7'-Dichlorofluorescein (DFC) by reactive oxygen species (LeBel et al., 1992; Jacobsen et al., 2008). In addition, in the cell free environment, DCFH-DA can be chemically hydrolyzed with 0.01 M NaOH to DCFH in order to measure materials' radical production ability (LeBel et al., 1992).

In the measurements THP-1 cells were seeded into 24-well plates (Wallac Visiplate, PerkinElmer, Belgium). Two washes with PBS were performed and DCFH-DA (0.01 mM diluted to PBS) was added to the cells for 1 h. Excess DCFH-DA was washed away with PBS followed by exposure with 3, 30 and 300 μg/ml NP suspensions (in PBS sonicated for 20 minutes) for 3 h with three replicates. A parallel experiment using DCFH was performed in cell-free environment (two replicates) and appropriate unlabelled controls were included to experiments. DFC was determined at λex 490 and λem 520 nm on a fluorescence spectrophotometer (Victor Wallac-2 1420, Perkin Elmer, Belgium). H_2O_2 (500 mM) was used as a positive control. The results were calculated as H_2O_2 concentrations [nM] using equation: H_2O_2 [nM] = 0.0004 × fluorescence -86.

3.5. Analysis of Cell Death (III)

The percentage of dead cells was analyzed by Cytotoxicity Detection KitPLUS (Roche Diagnostics GmbH, Mannheim, Germany) according to the manufacturer's instructions and the absorbance was determined at 490 nm with reference wavelength of 690 nm on spectrophotometer (Victor Wallac-2 1420, Perkin Elmer, Belgium). The percentage of apoptotic cells was studied with APOPercentage Apoptosis Assay (Biocolor Life Science Assays, Carrickfergus, UK) according to the instructions given by the manufacturer. Treated cells were photographed

with an Olympus DP70 Digital microscope camera connected to an Olympus IX71 (Olympus, Center Valley, PA) light microscope using DP Controller (version 2.2.1.227) (Olympus, Center Valley, PA) and DP Manager (version 2.2.1.195) software (Olympus, Center Valley, PA). The purple (apoptotic) and unstained (non-apoptotic) cells were counted manually, and the percentage of apoptotic cells was calculated.

3.6. Protein-nanomaterial interaction experiments (I)

The method for analysis of protein-ENM interaction was modified from MacCorkle et al. (2006). Cells (primary macrophages or epithelial cells) were collected, frozen and lysed with ME lysis buffer (1% Nonidet P40, 0.5% sodium deoxycholate, 80 mM MOPS, 2 mM EDTA pH 7.2) containing a protease inhibitor (Complete Mini, Roche Diagnostics GMBH, Mannheim, Germany) for 20 minutes on ice. Cell lysate (~1 mg protein/ml) was cleared by centrifugation (16 000 g, 5 minutes, +4°C) and exposed to sonicated (15 minutes) ENMs in ME lysis buffer. Final nanomaterial concentrations of 0.5, 0.05 or 0.005 mg/ml were used for the interaction experiments. Alternatively, diluted human plasma in ME buffer (~7 mg protein/ml) or undiluted plasma (70 mg protein/ml) was used. Protein concentrations of samples were determined with BioRad DC Protein Assay Kit (BioRad, Hercules, CA, US) according to the manufacturer's instructions. In order to avoid unspecific adsorption of proteins onto the walls of the test-tubes, low protein binding tubes were used (Protein LoBind tube, Eppendorf AG, Hamburg, Germany). Nanomaterial-cell lysate/plasma mixture was incubated at +4°C for 15 hours (or also one hour for plasma) in an end-to-end rotator (Grant-Bio PTR-30, Wolf Laboratories Limited, UK), after which nanomaterials were pelleted and unbound proteins were removed by washing the pellet six times with 20 mM Tris-MOPS, pH 7.4. After each wash, the nanomaterials were gently vortexed and centrifuged (16 000 g, 5 min, +4°C). ENM-bound proteins were removed from the nanomaterials by heating for 10 min at +70°C in 50 µl reducing sample buffer and analyzed in SDS-PAGE. Gels were stained with Coomassie blue dye. The gels were scanned and intensities of Coomassie stained protein bands were calculated with ImageQuant TL (GE Healthcare, Piscataway, NJ, US) software to quantify protein binding to the nanomaterials. Protein band intensities were compared to the intensity of a protein band with a known amount of protein analyzed in the same SDS-PAGE gel. Statistical analyses of were performed using GraphPad Prism 4 software (GraphPad Software, La Jolla, CA, US).

The effect of surfactant on protein-ENM interactions was studied by incubating natural porcine lung surfactant mixture (Curosurf®, Nycomed International Management GmbH, Zurich, Switzerland) with sonicated nanomaterials in ME

buffer (final concentration 1.2 μg/ml). After 15 minutes A549 epithelial cell lysate was added to the mixture. Incubation and analysis were performed as described above.

For protein-ENM interaction studies with cytoplasmic proteins, cytoplasm was extracted from primary macrophage cells with (ProteoJet Cytoplasmic™ and Nuclear Protein Extraction Kit, Fermentas International Inc, Burlington, ON, Canada) and mixed with sonicated nanoparticles in ME lysis buffer (final nanoparticle concentration 0.5 mg/ml) for 15 hours at +4°C in an end-to-end rotator. Removal of unbound proteins and analysis of bound proteins were carried out as described above.

The effect of pH on nanomaterial binding to proteins was studied with rTiO_2 coarse and r/aTiO_2 particles. A volume of 200 μl of cleared primary macrophage-cell lysate was exposed to 100 μl of sonicated particles (5 mg/ml) in ME lysis buffer and to 700 μl of different pH buffers. Binding of particles to proteins was analyzed as previously described. Buffers were: pH 6 (250 mM sodium acetate), pH 7.2 (ME lysis buffer) and pH 9 (100 mM Tris-HCl).

3.7. 2-D Difference Gel Electrophoresis (DIGE) (II and III)

Prior to DIGE labelling, salts and other contaminants were removed from the samples with 2-D Clean-Up Kit (GE Healthcare Biosciences, Pittsburgh, PA, US) and samples were resuspended in DIGE labelling buffer (7 M urea, 2 M thiourea, 30 mM tris-HCl, 4% (w/V) CHAPS). A total of 50 μg of protein per sample was used for analysis. DIGE minimum labelling was performed according to the manufacturer's instructions [Amersham CyDye DIGE fluors (minimal dye) for Ettan DIGE, GE Healthcare Biosciences, Pittsburgh, PA, US]. Internal standard was used to align the spots during analysis and to decrease technical variation. 18 cm pH interval 3-10 non-linear Immobiline™ DryStrips (IPG strips) (GE Healthcare Biosciences, Pittsburgh, PA, US) (II) / 18 cm SERVA IPG Blue strips 3-10 NL (SERVA Electrophoresis GmbH, Heidelberg, Germany) (III) were rehydrated for 6 hours and cup loading method was used to absorb proteins to the IPG strips. Each IPG strip was loaded with 50 μg of sample labelled with Cy5, 50 μg of sample labelled with Cy3 and 50 μg of internal standard, containing equal amount of all samples, labelled with Cy2. Isoelectric focusing (IEF) was performed with the Ettan IPGphor IEF system (GE Healthcare Biosciences, Pittsburgh, PA, US) and the second dimension separation of proteins by their size with polyacrylamide gel electrophoresis (SDS-PAGE) (Ettan DALTsix Electrophoresis Unit (GE Healthcare Biosciences, Pittsburgh, PA, US). After electrophoresis, the fluorescence of all three CyDyes was detected with Ettan DIGE Imager (GE Healthcare Biosciences, Pittsburgh, PA, US) and gels were then silver stained (Chevallet et al., 2006) for spot excision. DeCyder 2-D Differential Analysis Software v.7.0 (GE Healthcare

Biosciences, Pittsburgh, PA, US) was used for the spot detection, matching and statistical analysis. Spots with ≥ |1.5| fold change in expression compared to control, with Student's *t*-test *p*-values ≤ 0.01 (II) and ≤ 0.05 (III) were utilized for identification by mass spectrometry.

3.8. Protein identification and bioinformatics (I, II and III)

Coomassie (I) or silver (II and III) -stained protein bands (I) or spots (II and III) were cut from the gel, in-gel digested and the resulting peptides were extracted as previously described by Rostila and collaborators (2012). Peptide extracts were pooled and dried in a vacuum centrifuge. Each peptide mixture was analyzed by automated nanoflow capillary LC–MS/MS using a CapLC system (Waters, Milford, MA, USA) coupled to an electrospray ionization quadrupole time-of-flight mass spectrometer (Q-TOF Global, Waters). Reverse-phase separation of peptides was carried out using a 75 μm × 15 cm NanoEase Atlantis® dC18 column (Waters) at a flow rate of 250 nl/min. The peptides were eluted from the column with a linear gradient of 0–60% solvent B (0.1% formic acid in 95% acetonitrile) in 60 minutes. Solvent A was 0.1 % formic acid in 5 % acetonitrile. The obtained mass fragment spectra were searched against human entries [NCBInr (I) or SwissProt (II and III)] using Mascot software (Matrix Science Ltd., London, UK). Isoelectric point (pI) values were calculated from the nominal masses of protein hits in Mascot search. Information on post-translational modifications and gene ontology were gathered from the UniProt Protein knowledgebase (www.uniprot.org).

Hierarchical clustering and principal component analysis were performed for the identified proteins with DeCyder Extended Data Analysis software (GE Healthcare Biosciences, Pittsburgh, PA, US) (II).

In publication III, Cy2 standardized intensity values were exported from DeCyder and imported to R software version 3.0.0 (R Core Team 2013). Differentially secreted proteins were tested by the limma package (Smyth et al., 2012) implemented in bioconductor (Gentleman et al., 2004). First, a linear model (y ~ treatment + labeling + error) was fitted. Subsequently, pairwise comparisons between each treatment and control were evaluated by empirical Bayes and the proteins with the nominal P-value <0.01 were considered significant. In addition, proteins with ≥|1.5| fold change in expression as compared to control, with student's t-test P-value ≤0.05 were selected for DAVID analysis.

DAVID bioinformatics resources (http://david.abcc.ncifcrf.gov/) were used to identify enriched protein functional domains, gene ontologies or pathways in the identified proteins (Huang da et al., 2009) (II and III). Protein theoretical molecular weights and isoelectric points were calculated with ExPASy Compute MW/pI Tool (Gasteiger et al., 2005) (II).

3.9. Western Blotting (II and III)

Validation of interesting identified proteins was performed by Western blotting. About 3 µg cytoplasm proteins were loaded into precast 26-well 10-20% Criterion TGX gels (BioRad, Hercules, CA, US) and separated at 200 V for 50 min using Criterion Cell (BioRad, Hercules, CA, US) in Laemmli buffer. Proteins were the transferred onto Immobilion-P Transfer Membranes (Merck Millipore, Bedford, MA, US) at 300 mA for 2 h + 4°C with Criterion Blotter (BioRad, Hercules, CA, US). Sypro Ruby Protein Blot staining (BioRad, Hercules, CA, US) was performed according to the manufacturer's instructions in order to visualize the full protein content in the membranes.

Following primary antibody dilutions were used: 1:1000 for ANXA2 (ab54771, Abcam plc, Cambridge, UK), CATD (ab6313, Abcam plc, Cambridge, UK), SODM (HPA001814, Atlas Antibodies, Stockholm, Sweden), PRDX1 (HPA007730, Atlas Antibodies, Stockholm, Sweden), 1:500 for CLIC1 (HPA008917, Atlas Antibodies, Stockholm, Sweden) 1:2000 acetylated lysine (#9441, Cell Signaling Technology, Boston, MA, US) (II) 1 :1000 THIO (ab133524, Abcam plc, Cambridge, UK) and 1:1000 for 2AAA (ab154551, Abcam plc, Cambridge, UK) (III). 1:5000 dilution of HRP-conjugated secondary antibody was used (Dako, Glostrup, Denmark). Antibodies were diluted either into 5% non-fat milk in PBS or 0.05% tween-PBS. Immobilion Western HRP substrate (Merck Millipore, Bedford, MA, US) was added to the membranes and antibody stained protein bands were visualized with Image Quant LAS 4000 mini quantitative imager (GE Healthcare Biosciences, Pittsburgh, PA, US). ImageQuant TL (GE Healthcare Biosciences, Pittsburgh, PA, US) was used to analyze the intensities of protein bands.

In the two-dimensional western blots (II), the identities of acetylated protein spots were investigated by overlaying images of membranes detected against acetylation and PRDX1 (or acetylation and ANXA2) on top of each other by using the freeware ImageJ v.1.46 program downloaded from the internet (http://rsb.info.nih.gov/ij/).

4. RESULTS

4.1. Nanomaterial Protein-Corona Formation (I)

Prior to coming into contact with cells and tissues, ENMs are covered with proteins and lipids and this has a pronounced effect on their fate the body. Therefore, we decided to investigate the physicochemical properties governing protein-corona formation, by performing a protein-binding assay with eleven divergent materials.

It was first studied whether ENMs were phagocytized by cells and if so, did this have any effect on cell function. TEM micrographs revealed that all of the tested ENMs were internalized by lung epithelial cells and macrophages. While no materials could be detected in the nucleus, there were differences between the nanomaterial types in their intracellular localization. Most types of ENMs were located only inside vacuolar structures, whereas some material-species were residing both inside vesicles and free in the cytoplasm. These were $aTiO_2$, r/$aTiO_2$, $rTiO_2$ silica, $rTiO_2$ alumina and mwCNT. Only mwCNTs seemed to enter the cells passively by protruding through plasma membrane (I, Figure 1, Supporting Information Figures 1-4).

Protein-binding experiments were carried out using cell lysate proteins, cytoplasmic proteins and human plasma. Cell lysates were obtained from primary macrophages and A549 epithelial cells, while both diluted and undiluted human plasma were tested. Cytoplasm was extracted from primary macrophages. All materials were covered with plasma proteins, but greater differences were be detected in experiments with cell lysate proteins. Hydrophobic $rTiO_2$ silicone and swCNT were the only materials not to interact with cell lysate proteins, while $aTiO_2$, r/$aTiO_2$ and $rTiO_2$ silica were the most efficient binders of both cell lysate and plasma. Similar to $rTiO_2$ alumina, mwCNT and SiO_2, micro-sized particles, $rTiO_2$ coarse and quartz sand, seemed to interact more with plasma proteins than with cell lysate proteins (I, Figure 2A). A slight correlation could be found between particle size and the extent of the plasma protein interaction. This could not be detected with cell lysate proteins, nor could any correlation be detected between protein binding and zeta-potential or specific surface area (I, Supporting Information Figure 5).

Protein interaction studies were continued by coating the ENMs with surfactant prior to contact with cell lysate proteins. This mimics the events during lung exposure, where ENMs would first come into contact with the surfactant layer of the lungs before interacting with cells and tissues. The addition of surfactant reduced substantially the capacity of ENMs to interact with cell lysate proteins. Surfactant had the strongest effect on those materials that were the most efficient binders. Despite having a substantial effect on protein binding, surfactant addition did not change the interacting proteins (I, Figure 2B).

In these experiments, the major plasma proteins attaching to ENMs were the same regardless of the material and incubation time. The major binding proteins were identified by mass spectrometry as fibrinogen alpha, beta and gamma chains and immunoglobulin light chain proteins. In addition, several complement components, fibrinectin, apolipoprotein A, albumin and fibrin were found to be able to interact with the materials. All of the plasma proteins that became attached to ENMs were glycosylated. Conversely, the binding of cell lysate proteins was truly dependent on material species. The three titanium dioxides that were the most efficient protein binders shared major proteins in common, but differences could be detected in the less abundant proteins. Micro-sized rTiO_2 coarse interacted with different proteins than nano-sized titanium dioxides and alumina coated TiO_2 failed to interact significantly with any proteins (I, Figure 2C).

In an attempt to elucidate the mechanisms behind these phenomena, i.e. the possible ENM-protein interactions inside the cell, the materials were allowed to interact with extracted cytoplasmic proteins and the ENM-bound proteins were identified by mass spectrometry. The surface charge of titanium dioxide particles seemed to affect the protein binding - TiO_2 particles with negative zeta-potential, preferred proteins with high pI, having a positive charge at physiological pH, as their interaction partners. ENMs did not exhibit any preference with respect to the cellular function of bound proteins, with the exception of mwCNT, which adsorbed only cytoskeletal proteins. Some preference towards negatively charged calcium binding domains could be detected for analyzed titanium dioxide particles (I, Figures 2D and 3, Supporting Information 9).

The pH can significantly differ between cellular compartments, therefore the effect of pH on protein binding capability of uncoated TiO_2 nanoparticles was investigated. Compared to micro-sized TiO_2, which lost its protein binding ability completely at high pH values, the affinity of nano-sized titania towards cell lysate proteins declined only marginally (I, Figure 4A). Moreover, the nano-sized TiO_2 interacted mainly with unphosphorylated proteins, whereas coarse TiO_2 preferred proteins with multiple phosphorylation sites (I, Figures 4B and 4C).

4.2. Cytoplasmic Proteomic Changes Induced by TiO_2 Nanoparticles (II)

Publication (I) indicated that ENMs are able to enter cells and interact with intracellular proteins. Therefore, we decided to expose human primary macrophages to two of the most efficient protein adsorbers, silica coated $TiO_2$and uncoated TiO_2, and analyze the cytoplasmic protein expression changes using two-dimensional difference gel electrophoresis.

Exposure to TiO_2 nanoparticles resulted in altered expression of 112 proteins

spots (student's *t*-test $p \leq 0.01$, fold change $\geq |1.5|$) (II, Figure 1). Hierarchical clustering illustrated that even though the overall changes in protein expression patterns caused by the two particles were similar, $rTiO_2$ silica induced a more drastic change in the pattern (II, Figure 2A). Principal component analysis revealed that all datasets clustered into their own quadrants, except for one $r/aTiO_2$ dataset, which was located together with the $rTiO_2$ silica datasets (II, Figure 2B). Mass spectrometry was then utilized to identify the 112 protein spots with statistically significant expression changes. Several proteins had been post translationally modified or were proteoforms, since they were identified from more than one spot (Figure 8). As a result, final non-redundant list was obtained with a total of 62 proteins (II, Supplementary material 2).

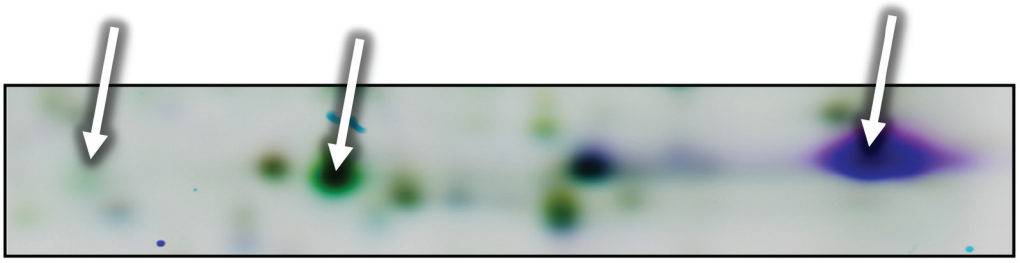

Figure 8. Peroxiredoxin-1 post translational modification after $nTiO_2$ exposure.
Three protein spots, which were all identified as peroxiredoxin-1. The abundance of the purple protein spot was decreased in the macrophage cytoplasm after $nTiO_2$ exposure, while the quantity of the green spots was increased in the cytoplasm of the treated macrophages.

TiO_2 treatment had caused up-regulation of 33 and down-regulation of 29 proteins. Many proteins with changed patterns were linked to cytoskeleton or metabolism, but also responses to stress, inflammation and apoptosis were featured (II, Supplementary material 2). The identified proteins were analyzed with DAVID bioinformatics resources (Huang da et al., 2009) to determine whether some gene ontologies (GO), protein functional domains or biological processes had become enriched. As expected, cytoplasm and GO cytosol were among the most enriched terms associated with the identified proteins, while DAVID analysis also recognized acetylation as a highly enriched PTM: almost 70% of the identified proteins contained possible acetylation sites (Table 6). N-terminal protein acetylation could be detected by mass spectrometry in two down-regulated annexin A2 (ANXA2) spots and in one up-regulated ANXA2 spot, also, one heat shock protein contained lysine acetylation. Other GO terms revealed by DAVID analysis could be grouped into three categories: vesicles/endocytosis, cytoskeleton and metabolism. Protein folding, response to inorganic substance and immune response were also represented although with lower statistical significance (II, Table II).

Table 6. Identified proteins with known acetylation sites

Access.	Protein name	Access.	Protein name
Q01518	Adenylyl cyclase-associated protein 1	P26038	Moesin
P13798	Acylamino-acid-releasing enzyme	Q06830	Peroxiredoxin-1
P52566	Rho GDP dissociation inhibitor 2	P32119	Peroxiredoxin-2
P60709	Actin, cytoplasmic 1	P18669	Phosphoglycerate mutase 1
P63261	Actin, cytoplasmic 2	P60891	Ribose-phosphate pyrophosphokinase 1
P04083	Annexin A1	P17980	26S protease regulatory subunit 6A
P50995	Annexin A11	Q9NVA2	Septin-11
P07355	Annexin A2	P48594	Serpin B4
P78371	T-complex protein 1 subunit beta	P14618	Pyruvate kinase isozymes M1/M2
O00299	Chloride intracellular channel protein 1	P50990	T-complex protein 1 subunit theta
P11413	Glucose-6-phosphate 1-dehydrogenase	P60842	Eukaryotic initiation factor 4A-I
P34932	Heat shock 70kDa protein 4	P06753	Tropomyosin alpha-3 chain
P07900	Heat shock protein HSP 90-alpha	P07437	Tubulin beta chain
P08238	Heat shock protein HSP 90-beta	P54577	Tyrosine--tRNA ligase, cytoplasmic
Q09028	Histone-binding protein RBBP4	P08670	Vimentin
P13796	Plastin-2	P29350	Tyrosine-protein phosphatase non-receptor type 6
P63244	Guanine nucleotide-binding protein subunit beta-2-like 1	P15153	Ras-related C3 botulinum toxin substrate 2
P22626	Heterogeneous nuclear ribonucleoproteins A2/B1	P04179	Superoxide dismutase [Mn], mitochondrial
P31153	S-adenosylmethionine synthetase isoform type-2	Q9Y3Z3	SAM domain and HD domain-containing protein 1
Q13200	26S proteasome non-ATPase regulatory subunit 2	O15144	Actin related protein 2/3 complex, subunit 2

Exposure to nano-sized TiO_2 resulted in an increase of oxidative stress related proteins. Chloride intracellular channel protein 1 (CLIC1) and superoxide dismutase 2 (SODM), linked to redox regulation (Averaimo et al., 2010; Than et al., 2009), were up-regulated after TiO_2 treatment (II, Figures 1 and 3). Annexin A2 (ANXA2) and peroxiredoxin-1 (PRDX1), also involved in the oxidative stress response (Madureira et al., 2011; Sue et al., 2005), were identified from multiple spots. ENM exposure resulted in processing of ANXA2 protein as the up-regulated

ANXA2 spots displayed a distinctly different localization in the gel than the down-regulated ANXA2 spots, which were localized according to their theoretical isoelectric point (pI) and molecular weight (MW). As verified by the combination of mass spectrometry and pI and MW calculations, three down-regulated ANXA2 spots were most probably lacking part of their C-terminal (II, Figures 1 and 3). For the PRDX1 spots, ENM treatment produced a pI shift from basic to acidic side in the gel but did not affect MW (Figure 8; II, Figures 1 and 3). This might be an indication of ROS production in the cells, since the appearance of the acidic PRDX1 spots has been linked to oxidative stress (Rabilloud et al., 2002). The expression of cathepsin D (CATD) (II, Figures 1 and 3) was also increased after TiO_2 treatment. CATD overexpression has been previously reported after asbestos exposure (Sjöstrand et al., 1989).

Western blotting was used to not only validate findings from 2D-DIGE analysis but also to investigate if these protein expression changes were dependent on the particle size, since fine-sized TiO_2 has been claimed to be essentially inert. The cytoplasmic protein levels of SODM and CLIC1 detected with antibodies concurred with the 2D-DIGE results (II, Figure 4). The amount of the 48 kDa single-chain intermediate of CATD could be confirmed by western blotting. Similarly, the amount of mature 34 kDa CATD was also elevated after $nTiO_2$ treatment, however not in a statistically significant manner (II, Figure 4C). SODM expression was not size-dependent as coarse TiO_2 particles were able to induce similar protein levels changes to nano-sized TiO_2 (II, Figure 4A). However, the $rTiO_2$ coarse particles did not cause elevated expression of CLIC1 and CATD, i.e. the differential expression of these proteins only occurred after exposure to nano-sized TiO_2 (II, Figure 4B and 4C). Interestingly, A549 epithelial cells exposed under the same conditions to the same materials did not exhibit similar expression of SODM, CLIC1 and CATD to macrophages (data not shown).

Acetylation was a highly enriched PTM in the identified proteins according to DAVID analysis (Table 6; II, Table II). In addition, the functions of both ANXA2 and PRDX1 have been reported to be affected by acetylation (Parmigiani et al., 2008; Nazmi et al., 2012). Therefore, we decided to examine the overall lysine acetylation of cytoplasmic proteins after exposure to nano-sized and coarse TiO_2 with western blotting. A statistically significant difference could be observed in the amount of lys-acetylated proteins after exposure to both $nTiO_2$s, whereas the levels of lys-acetylated cytoplasmic proteins in coarse TiO_2 treated cells were not significantly elevated (II, Figure 4D).

4.3. The effects of carbon nanotube exposure to protein secretion of macrophages (III)

The logical continuum after investigating intracellular proteome changes induced by nano-sized TiO_2 was to study the changes occurring in protein secretion by human primary macrophages after ENM exposure. 2D-DIGE was again utilized. This time, long rigid (R CNTs) and long tangled multi-walled carbon nanotubes (T CNTs) were used as the exposure agents, while crocidolite asbestos, a well-studied high aspect ratio fibrous material, was used as the positive control. This study set-up made it possible to assess nanomaterial safety taking both size and shape into account.

Prior to 2D-DIGE analysis, a pilot study was performed by exposing macrophages for 6 and 18 hours to the materials. Cell death and protein secretion were investigated to determine the appropriate duration of the exposure. On that basis an exposure time of six hours was selected. 2D-DIGE analysis and identification of secreted proteins was then followed by a bioinformatics analysis (III, Figure 1). R CNT exposure resulted in changed secretion of 37 protein spots (empirical Bayes nominal P-value < 0.01), when compared to the secretome of unexposed macrophages. T CNT treatment altered the secretion of 12 and asbestos changed 5 protein spots. After mass spectrometry and database searches, a total of 29 different proteins were identified (III, Figure 2, Supplementary material S2).

Hierarchical clustering and PCA analysis revealed that the secretome profiles of R CNT and asbestos exposed macrophages resembled each other, while the T CNT secretome had a distinct profile (III, Figure 3). However, the Venn diagram indicated that the R CNT and asbestos groups shared only 4 proteins, while T CNT and R CNT shared 5. No common secreted proteins were found between all exposure groups, this was also the apparent in the comparison between asbestos and T CNT groups. R CNT treatment triggered the release of 28 unique proteins from the macrophages. The numbers of unique secreted proteins after T CNT and asbestos exposures were seven and one, respectively (III, Figure 4).

When looking more closely at the secretion levels of individual proteins after different fiber treatments, it became evident the proteins could be categorized into three different groups. In the first group, the proteins were secreted most efficiently after R CNT treatment. This group included lysosomal cathepsins, cathepsin B (CATB, mature 30 kDa), CATD (mature 34 kDa), and cathepsin H (CATH, mature 25 kDa). In addition, cofilin-1 which is linked to restraining phagocytosis and oxidative stress (Morato-Marques et al., 2011) and several inflammation-related proteins were also categorized in the first group, i.e. cystatin-B (CYTB), Peptidyl-prolyl cis-trans isomerase A (PPIA) and heat shock protein beta-1 (HSPB1) (Turk and Bode, 1991; Rodriguez-Franco et al., 2012; Sherry et al., 1992; Gwinn et al.,

2006; Arrigo, 2007) (III, Figure 5A). The second group comprised of proteins with decreased secretion from macrophages after R CNT exposure. Calreticulin (CALR), expressed in the surface of apoptotic cells (Raghavan et al., 2013) and superoxide dismutase 2 (SODM) which has a role in redox homeostasis and in inflammation (Than et al., 2009) fell into this group (III, Figure 5B). The third group included three proteoforms of serine/threonine-protein phosphatase 2A 65 kDa regulatory subunit A alpha isoform (2AAA), which has been also linked to inflammation (Wallace et al., 2012). This protein was only secreted after T CNT treatment (Figure 5C). 2AAA secretion could be also validated with western blotting (III, Supplementary material S3).

The identified proteins were then analyzed with DAVID to clarify the enriched pathways and GOs. Since DAVID is not able to analyze small protein lists reliably, a more lenient statistical test (student's *t*-test $p < 0.05$, fold change $\geq |1.5|$) was used to produce a larger list (III, Supplementary material S4). The most evident enriched KEGG pathway was lysosome, consisting of CATB, CATD, CATH and CATS, and this was detected after exposure to all materials. In contrast, antigen processing and presentation were not enriched after T CNT treatment (III, Supplementary materials S5 and S6). Lysosome was the only enriched term in the T CNT secretome, whereas the asbestos secretome included lysosome, vesicles and cellular response to stress. Again, R CNTs seemed to cause the greatest activation in macrophages: apoptosis, endoplasmic reticulum, inflammatory response, protease inhibition, redox-active center, signaling, lysosome and vesicles were all enriched after R CNT treatment (III, Supplementary materials S5 and S6).

Since DAVID analysis revealed that apoptosis related proteins were enriched only in the R CNT secretome (III, Figure 6A), the effects of fibers to cell viability were investigated by using two different methods: LDH, which detects general cell death and ApoPercentage, which identifies only apoptotic cells. LDH assay revealed that 5-10% of the cells died after six hour treatments with R CNT and asbestos (III, Figure 6B). ApoPercentage assay yielded similar results to DAVID analysis: only R CNT triggered apoptosis to macrophages, with 10% of the cells being in apoptosis after 18 h (III, Figure 6B, 6C and 6D).

4.4. Comparison of the effects of $nTiO_2$s and CNTs on macrophages (II and III)

Even though the two DIGE experiments differ from each other in the exposure time (24 h vs. 6 hours) and in the studied protein fraction (cytoplasm vs. secretome), the R CNTs seemed to be the most hazardous ENM to primary macrophages. Both $nTiO_2$ species seemed to cause similar changes in the cytoplasmic proteome of macrophages: several proteins with changed abundance were related to

phagocytosis and cytoskeleton (II, Supplementary material 2). Some proteins with changed abundances after exposure to $nTiO_2$ were linked to oxidative stress, however cellular and acellular ROS measurements indicated that neither of the $nTiO_2$s were capable of triggering oxidative stress (II, Supplementary material 5). Of the fibrous materials, only R CNT was capable of causing extensive cell death and apoptosis to macrophages (III, Figure 6). In addition, R CNT triggered the most prominent secretion of lysosomal cathepsins and inflammation related proteins (III, Figure 5). When comparing all the ENMs, the DAVID analysis indicated that cell death associated proteins were enriched only in the secretome of R CNT exposed macrophages (Table 7).

Table 7. Comparison of the ten most enriched terms associated to the identified proteins after exposure to ENMs. *Data obtained from DAVID functional annotation chart.*

$nTiO_2$ (cytoplasmic)	**T CNT (secreted)**	**R CNT (secreted)**
acetylation	acetylation	acetylation
cytoplasm	cysteine proteinase	cytoplasm
cytosol	Peptidase C1A, papain C-terminal	enzyme inhibitor activity
melanosome	Peptidase C1A, papain	regulation of apoptosis
pigment granule	Pept_C1	regulation of programmed cell death
phosphoprotein	papain	regulation of cell death
structural constituent of cytoskeleton	soluble fraction	acetylated amino end
nucleotide-binding	Peptidase, cysteine peptidase active site	disulfide bond
acetylated amino end	zymogen	calcium binding
soluble fraction	Protease	disulfide bond

5. DISCUSSION

Engineered nanomaterials are already a part of our everyday life. They are used in a multitude of products, such as coatings, paints and electronics, where consumers do not come into direct contact with them. However, ENMs are also added in food and cosmetics, even used as drug carriers – meaning that some ENMs are able interact with human body. Therefore, in order to ensure that the benefits of ENMs can be fully realized, the health effects of ENMs must be thoroughly studied. Proteomics is a new strategy for nanosafety investigations. Proteomic methods aim to detect and quantify the proteins that are expressed in cells, tissues or biofluids at a certain time point. Today, proteomic experiments are able to identify thousands of proteins, making it possible to identify activated and attenuated processes and cascades after a given stimulus. Moreover, protein post translational modifications can be detected, which adds another information layer to the data obtained from proteomic exercises. In this thesis, proteomics was utilized to characterize the biological effects of ENMs. We found that the surface activity of ENMs is a key factor governing ENM-protein interactions. Furthermore, the binding of ENMs to cytoplasmic proteins might trigger adverse effects to cells. Results also showed that macrophages exposed to nano-sized TiO_2 undergo cytoplasmic proteome changes attributable to active ENM uptake and processing and that $nTiO_2$ treatment triggers acetylation of cytoplasmic proteins. Moreover, we found that rigid CNTs and asbestos exposure causes similar protein secretion from macrophages, while tangled CNTs inflict a distinct response. R CNT treatment also triggered apoptosis in macrophages, which was not observed in T CNT and asbestos exposed cells.

5.1. ENM-protein interactions (I)

Nanomaterials have been postulated to be covered by proteins thus forming a protein corona on top of the ENM. The vast majority of ENM protein corona studies have investigated the interactions between ENMs and plasma proteins (Monopoli et al., 2011; Tenzer et al., 2013; Cedervall et al., 2007; Göppert and Muller, 2005; Tenzer et al., 2011). The ENM-lipid corona has also been investigated. One study revealed that high density lipoproteins, namely apolipoproteins adhere strongly to copolymer nanoparticles (Hellstrand et al., 2009), while another study found that swCNTs were coated with apolipoproteins and surfactant proteins (Kapralov et al., 2012). Data from our study indicated that certain TiO_2 nanoparticles bind significantly more plasma proteins than other ENMs. The major proteins forming the plasma corona for ENMs were fibrinogen alpha, beta and gamma chain and immunoglobulin light chain. In contrast to the results by Jung and collaborators

(2003), we did not observe fibrinogen replacement from silica surface by other plasma proteins. One reason could be that structural changes had occurred in protein domains. In agreement with the plasma corona data, many common proteins, such as complement C4-A, complement factor H, and Ig mu chain C region have been found in other plasma protein corona studies. However, these reports did not describe fibrinogen as being the major adhering protein, while also reporting apolipoprotein A-I as a significant interacting protein (Tenzer et al., 2013; Tenzer et al., 2011; Lundqvist et al., 2011). These differences might be due to different exposure conditions such as the buffer used in the interactions. Albumin is another commonly reported high abundance protein adhering with ENMs, which was present only at low quantities in our studies. This might be explained by long interaction time used here (15 h), since Tenzer and collaborators (2013) reported that albumin can be gradually replaced by other proteins from the surface of some ENMs over the time (0.5 - 120 minutes).

When ENM interactions with cytoplasmic proteins were analyzed, the same $nTiO_2$ species were binding most proteins, while other ENMs bound cytosolic proteins even less than plasma proteins. This is an indication that the formation of the plasma protein corona is an active process involving recognition and tagging of foreign molecules by opsonins such as fibrinogen, immunoglobulins and complement components (Walkey and Chan, 2012). In contrast, the interactions between cytosolic proteins and ENMs seem to occur by passive reactions influenced by ENM physicochemical properties.

One of the main reasons behind the success of ENM is their easily modifiable surface (Nel et al., 2006). The surface reactivity of these kinds of molecules is dependent upon many characteristics such as solubility, zeta potential, surface area, charge and hydrophobicity. Modifications to the particle surface also alter the surface reactivity of ENMs which critically affects their capacity to interact with proteins. As an example, uncoated anatase and rutile $nTiO_2$ particles interact with cell lysate proteins similarly, while the protein binding of alumina coated $nTiO_2$ particles is hardly detectable. Another clearly distinguishable particle property influencing ENM protein interactions is hydrophobicity, $rTiO_2$ silicone is a good example of this kind of particle since this did not adhere to cell lysate proteins in the present investigations. In contrast, $rTiO_2$ silica and $rTiO_2$ alumina, two ENMs that have similar sizes, zeta potentials, surface areas and phase structures, interact with cell lysate proteins with completely different efficiencies. Thus one must conclude that, solubility, surface area and polyform are not able to explain the protein-ENM interactions observed here. Therefore, while the influence of ENM surface reactivity on protein binding is evident, it is unclear which physicochemical property is the main determinant of protein binding.

If ENMs enter the body via the respiratory system, they first come into contact with lung surfactant (Bakshi et al., 2008; Schleh et al., 2009). Therefore,

we studied how pre-coating the ENMs with lung surfactant would affect the protein corona formation. It was found that, the quantity of adsorbing proteins diminished significantly, however the proteins forming the corona remained the same. This indicates that surfactant molecules merely diminish the ENM surface area available for binding.

Many toxicological effects induced by ENMs have been described to be mediated by ROS generation (Donaldson et al., 2013; Shvedova et al., 2012). However, physical interactions between ENMs and cellular proteins might also create some problems. For example, the binding of asbestos fibers to proteins regulating cytoskeleton organization and mitotic processes has been claimed to cause chromosome instability (MacCorkle et al., 2006). Similarly, the present data reveal that mwCNT fibers can interact with only cytoskeletal proteins such as vimentin. Moreover, ENMs seem to bind to cytosolic proteins involved in metabolism, protein biosynthesis, response to stress and cell differentiation, therefore possibly interfering with many critical cellular functions and the mediating toxicological outcomes through physical interactions.

One possible mechanism of $nTiO_2$ toxicity can be caused by reactivity changes caused by pH. Microscale TiO_2 is being routinely used for extraction of phosphorylated proteins from complex mixtures (Yu et al., 2009). This mechanism is based on the ability of TiO_2 to bind phosphoproteins very efficiently at pH 6. The bound proteins can then be eluted by elevating the pH. In contrast, $nTiO_2$ particles seem to bind proteins by different mechanism since the binding ability decreased only slightly in higher pH. Taken together, the effect of pH on protein ENM interactions is dependent on the particles not the proteins. When ENMs are ingested by phagocytosis they are retained within vesicles, which mature gradually from phagosomes to lysosomes (Canton and Battaglia, 2012). The low pH inside lysosomes might enhance $nTiO_2$ interactions with proteins, possibly leading to lysosomal rupture and the release of ENMs to cytoplasm.

Overall, our results from protein corona studies indicate that surface reactivity of ENMs has a significant role in protein binding, however more studies will be needed to clarify which particle property has the greatest effect on the protein corona. In plasma, however, since most proteins covering ENMs are opsonins, the ENM protein reactions might be a mixture of physicochemical interactions and active tagging of exogenous molecules. Moreover, ENM interactions with cytoplasmic proteins might represent a new source of toxic effects.

5.2. ENM uptake (I)

Several studies have reported that ENMs are internalized by macrophages and lung epithelial cells both *in vitro* and *in vivo* (Rossi et al., 2010b; Shi et al., 2013; Simon-Deckers et al., 2008). Similarly, all ENMs used in the present studies were ingested by phagocytic cells and lung epithelial cells. TEM micrographs revealed that most of the particle species were residing within vacuolar structures, indicating that ENMs might be taken in by phagocytosis or pinocytosis as reviewed by Canton and Battaglia (2012). The only exceptions, circumventing classic endocytic pathways, were individual mwCNTs which seemed to penetrate through the cell membrane and enter cells passively, and this might result in physical damage and makes possible for the fibers to interact with cytoplasmic proteins (Canton and Battaglia, 2012; Kettiger et al., 2013; Dumortier, 2013). ENMs were not detected inside the nucleus in the exposure conditions used here, although it has been postulated as being possible (Unfried et al., 2007).

5.3. Health effects of nano-sized TiO_2 (II)

Previously, nano-sized TiO_2 has been shown to induce various adverse effects both *in vitro* and *in vivo*, ranging from ROS formation to lung inflammation (Rossi et al., 2010a; Rossi et al., 2010b; Shi et al., 2013; Shvedova et al., 2013). Proteomics have been utilized in relatively few studies investigating health effects of the $nTiO_2$ (Gao et al., 2011; Ge et al., 2011; Gonçalves et al., 2010; Tilton et al., 2013). We asked, what are the changes in cytoplasmic protein expression in macrophages treated with silica coated $nTiO_2$ ($rTiO_2$ silica) and uncoated $nTiO_2$ ($r/aTiO_2$), since it was already known that these $nTiO_2$s are present free in the cytoplasm of the macrophages and there they are capable of adsorbing cytoplasmic proteins (I). The enrichment analysis of differently regulated proteins revealed that many proteins are associated with carbohydrate metabolism and cell motion, which was not surprising since the macrophages were seen to be actively engulfing and processing TiO_2 NPs (I).

Several up-regulated proteins (SODM, PRDX1, CLIC1 and ANXA2) after $nTiO_2$ treatment are related to redox homeostasis, indicating that $nTiO_2$s might be evoking oxidative stress, which has been frequently reported as a mediator of ENM toxicity (Palomäki et al., 2011; Shvedova et al., 2012; Li et al., 2013; Sharma et al., 2007; Shvedova et al., 2007). However, acellular and cellular ROS measurements indicated that $rTiO_2$ silica and $r/aTiO_2$ are not able to induce ROS production, implying that up-regulation of these proteins might be due to oxidative burst, a mechanism known to be present in phagocytes for processing ingested material (Shvedova et al., 2012).

Exposing macrophages to nano- and micro-sized TiO_2 induced the up-regulation of superoxide dismutase 2 in the cytoplasm. SODM is known to be up-regulated in oxidative stress and it has been shown to have a tumor suppressor function. This enzyme is located in mitochondrial matrix and it functions as a ROS scavenger by catalyzing the conversion of reactive radicals into H_2O_2 and oxygen (Culotta et al., 2006; Kaminski et al., 2012). SODM production has been also postulated to be activated in antimicrobial defense, protecting immune cells from ROS formation during microbial infection (Rakkola et al., 2007). In agreement with the present results, Taira and collaborators (2006) have reported elevated SODM expression in macrophage-like cells levels after 0.2-0.3 μm TiO_2 exposure. Moreover, Mazzoli-Rocha and others (2010) have claimed that SODM expression is elevated by ROS derived from particulate exposure, further indicating that SODM is a major antioxidant enzyme but is not specific for nanomaterials.

CLIC1 is a metamorphic ion channel which can exist either soluble in the cytoplasm or integrated into membranes. It has been shown to have an effect on phagosome maturation of macrophages (Jiang et al., 2012) and epithelial cell growth and migration (Tung and Kitajewski, 2010). Over-expression of CLIC1 has been described in cancer cells and tissues (Wang et al., 2012a; Wang et al., 2012b). It was observed that cytoplasmic CLIC1 was up-regulated only after exposure to nano-sized TiO_2 which is in contrast to results obtained by Cha and others (2007) showing that levels of CLIC1 were elevated after coarse TiO_2 exposure. The conflicting results might be due to differing cell types (BEAS-2B vs. primary macrophages) and sample fractionation (cell lysate vs. cytoplasmic proteins) used in the experiments or the exposure times, since Cha and collaborators claimed that CLIC1 protein levels returned to baseline after 48 hours.

Cathepsin D, which normally resides in lysosomes, has been reported to be released into the cytoplasm after the oxidative stress induced peroxidation of lysosomal lipids (Castino et al., 2007; Zaidi et al., 2008). Furthermore, permeabilization of lysosome membrane and the subsequent release of CATD into cytoplasm has been postulated to precede the triggering of apoptosis (Benes et al., 2008). Both $nTiO_2$ species induced up-regulation of both single-chain intermediate (48 kDa) and mature (34 kDa) CATD in macrophage cytoplasm. Therefore, the oxidative burst discussed earlier might contribute to permeabilization of lysosomes. It should be noted, though, that no clear signs of apoptosis were detected in the exposed macrophages. Alternatively, $nTiO_2$s themselves might play a role in lysosome rupture by a so-called proton sponge effect. However, this effect has been characterized for cationic ENMs (Nel et al., 2009), whereas $nTiO_2$s used in the present experiments carry negative surface charge.

Peroxiredoxins act as signaling molecules and as H_2O_2 reducing enzymes (Hall et al., 2009). When cells undergo oxidative stress, PRDX1 molecules form

oligomeric complexes, which function as super chaperones, and protect other proteins form degradation (Jang et al., 2004). PRDX1 has been claimed to be up-regulated in several cancers. The elevated expression has been observed both in tissues (Maxwell et al., 2011; Zhang et al., 2009) and in the plasma of the patients (Rostila et al., 2012). Three peroxiredoxin-1 spots were identified to be differentially expressed after $nTiO_2$ treatment. ENM exposure seemed to induce a pI shift to PRDX1, which might be because of acetylation. Acetylation has been claimed to enhance the reducing activity of PRDX1 and to be a way to protect the protein from overoxidation, which results in inactivation of the protein (Parmigiani et al., 2008). Therefore, the pI shift of PRDX1 might be a sign of the need for elevated reducing activity in macrophages, possibly because of extensive phagocytosis of $nTiO_2$.

Annexin A2, a calcium binding protein involved in cell signaling, vesicle transport and cell-cell contacts was also identified in several different protein spots. ANXA2 can also act as a scaffold in membrane-cytoskeleton reorganization (Gerke et al., 2005). The fragmented ANXA2 spots present in our study might originate in the detachment of ANXA2 molecules from membranes, which has been claimed to occur by proteolytic cleavage (Babiychuk et al., 2002). The cleavage and detachment of ANXA2 from the membranes after ENM exposure might cause membrane rearrangement and possibly disturb segregation-dependent cell signaling events.

Acetylation was the only major PTM that appeared to be enriched in macrophages after treatment with $nTiO_2$. Reversible lysine acetylation is known to regulate histones, which are the most well-known proteins affected by acetylation (Pehar and Puglielli, 2013; Choudhary et al., 2009). However, lysine acetylation has been also postulated to control the activity of many proteins linked to cytoskeleton dynamics (Choudhary et al., 2009), metabolic homeostasis (Xu et al., 2013) and protein folding (Choudhary et al., 2009) and degradation (Xiong and Guan, 2012). The general lysine acetylation was elevated in cytoplasmic proteins of macrophages. Moreover, many of the proteins with altered expression after $nTiO_2$ treatment are also regulated by lysine acetylation. Arp2/3 complex subunit, the small rho GDP dissociation inhibitor, vimentin, actin and tubulin are all involved in the regulation of cytoskeleton dynamics (Choudhary et al., 2009), similarly pyruvate kinase (Xiong and Guan, 2012), heat shock protein HSP 90-alpha, ANXA2, SODM, phosphoglycerate mutase 1 (Choudhary et al., 2009), all governed by lysine acetylation, underwent expression changes after $nTiO_2$ exposure. Overall, lysine acetylation might be a distinct result of $nTiO_2$ exposure or another indication of macrophage activation.

5.4. Health effects of carbon nanotubes (III)

Several reports have been published where certain types of carbon nanotubes have induced toxic outcomes *in vitro* and *in vivo* prompting comparisons to asbestos-like effects (Palomäki et al., 2011; Poland et al., 2008; Xiong and Guan, 2012; Takagi et al., 2008). The main reasons behind CNT toxicity have been postulated as being impaired clearance from the lung due to the high aspect ratio of CNTs (Ryman-Rasmussen et al., 2009), impurities leading to ROS formation (Shvedova et al., 2012) and fiber diameter (Gernand and Casman, 2013). Most recently Shvedova and others (2013) reported that swCNTs and carbon nanofibers (CNFs) were able to induce bronchopneumonia and fibrosis one year post-exposure. Disturbingly, large amounts of the materials were still residing in the mice lung after one year. They postulated that CNT toxicity emanated from the chemical composition and surface area.

Inflammation is another clear effect noted after CNT exposure. Activation of NLRP3 inflammasome, a central player in inflammation cascade, has been demonstrated in particle-induced inflammation (Bhattacharya et al., 2009). Related to this, the NLRP3 inflammasome could be shown to be activated in macrophages after exposure to long rigid mwCNTs (R CNTs), whereas long tangled mwCNTs (T CNTs) and asbestos could not (Palomäki et al., 2011). In our experiments, several of the proteins secreted only after R CNT exposure were linked to inflammation, i.e. CYTB, PPIA and HSPB1 (Gwinn and Vallyathan, 2006; Rodriguez-Franco et al., 2012; Salari et al., 2013). For example elevated PPIA levels have been reported in inflamed tissue and in BAL of mice with asthmatic lung inflammation (Gwinn and Vallyathan, 2006). The secretion of these proteins, which occurs from macrophages during their initial response against foreign molecules, together with already proven inflammasome activation is an indication that there is the onset of inflammatory responses after R CNT exposure.

All materials activated lysosome pathway in macrophages according to DAVID analysis, but only asbestos and R CNT were able to trigger expression of those proteins related to antigen processing and presentation. This in contrast to work conducted by Tilton et al. (2013) who reported that antigen presentation was activated in THP-1 and SAE cells after exposure to tangled CNT and TiO_2 nanobelts. Most probably cell lines react to stimuli with different sensitivities. DAVID analysis was also different able to reveal that only R CNT treatment induced secretion of apoptosis related proteins and this could be verified by the functional validation. Apoptosis and necrosis, which are believed to occur at the onset of silicosis, have been demonstrated in crystalline silica exposed cells (Joshi and Knecht, 2013). Therefore, apoptosis might be a potential mediator of R CNT induced toxicity.

Macrophages secreted lysosomal cathepsin B and pro-cathepsin H after exposure to all materials. However, asbestos and R CNT treated macrophages secreted also large amounts of cathepsin D and cathepsin S, which were not secreted by T CNT exposed cells. This might indicate that rigid fibers evoke more severe lysosomal damage, since the leakage of lysosomal proteins is linked to lysosomal rupture which, in turn, can initiate inflammatory reactions (Strowig et al., 2012). In agreement with this hypothesis, lysosomal damage and subsequent NLRP3 inflammasome activation have been observed in R CNT and asbestos exposed macrophages but not in T CNT treated (Palomäki et al., 2011). A hallmark of NLRP3 inflammasome activation is secretion of the IL-1 family cytokines; NLRP3 inflammasome activates caspase-1 which cleaves pro-IL-1 family cytokines into mature cytokines which are then secreted. At the same time, NLRP3 regulates pyroptosis which is a distinct form of programmed cell death. Cells undergoing pyroptosis release their contents and trigger pro-inflammatory effects in the surrounding tissue (Strowig et al., 2012; Bergsbaken et al., 2009). While IL-1 family cytokines were not detected in the present exposures, activation of NLRP3 inflammasome cannot be ruled out since secretion of IL-1 family cytokines is dependent upon an activation step, usually performed by LPS (lipopolysaccharide) treatment, which was not conducted in the present experiments. Moreover, R CNT induced LDH leakage from macrophages after 18 hours - which can occur in both necrosis and pyroptosis (Bergsbaken et al., 2009). Therefore, one cannot exclude the possibility that R CNT induced toxicity, for example as encountered in the severe inflammation in mice lung, is due to pyroptosis.

5.5. Key points observed in the experiments

r/aTiO_2 and rTiO_2 silica interacted similarly with cytoplasmic proteins, while the most toxic ENM, R CNT, did not adhere with proteins at all (Data not shown), suggesting that ENM-protein interactions are not the cause of ENM health effects at least in these experiments. However, the protein binding capability of R CNTs was not investigated in lower pH, the environment inside the lysosomes. 2D DIGE analysis showed that silica coated nTiO_2 and uncoated TiO_2 evoked similar proteome changes to macrophages, while in *in vivo* experiments silica coated nTiO_2 was the only material capable of triggering neutrophilia in mice lung (Rossi et al., 2010b), therefore the macrophages might not play a crucial role in the lung inflammation caused by rTiO_2 silica.

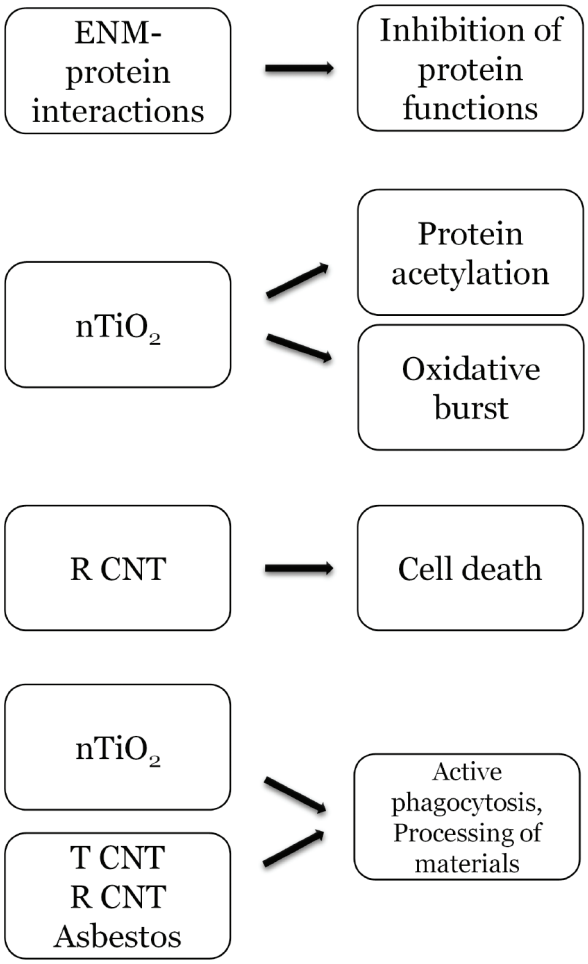

Figure 9. Summary of the observed biological effects caused by tested materials.

There were no clear similarities in the effects induced by $nTiO_2$ exposure and CNT exposure, which is most probably because the analyzed protein fractions were different in the experiments. The only set of proteins with elevated abundance in both macrophage cytoplasm after $nTiO_2$ treatment and in the secretome after exposure to R CNT, T CNT and asbestos were cathepsins. Since they are lysosomal proteins, the elevation of cathepsin levels might be a sign of lysosomal damage (Strowig et al., 2012). However, only rigid CNT were able to trigger significant cell death, a known consequence of lysosomal rupture (Brunk et al., 1997) (Figure 9).

6. CONCLUSIONS AND FUTURE PERSPECTIVES

In this study, we investigated the effects of ENMs on their journey from the early stages when they enter the body: first focusing on their interactions with plasma and cytoplasmic proteins and then evaluating their effects on crucial cells evoking immune responses.

Upon entering the body, ENMs are immediately covered with biomolecules such as proteins and lipids, forming a corona around the ENMs. We observed that the surface reactivity of ENMs plays a crucial role in protein corona formation, however, the main characteristic determining the protein binding efficiency could not be distinguished. Nonetheless, a difference was detected in the mechanism of corona formation between plasma and cytosolic proteins - plasma protein corona formation seemed to depend on both surface reactivity of ENMs and active protein tagging by opsonin proteins, whereas cytosolic protein interactions were solely surface reactivity dependent. The interactions of ENMs and cytoplasmic proteins might be a mechanism of ENM induced toxicity, impairing normal cellular processes. Since the ENM protein corona plays a crucial role in defining the uptake, toxicity and fate, the analysis of ENM protein interactions should be included in their routine characterization before assessing any other effects.

To gain more information about the first contacts with cells, the entry of ENMs to macrophages and lung epithelial cells was examined with transmission electron microscopy. All materials were internalized by both cell types and ENMs were mainly located inside vesicles. At the same time, it was observed that some portion of $aTiO_2$, $r/aTiO_2$, $rTiO_2$ silica, $rTiO_2$ alumina and mwCNTs appeared to be free in the cytoplasm enabling interactions with cytoplasmic proteins, while mwCNTs were also detected to be protruding through the plasma membrane.

The cytoplasmic proteome changes in the macrophages exposed to silica coated and uncoated TiO_2 revealed that silica coated TiO_2 particles had induced stronger changes in protein expression than uncoated TiO_2s. Most of the protein expression changes were due to prominent phagocytosis, although, signs of oxidative burst and possible oxidative stress could also be detected. Moreover, exposure to $nTiO_2$ triggered acetylation of cytoplasmic proteins. Finally, since macrophages are major effector cells involved in various inflammatory reactions, we analyzed secretome changes of macrophages after stimulation with long rigid mwCNTs, long tangled mwCNTs and crocidolite asbestos. It was observed that R CNT and asbestos treatment resulted in similar protein secretions. The following bioinformatics analyses revealed that the proteins secreted by R CNT exposed macrophages were related to inflammation and apoptosis. One can speculate that the severe toxicity of R CNTs might occur because of lysosome damage, inflammasome activation and, possibly, pyroptosis.

Proteomics proved to be a useful method for evaluating global changes of both intracellular and extracellular proteomes. In addition, large amounts of information on how ENMs modified cellular function could be gathered. Both investigations utilizing 2D-DIGE revealed over 100 differentially regulated proteins and their proteoforms. Moreover, simple proteomic experiments were effective in analyzing the protein corona of different ENMs, providing useful information for estimating how ENMs influence to cells. By utilizing MS-based proteomic methods, even greater proteome coverage and dynamic range would have been achieved. Gel-free proteomics exercises would have also been more readily combined with other systems biology approaches, e.g. transcriptomics.

Since ENMs are highly heterogeneous in their shapes, sizes and surface reactivities, their toxicity is very difficult to predict. Therefore, simple, robust and high-throughput methods capable of screening large numbers of ENMs are needed to map the characteristics which determine possible toxic effects. At present, proteomics is rarely utilized in ENM safety research. Proteomics could provide a high-throughput solution to nanosafety field, since the newest MS-based proteomics assays are able to produce vast amounts of both qualitative and quantitative data. This data could be utilized not only for safety analysis but also for the discovery of novel biomarkers of ENM exposure.

Plenty of research is still needed before all the factors influencing ENM associated risks to living organisms are revealed. However, the information already known should be used in ENM design to control the harmfulness of new nanomaterials. For example, since long and stiff CNTs seem to cause problems, the easiest form of protection from putative adverse effects would be to reduce the fiber length, if possible. Adoption of the safe-by-design principle is imperative in order to ensure the full realization of the potential of ENMs. Another important point to be kept in mind is that while some forms of ENMs seem to be even more hazardous than asbestos, the majority of ENMs appear to be inert and incapable of triggering serious health effects. Therefore, all ENMs must not be deemed dangerous. Nevertheless, since currently the amount of information about the safety of ENMs is limited, the best way to protect the population against possible adverse effects is to minimize the probability of exposure.

7. ACKNOWLEDGEMENTS

This work was performed in the Unit of Systems Toxicology at the Finnish Institute of Occupational Health (FIOH) in Helsinki. I thank Professor Harri Vainio, the director general of FIOH for providing us the excellent research facilities.

I would like to sincerely thank my supervisors, docent Anne Puustinen and Professor Harri Alenius, for giving me a chance to work in such an interesting project. It was a privilege to be involved in the forefront of ENM safety research and I believe that it will have a profound impact on my future. In addition to the science, I thank my supervisors for the being genuinely interested in my future and for providing me help in any matter if needed. However, one thing I still do not understand is how to calculate the points in Mahjong.

I am super grateful to my thesis reviewers, docent Tuula Nyman and Professor Kirsi Vähäkangas, for making this book much better. Your help was indispensable and you have done the hardest work. I hope that you have not suffered from headaches while reading the first version of this thesis. I also thank Ewen MacDonald for efficient and detailed language revision for this thesis.

I thank my co-authors for being flexible, understanding, efficient and professional. I owe my gratitude to Professor Kai Savolainen for being inspiring, available, always positive and for helping me in any given problem. I am so grateful to you, Jaana Palomäki, my closest colleague to whom I could always trust and share all the joys and sorrows, both work related and personal. Most importantly, thank you for being a true friend. Never lose your passion and always believe in yourself! I am also grateful to Niina Ahonen, who taught me the ways of the proteomics lab. I think that I was not always the easiest of pupil but I must say that I can now certainly clean the lab better than most. I thank you also for helping me every time in the lab and giving me good baby advice. I wish to thank Minnamari Vippola for always providing the new EM figures again and again and again and again. I owe my gratitude to Pia Kinaret for the excellent bioinformatics analyses and for all the laughs in the lab and in the KM. And thanks also for selling me Wades bike. I also wish to thank Dario Greco for performing the bioinformatics analyses and for familiarizing us all to bioinformatics. I promise to beat you next time in sushi eating.

I thank all the former and present members of the Unit of Systems toxicology (Ossian Saris, Anna-Mari Walta, Kristiina Sirola, Annina Rostila, Henrik Wolff, Santtu Hirvikorpi, Sari Tillander, Alina Suomalainen, Nanna Fyhrquist, Johanna Kerminen, Päivi Kankkunen, Piia Karisola, Marja-Leena Majuri, Sari Lehtimäki, Terhi Savinko, Sara Vilske, Lea Pylkkänen, Vittorio Fortino, Sandra Söderholm, Päivi Alander, Joonas Koivisto, Joe Ndika, Johanna Vendelin, Olli Laine, Hanna Lindberg, Hannu Norppa and Jarkko Tornaeus). You are the ones who made the incredible atmosphere in the lab. Everyone was supporting each other and had time

to help one another no matter how much in a hurry they were. I can honestly say that I have not had a single morning where I did not want to go to work during my n years at FIOH. That was all because of you. I want to thank you Sampsa Matikainen for all seven scientific discussions and for the 4972 football discussions. It was very nice to get the mind off from the work and discuss something completely different during coffee breaks. Thank you so much Marit Ilves for all the help and for being a great friend. I will never drink tequila with you again. I am grateful to you Maili Lehto for helping me whenever I did not understand something about immunology (that was often) and for being the best roommate. I want to thank you also for all the help for my thesis, you have really helped to make it better. I think that Maili has had to listen to Basso Radio more than the average researcher in our institute. I am grateful to you Elina Välimäki for all the support in the science and also for all the gossiping while changing the media, it was fun. Next, I wish to thank Laura Teirilä for being always super helpful and for your positive attitude which is truly contagious. I thank Elina Rydman for all the help. It was nice to be one of the girls - I will never forget the kysta discussions. I owe my gratitude to Ville Veckman for being an inspirational researcher and offering me great cooking advice. I thank you for always having time to visit the McD when the others were boring. I also wish to thank Esa Vanhala who taught me to operate the TEM, which was incredibly interesting. You always had the time to repair the microscope after I had messed up with the settings. I thank you Juho Miettinen for teaching me most of the molecular biology techniques I know at the Kartsa-lab. I also want to thank Amica for providing me food, especially the siemensekoitus is thanked.

I want to thank all my friends from the real life (Kalle, Antti, Satu, Petri, Lauri, Mäksä, Ida, Toni, Krista, Jähi, Make, Pade, Tiina, Olli, Ile, Aksu, Taru, Janne F, Harri, Ridge, Kossu, Teemu kuusamosta and kuusamo Teemun veli Timppa) for not asking any questions of my work - you would have been bored to death. I am grateful for your support and for all the fun moments: the Pori Jazzes, Åres, Tahkos, Lanzarotes, crayfish parties, beers and the evenings at mäksän faija.

I thank my parents from the bottom of my heart for all the help and support they have given me. You have always been there for me all my life and helped me tremendously during my Master's studies in Jyväskylä, and during my Ph.D studies. I also wish to thank Pirkko, Seppo, Riikka, Ulla and Teemu for their support and all the great moments we have shared. The warmest thanks go to my family Päivi, Aaro and Nano. I thank you Päivi for being so supportive in whatever I do and for being flexible and understanding – I know I am not always the easiest of person. You are my love and my best friend. I thank you Aaro for teaching me how to approach life – you wake up every day with a smile on your face wondering what new and exciting is going to happen today. Everyone should learn from your example. It is amazing how much you learn everyday and you are so much fun to be around.

This work was funded by The Finnish Work Environment Fund (grants 107231 and 110168) and The Academy of Finland.

8. REFERENCES

Aparicio-Bautista, D.I., J.I. Perez-Carreon, N. Gutierrez-Najera, J.P. Reyes-Grajeda, J. Arellanes-Robledo, V.R. Vasquez-Garzon, M.N. Jimenez-Garcia, and S. Villa-Trevino. 2013. Comparative proteomic analysis of thiol proteins in the liver after oxidative stress induced by diethylnitrosamine. Biochim.Biophys.Acta. 1834:2528-2538.

Arrigo, A.P. 2007. The cellular "networking" of mammalian Hsp27 and its functions in the control of protein folding, redox state and apoptosis. Adv.Exp. Med.Biol. 594:14-26.

Aschberger, K., C. Micheletti, B. Sokull-Kluttgen, and F.M. Christensen. 2011. Analysis of currently available data for characterising the risk of engineered nanomaterials to the environment and human health--lessons learned from four case studies. Environ.Int. 37:1143-1156.

Ashburner, M., C.A. Ball, J.A. Blake, D. Botstein, H. Butler, J.M. Cherry, A.P. Davis, K. Dolinski, S.S. Dwight, J.T. Eppig, M.A. Harris, D.P. Hill, L. Issel-Tarver, A. Kasarskis, S. Lewis, J.C. Matese, J.E. Richardson, M. Ringwald, G.M. Rubin, and G. Sherlock. 2000. Gene ontology: tool for the unification of biology. The Gene Ontology Consortium. Nat.Genet. 25:25-29.

Auvynet, C., S. Moreno, E. Melchy, I. Coronado-Martínez, J.L. Montiel, I. Aguilar-Delfin, and Y. Rosenstein. 2013. Galectin-1 promotes human neutrophil migration. Glycobiology. 23:32-42.

Averaimo, S., R.H. Milton, M.R. Duchen, and M. Mazzanti. 2010. Chloride intracellular channel 1 (CLIC1): Sensor and effector during oxidative stress. FEBS Lett. 584:2076-2084.

Babiychuk, E.B., K. Monastyrskaya, F.C. Burkhard, S. Wray, and A. Draeger. 2002. Modulating signaling events in smooth muscle: cleavage of annexin 2 abolishes its binding to lipid rafts. Faseb j. 16:1177-1184.

Bakshi, M.S., L. Zhao, R. Smith, F. Possmayer, and N.O. Petersen. 2008. Metal nanoparticle pollutants interfere with pulmonary surfactant function *in vitro*. Biophys.J. 94:855-868.

Benes, P., V. Vetvicka, and M. Fusek. 2008. Cathepsin D--many functions of one aspartic protease. Crit.Rev.Oncol.Hematol. 68:12-28.

Bergsbaken, T., S.L. Fink, and B.T. Cookson. 2009. Pyroptosis: host cell death and inflammation. Nat.Rev.Microbiol. 7:99-109.

Bermudez, E., J.B. Mangum, B.A. Wong, B. Asgharian, P.M. Hext, D.B. Warheit, and J.I. Everitt. 2004. Pulmonary Responses of Mice, Rats, and Hamsters to Subchronic Inhalation of Ultrafine Titanium Dioxide Particles. Toxicol.Sci. 77:347-357.

Bertini, R., O.M. Howard, H.F. Dong, J.J. Oppenheim, C. Bizzarri, R. Sergi, G. Caselli, S. Pagliei, B. Romines, J.A. Wilshire, M. Mengozzi, H. Nakamura, J. Yodoi, K. Pekkari, R. Gurunath, A. Holmgren, L.A. Herzenberg, L.A. Herzenberg, and P. Ghezzi. 1999. Thioredoxin, a redox enzyme released in infection and inflammation, is a unique chemoattractant for neutrophils, monocytes, and T cells. J.Exp.Med. 189:1783-1789.

Bhattacharya, K., M. Davoren, J. Boertz, R.P. Schins, E. Hoffmann, and E. Dopp. 2009. Titanium dioxide nanoparticles induce oxidative stress and DNA-adduct formation but not DNA-breakage in human lung cells. Part.Fibre Toxicol. 6:17-8977-6-17.

Bondarenko, P.V., D. Chelius, and T.A. Shaler. 2002. Identification and relative quantitation of protein mixtures by enzymatic digestion followed by capillary reversed-phase liquid chromatography-tandem mass spectrometry. Anal.Chem. 74:4741-4749.

Brouwer, D.H. 2012. Control banding approaches for nanomaterials. Ann.Occup. Hyg. 56:506-514.

Brunk, U.T., H. Dalen, K. Roberg, and H.B. Hellquist. 1997. Photo-oxidative disruption of lysosomal membranes causes apoptosis of cultured human fibroblasts. Free Radic.Biol.Med. 23:616-626.

Canton, I., and G. Battaglia. 2012. Endocytosis at the nanoscale. Chem.Soc.Rev. 41:2718-2739.

Castino, R., N. Bellio, G. Nicotra, C. Follo, N.F. Trincheri, and C. Isidoro. 2007. Cathepsin D–Bax death pathway in oxidative stressed neuroblastoma cells. Free Radical Biology and Medicine. 42:1305-1316.

Cedervall, T., I. Lynch, S. Lindman, T. Berggård, E. Thulin, H. Nilsson, K.A. Dawson, and S. Linse. 2007. Understanding the nanoparticle-protein corona using methods to quntify exchange rates and affinities of proteins for nanoparticles. Proc.Natl.Acad.Sci.U.S.A. 104:2050-2055.

Cha, M., T. Rhim, K.H. Kim, A. Jang, Y. Paik, and C. Park. January 2007. Proteomic Identification of Macrophage Migration-inhibitory Factor upon Exposure to TiO_2 Particles. Mol.Cell.Proteomics. 6:56-63.

Chaudhry, Q., M. Scotter, J. Blackburn, B. Ross, A. Boxall, L. Castle, R. Aitken, and R. Watkins. 2008. Applications and implications of nanotechnologies for the food sector. Food.Addit.Contam.Part A.Chem.Anal.Control.Expo.Risk Assess. 25:241-258.

Chevallet, M., S. Luche, and T. Rabilloud. 2006. Silver staining of proteins in polyacrylamide gels. Nat.Protocols. 1:1852-1858.

Choi, H., D. Ghosh, and A.I. Nesvizhskii. 2008. Statistical validation of peptide identifications in large-scale proteomics using the target-decoy database search strategy and flexible mixture modeling. J.Proteome Res. 7:286-292.

Choudhary, C., C. Kumar, F. Gnad, M.L. Nielsen, M. Rehman, T.C. Walther, J.V. Olsen, and M. Mann. 2009. Lysine Acetylation Targets Protein Complexes and Co-Regulates Major Cellular Functions. Science. 325:834-840.

Coombs, K.M. 2011. Quantitative proteomics of complex mixtures. Expert Rev. Proteomics. 8:659-677.

Culotta, V.C., M. Yang, and T.V. O'Halloran. 2006. Activation of superoxide dismutases: Putting the metal to the pedal. Biochim.Biophys.Acta. 1763:747-758.

Dayon, L., A. Hainard, V. Licker, N. Turck, K. Kuhn, D.F. Hochstrasser, P.R. Burkhard, and J.C. Sanchez. 2008. Relative quantification of proteins in human cerebrospinal fluids by MS/MS using 6-plex isobaric tags. Anal.Chem. 80:2921-2931.

Deutsch, E.W., H. Lam, and R. Aebersold. 2008. Data analysis and bioinformatics tools for tandem mass spectrometry in proteomics. Physiol.Genomics. 33:18-25.

Desaire, H. 2013. Glycopeptide analysis, recent developments and applications. Mol.Cell.Proteomics. 12:893-901.

De Volder, M.F., S.H. Tawfick, R.H. Baughman, and A.J. Hart. 2013. Carbon nanotubes: present and future commercial applications. Science. 339:535-539.

Donaldson, K., C.A. Poland, F.A. Murphy, M. Macfarlane, T. Chernova, and A. Schinwald. 2013. Pulmonary toxicity of carbon nanotubes and asbestos - Similarities and differences. Adv.Drug Deliv.Rev.

Dostert, C., V. Petrilli, R. Van Bruggen, C. Steele, B.T. Mossman, and J. Tschopp. 2008. Innate immune activation through Nalp3 inflammasome sensing of asbestos and silica. Science. 320:674-677.

Dumortier, H. 2013. When carbon nanotubes encounter the immune system: Desirable and undesirable effects. Adv.Drug Deliv.Rev.

Dutta, D., S.K. Sundaram, J.G. Teeguarden, B.J. Riley, L.S. Fifield, J.M. Jacobs, S.R. Addleman, G.A. Kaysen, B.M. Moudgil, and T.J. Weber. 2007. Adsorbed proteins influence the biological activity and molecular targeting of nanomaterials. Toxicol.Sci. 100:303-315

Egas, D.A., and M.J. Wirth. 2008. Fundamentals of protein separations: 50 years of nanotechnology, and growing. Annu.Rev.Anal.Chem. 1:833-855.

Elsaesser, A., and C.V. Howard. 2012. Toxicology of nanoparticles. Adv.Drug Deliv.Rev. 64:129-137.

Eng, J.K., A.L. McCormack, and J.R. Yates. 1994. An approach to correlate tandem mass spectral data of peptides with amino acid sequences in a protein database. J.Am.Soc.Mass Spectrom. 5:976-989.

EU 2012. Communication on the Second Regulatory Review on Nanomaterials

http://eur-lex.europa.eu/LexUriServ/LexUriServ.o?uri=COM:2012:0572:FIN:en:PDF

Fadeel, B., Pietroiusti, A., and A.A Shvedova. 2012. Adverse Effects of Engineered Nanomaterials: Exposure, Toxicology, and Impact on Human Health, 1st Edition, Academic Press, Chapter 5: Critical Evaluation of Toxicity Tests pp. 63-84

Fokkens, W.J., and R.A. Scheeren. 2000. Upper airway defence mechanisms. Paediatr.Respir.Rev. 1:336-341.

Gao, Y., N.V. Gopee, P.C. Howard, and L.R. Yu. 2011. Proteomic analysis of early response lymph node proteins in mice treated with titanium dioxide nanoparticles. J.Proteomics. 74:2745-2759.

Garcia-Lorenzo, A., A.M. Rodriguez-Pineiro, F.J. Rodriguez-Berrocal, M.P. Cadena, and V.S. Martinez-Zorzano. 2012. Changes on the Caco-2 Secretome through Differentiation Analyzed by 2-D Differential In-Gel Electrophoresis (DIGE). Int.J.Mol.Sci. 13:14401-14420.

Gasteiger, E., C. Hoogland, A. Gattiker, S. Duvaud, M. Wilkins, R. Appel, and A. Bairoch. 2005. Protein Identification and Analysis Tools on the ExPASy Server. In J. Walker, editor. Humana Press. 571-607.

Ge, C., J. Du, L. Zhao, L. Wang, Y. Liu, D. Li, Y. Yang, R. Zhou, Y. Zhao, Z. Chai, and C. Chen. 2011. Binding of blood proteins to carbon nanotubes reduces cytotoxicity. Proc.Natl.Acad.Sci.U.S.A. 108:16968-16973.

Ge, Y., M. Bruno, K. Wallace, W. Winnik, and R.Y. Prasad. 2011. Proteome profiling reveals potential toxicity and detoxification pathways following exposure of BEAS-2B cells to engineered nanoparticle titanium dioxide. Proteomics. 11:2406-2422.

Ge, Y., J.H. Priester, L.C. Van De Werfhorst, J.P. Schimel, and P.A. Holden. 2013. Potential Mechanisms and Environmental Controls of TiO_2 Nanoparticle Effects on Soil Bacterial Communities. Environ.Sci.Technol. 47:14411-14417.

Gentleman R.C., V.J. Carey, D.M. Bates, B. Bolstad, M. Dettling, S. Dudoit, B. Ellis, L. Gautier, Y. Ge, J. Gentry, K. Hornik, T. Hothorn, W. Huber, S. Iacus, R. Irizarry, F. Leisch, C. Li, M. Maechler, A.J. Rossini, G. Sawitzki, C. Smith, G. Smyth, L. Tierney, J.Y. Yang, and J. Zhang. 2004. Bioconductor: open software development for computational biology and bioinformatics. Genome Biol. 5:R80.

George, S., S. Pokhrel, T. Xia, B. Gilbert, Z. Ji, M. Schowalter, A. Rosenauer, R. Damoiseaux, K.A. Bradley, L. Madler, and A.E. Nel. 2010. Use of a rapid cytotoxicity screening approach to engineer a safer zinc oxide nanoparticle through iron doping. ACS Nano. 4:15-29.

Gerke, V., C.E. Creutz, and S.E. Moss. 2005. Annexins: Linking Ca2+ signalling to membrane dynamics. Nat.Rev.Mol.Cell Biol. 6:449-461.

Gernand, J.M., and E.A. Casman. 2013. A Meta-Analysis of Carbon Nanotube Pulmonary Toxicity Studies-How Physical Dimensions and Impurities Affect the Toxicity of Carbon Nanotubes. Risk Anal.

Gonçalves, D.M., S. Chiasson, and D. Girard. 2010. Activation of human neutrophils by titanium dioxide (TiO2) nanoparticles. Toxicol.In Vitro. 24:1002-1008.

Gottschalk, F., T. Sonderer, R.W. Scholz, and B. Nowack. 2009. Modeled environmental concentrations of engineered nanomaterials (TiO(2), ZnO, Ag, CNT, Fullerenes) for different regions. Environ.Sci.Technol. 43:9216-9222.

Gottschalk, F., and B. Nowack. 2011. The release of engineered nanomaterials to the environment. J.Environ.Monit. 13:1145-1155.

Graves, P.R., and T.A. Haystead. 2002. Molecular biologist's guide to proteomics. Microbiol.Mol.Biol.Rev. 66:39-63.

Grieger, K.D., A. Baun, and R. Owen. 2010. Redefining risk research priorities for nanomaterials. J.Nanopart Res. 12:383-392.

Gupta, S., and M. Tripathi. 2011. A review of TiO_2 nanoparticles. Chinese Science Bulletin. 56:1639-1657.

Gwinn, M.R., and V. Vallyathan. 2006. Nanoparticles: health effects--pros and cons. Environ.Health Perspect. 114:1818-25.

Gwinn, W.M., J.M. Damsker, R. Falahati, I. Okwumabua, A. Kelly-Welch, A.D. Keegan, C. Vanpouille, J.J. Lee, L.A. Dent, D. Leitenberg, M.I. Bukrinsky, and S.L. Constant. 2006. Novel approach to inhibit asthma-mediated lung inflammation using anti-CD147 intervention. J.Immunol. 177:4870-4879.

George, S., T. Xia, R. Rallo, Y. Zhao, Z. Ji, S. Lin, X. Wang, H. Zhang, B. France, D. Schoenfeld, R. Damoiseaux, R. Liu, S. Lin, K.A. Bradley, Y. Cohen, and A.E. Nel. 2011. Use of a high-throughput screening approach coupled with *in vivo* zebrafish embryo screening to develop hazard ranking for engineered nanomaterials. ACS Nano. 5:1805-1817.

Gygi, S.P., B. Rist, S.A. Gerber, F. Turecek, M.H. Gelb, and R. Aebersold. 1999. Quantitative analysis of complex protein mixtures using isotope-coded affinity tags. Nat.Biotechnol. 17:994-999.

Göppert, T.M., and R.H. Müller. 2005. Adsorption kinetics of plasma proteins on solid lipid nanoparticles for drug targeting. Int.J.Pharm. 302:172-186.

Görg, A., W. Weiss, and M.J. Dunn. 2004. Current two-dimensional electrophoresis technology for proteomics. Proteomics. 4:3665-3685.

Hall, A., P.A. Karplus, and L.B. Poole. 2009. Typical 2-Cys peroxiredoxins -- structures, mechanisms and functions. FEBS J. 276:2469-2477.

Hamelin, C., E. Cornut, F. Poirier, S. Pons, C. Beaulieu, J.P. Charrier, H. Haidous, E. Cotte, C. Lambert, F. Piard, Y. Ataman-Onal, and G. Choquet-Kastylevsky. 2011. Identification and verification of heat shock protein 60 as a potential serum marker for colorectal cancer. FEBS J. 278:4845-4859.

Haniu, H., N. Komori, N. Takemori, A. Singh, J.D. Ash, and H. Matsumoto. 2006. Proteomic trajectory mapping of biological transformation: Application to developmental mouse retina. Proteomics. 6:3251-61.

Harris, J.G., R.J. Flower, and M. Perretti. 1995. Alteration of neutrophil trafficking by a lipocortin 1 N-terminus peptide. Eur.J.Pharmacol. 279:149-157.

Heister, E., E.W. Brunner, G.R. Dieckmann, I. Jurewicz, and A.B. Dalton. 2013. Are carbon nanotubes a natural solution? Applications in biology and medicine. ACS Appl.Mater.Interfaces. 5:1870-1891.

Hellstrand, E., I. Lynch, A. Andersson, T. Drakenberg, B. Dahlbäck, K.A. Dawson, S. Linse, and T. Cedervall. 2009. Complete high-density lipoproteins in nanoparticle corona. FEBS J. 276:3372-3381.

Hempel, K., F.A. Herbst, M. Moche, M. Hecker, and D. Becher. 2011. Quantitative proteomic view on secreted, cell surface-associated, and cytoplasmic proteins of the methicillin-resistant human pathogen Staphylococcus aureus under iron-limited conditions. J.Proteome Res. 10:1657-1666.

Huang da, W., B.T. Sherman, and R.A. Lempicki. 2009. Systematic and integrative analysis of large gene lists using DAVID bioinformatics resources. Nat.Protoc. 4:44-57.

Hsu, J.L., S.Y. Huang, N.H. Chow, and S.H. Chen. 2003. Stable-isotope dimethyl labeling for quantitative proteomics. Anal.Chem. 75:6843-6852.

Iijima, S. 1991. Helical microtubules of graphitic carbon. Nature. 354:56-58.

Jacobsen, N.R., G. Pojana, P. White, P. Moller, C.A. Cohn, K.S. Korsholm, U. Vogel, A. Marcomini, S. Loft, and H. Wallin. 2008. Genotoxicity, cytotoxicity, and reactive oxygen species induced by single-walled carbon nanotubes and C(60) fullerenes in the FE1-Mutatrade markMouse lung epithelial cells. Environ.Mol. Mutagen. 49:476-487.

Jang, H.H., K.O. Lee, Y.H. Chi, B.G. Jung, S.K. Park, J.H. Park, J.R. Lee, S.S. Lee, J.C. Moon, J.W. Yun, Y.O. Choi, W.Y. Kim, J.S. Kang, G. Cheong, D. Yun, S.G. Rhee, M.J. Cho, and S.Y. Lee. 2004. Two Enzymes in One: Two Yeast Peroxiredoxins Display Oxidative Stress-Dependent Switching from a Peroxidase to a Molecular Chaperone Function. Cell. 117:625-635.

Jariwala, D., V.K. Sangwan, L.J. Lauhon, T.J. Marks, and M.C. Hersam. 2013. Carbon nanomaterials for electronics, optoelectronics, photovoltaics, and sensing. Chem.Soc.Rev. 42:2824-2860.

Jedlovszky-Hajdu, A., F.B. Bombelli, M.P. Monopoli, E. Tombacz, and K.A. Dawson. 2012. Surface coatings shape the protein corona of SPIONs with relevance to their application *in vivo*. Langmuir. 28:14983-14991.

Jiang, J., G. Oberdörster, and P. Biswas. 2009. Characterization of size, surface charge, and agglomeration state of nanoparticle dispersions for toxicological studies. J.Nanopart.Res. 11:77-89.

Jiang, L., K. Salao, H. Li, J.M. Rybicka, R.M. Yates, X.W. Luo, X.X. Shi, T. Kuffner, V.W. Tsai, Y. Husaini, L. Wu, D.A. Brown, T. Grewal, L.J. Brown, P.M.G. Curmi, and S.N. Breit. 2012. Intracellular chloride channel protein CLIC1 regulates macrophage function through modulation of phagosomal acidification. J.Cell Sci. 125:5479-5488.

Johnston, H., G. Pojana, S. Zuin, N.R. Jacobsen, P. Moller, S. Loft, M. Semmler-Behnke, C. McGuiness, D. Balharry, A. Marcomini, H. Wallin, W. Kreyling, K. Donaldson, L. Tran, and V. Stone. 2013. Engineered nanomaterial risk. Lessons learnt from completed nanotoxicology studies: potential solutions to current and future challenges. Crit.Rev.Toxicol. 43:1-20.

Joshi, G.N., and D.A. Knecht. 2013. Silica phagocytosis causes apoptosis and necrosis by different temporal and molecular pathways in alveolar macrophages. Apoptosis. 18:271-285

Juncadella, I.J., A. Kadl, A.K. Sharma, Y.M. Shim, A. Hochreiter-Hufford, L. Borish, and K.S. Ravichandran. 2013. Apoptotic cell clearance by bronchial epithelial cells critically influences airway inflammation. Nature. 493:547-551.

Jung, S.Y., S.M. Lim, F. Albertorio, G. Kim, M.C. Gurau, R.D. Yang, M.A. Holden, and P.S. Cremer. 2003. The Vroman effect: a molecular level description of fibrinogen displacement. J.Am.Chem.Soc. 125:12782-12786.

Kaminski, M.M., D. Roth, S. Sass, S.W. Sauer, P.H. Krammer, and K. Gulow. 2012. Manganese superoxide dismutase: a regulator of T cell activation-induced oxidative signaling and cell death. Biochim.Biophys.Acta. 1823:1041-1052.

Kapralov, A.A., W.H. Feng, A.A. Amoscato, N. Yanamala, K. Balasubramanian, D.E. Winnica, E.R. Kisin, G.P. Kotchey, P. Gou, L.J. Sparvero, P. Ray, R.K. Mallampalli, J. Klein-Seetharaman, B. Fadeel, A. Star, A.A. Shvedova, and V.E. Kagan. 2012. Adsorption of surfactant lipids by single-walled carbon nanotubes in mouse lung upon pharyngeal aspiration. ACS Nano. 6:4147-4156.

Karas, M., D. Bachmann, and F. Hillenkamp. 1985. Influence of the wavelength in high- irradiance ultraviolet laser desorption mass spectrometry of organic molecules. Anal.Chem. 57:2935-2939.

Kettiger, H., A. Schipanski, P. Wick, and J. Huwyler. 2013. Engineered nanomaterial uptake and tissue distribution: from cell to organism. Int.J.Nanomedicine. 8:3255-3269.

Kolosnjaj-Tabi, J., K.B. Hartman, S. Boudjemaa, J.S. Ananta, G. Morgant, H. Szwarc, L.J. Wilson, and F. Moussa. 2010. *In vivo* behavior of large doses of ultrashort and full-length single-walled carbon nanotubes after oral and intraperitoneal administration to Swiss mice. ACS Nano. 4:1481-1492.

Kroto, H.W., J.R. Heath, S.C. O'Brien, R.F. Curl, and R.E. Smalley. 1985. C60: Buckminsterfullerene. Nature. 318:162-163.

Krug, H.F., and P. Wick. 2011. Nanotoxicology: an interdisciplinary challenge. Angew.Chem.Int.Ed Engl. 50:1260-1278.

Lambrecht, B.N., and H. Hammad. 2012. The airway epithelium in asthma. Nat. Med. 18:684-692.

LeBel, C.P., H. Ischiropoulos, and S.C. Bondy. 1992. Evaluation of the probe 2',7'-dichlorofluorescin as an indicator of reactive oxygen species formation and oxidative stress. Chem.Res.Toxicol. 5:227-231.

Lelong, C., M. Chevallet, H. Diemer, S. Luche, A. Van Dorsselaer, and T. Rabilloud. 2012. Improved proteomic analysis of nuclear proteins, as exemplified by the comparison of two myeloid cell lines nuclear proteomes. J.Proteomics. 77:577-602.

Li, B., Y. Ze, Q. Sun, T. Zhang, X. Sang, Y. Cui, X. Wang, S. Gui, D. Tan, M. Zhu, X. Zhao, L. Sheng, L. Wang, F. Hong, and M. Tang. 2013. Molecular mechanisms of nanosized titanium dioxide-induced pulmonary injury in mice. PLoS One. 8:e55563.

Li, J., Q. Li, J. Xu, J. Li, X. Cai, R. Liu, Y. Li, J. Ma, and W. Li. 2007. Comparative study on the acute pulmonary toxicity induced by 3 and 20nm TiO(2) primary particles in mice. Environ.Toxicol.Pharmacol. 24:239-244.

Liao, C.M., Y.H. Chiang, and C.P. Chio. 2008. Model-based assessment for human inhalation exposure risk to airborne nano/fine titanium dioxide particles. Sci. Total Environ. 407:165-177.

Lin, S., Y. Zhao, A.E. Nel, and S. Lin. 2013. Zebrafish: an *in vivo* model for nano EHS studies. Small. 9:1608-1618.

Lindberg, H.K., G.C. Falck, J. Catalan, A.J. Koivisto, S. Suhonen, H. Jarventaus, E.M. Rossi, H. Nykasenoja, Y. Peltonen, C. Moreno, H. Alenius, T. Tuomi, K.M. Savolainen, and H. Norppa. 2012. Genotoxicity of inhaled nanosized TiO(2) in mice. Mutat.Res. 745:58-64.

Lindberg, H.K., G.C.-. Falck, S. Suhonen, M. Vippola, E. Vanhala, J. Catalán, K. Savolainen, and H. Norppa. 2009. Genotoxicity of nanomaterials: DNA damage and micronuclei induced by carbon nanotubes and graphite nanofibres in human bronchial epithelial cells *in vitro*. Toxicol.Lett. 186:166-173.

Liu, H., R.G. Sadygov, and J.R. Yates 3rd. 2004. A model for random sampling and estimation of relative protein abundance in shotgun proteomics. Anal.Chem. 76:4193-4201.

Liu, H.L., Y.L. Zhang, N. Yang, Y.X. Zhang, X.Q. Liu, C.G. Li, Y. Zhao, Y.G. Wang, G.G. Zhang, P. Yang, F. Guo, Y. Sun, and C.Y. Jiang. 2011. A functionalized single-walled carbon nanotube-induced autophagic cell death in human lung cells through Akt-TSC2-mTOR signaling. Cell.Death Dis. 2:e159.

Liu, R., S. Lin, R. Rallo, Y. Zhao, R. Damoiseaux, T. Xia, S. Lin, A. Nel, and Y. Cohen. 2012. Automated phenotype recognition for zebrafish embryo based *in vivo* high throughput toxicity screening of engineered nano-materials. PLoS One. 7:e35014.

Lohcharoenkal, W., L. Wang, T.A. Stueckle, C.Z. Dinu, V. Castranova, Y. Liu, and Y. Rojanasakul. 2013. Chronic Exposure to Carbon Nanotubes Induces Invasion of Human Mesothelial Cells through Matrix Metalloproteinase-2. ACS Nano.

Lundby, A., and J.V. Olsen. 2011. GeLCMS for in-depth protein characterization and advanced analysis of proteomes. Methods Mol.Biol. 753:143-155.

Lundqvist, M., J. Stigler, T. Cedervall, T. Berggard, M.B. Flanagan, I. Lynch, G. Elia, and K. Dawson. 2011. The evolution of the protein corona around nanoparticles: a test study. ACS Nano. 5:7503-7509.

Lunov, O., T. Syrovets, C. Loos, J. Beil, M. Delacher, K. Tron, G.U. Nienhaus, A. Musyanovych, V. Mailander, K. Landfester, and T. Simmet. 2011. Differential uptake of functionalized polystyrene nanoparticles by human macrophages and a monocytic cell line. ACS Nano. 5:1657-1669.

Luo, E., G. Song, Y. Li, P. Shi, J. Hu, and Y. Lin. 2013. The toxicity and pharmacokinetics of carbon nanotubes as an effective drug carrier. Curr.Drug Metab. 14:879-890.

Lynch, I., T. Cedervall, M. Lundqvist, C. Cabaleiro-Lago, S. Linse, and K.A. Dawson. 2007. The nanoparticle-protein complex as a biological entity; a complex fluids and surface science challenge for the 21st century. Adv.Colloid Interface Sci. 134-135:167-174.

Lynch, I., and K.A. Dawson. 2008. Protein-nanoparticle interactions. Nano Today. 3:40-47.

MacCorkle, R.A., S.D. Slattery, D.R. Nash, and B.R. Brinkley. 2006. Intracellular protein binding to asbestos induces aneuploidy in human lung fibroblasts. Cell Motil.Cytoskeleton. 63:646-657.

Madureira, P.A., R. Hill, V.A. Miller, C. Giacomantonio, P.W. Lee, and D.M. Waisman. 2011. Annexin A2 is a novel cellular redox regulatory protein involved in tumorigenesis. Oncotarget. 2:1075-1093.

Maier, T., M. Guell, and L. Serrano. 2009. Correlation of mRNA and protein in complex biological samples. FEBS Lett. 583:3966-3973.

Malik, R., K. Dulla, E.A. Nigg, and R. Korner. 2010. From proteome lists to biological impact--tools and strategies for the analysis of large MS data sets. Proteomics. 10:1270-1283.

Mangum, J.B., E.A. Turpin, A. Antao-Menezes, M.F. Cesta, E. Bermudez, and J.C. Bonner. 2006. Single-walled carbon nanotube (SWCNT)-induced interstitial fibrosis in the lungs of rats is associated with increased levels of PDGF mRNA and the formation of unique intercellular carbon structures that bridge alveolar macrophages in situ. Part Fibre Toxicol. 3:15.

Maxwell, G.L., B.L. Hood, R. Day, U. Chandran, D. Kirchner, V.S.K. Kolli, N.W. Bateman, J. Allard, C. Miller, M. Sun, M.S. Flint, C. Zahn, J. Oliver, S. Banerjee, T. Litzi, A. Parwani, G. Sandburg, S. Rose, M.J. Becich, A. Berchuck, E. Kohn, J.I. Risinger, and T.P. Conrads. 2011. Proteomic analysis of stage I endometrial cancer tissue: Identification of proteins associated with oxidative processes and inflammation. Gynecol.Oncol. 121:586-594.

Mazzoli-Rocha, F., S. Fernandes, M. Einicker-Lamas, and W.A. Zin. 2010. Roles of oxidative stress in signaling and inflammation induced by particulate matter. Cell Biol.Toxicol. 26:481-498.

Monopoli, M.P., D. Walczyk, A. Campbell, G. Elia, I. Lynch, F.B. Bombelli, and K.A. Dawson. 2011. Physical-chemical aspects of protein corona: relevance to *in vitro* and *in vivo* biological impacts of nanoparticles. J.Am.Chem.Soc. 133:2525-2534.

Morato-Marques M, M.R. Campos, S. Kane, A.P. Rangel, C. Lewis, M.N. Ballinger, S.H. Kim, M. Peters-Golden, S. Jancar, and C.H. Serezani. 2011. Leukotrienes target F-actin/cofilin-1 to enhance alveolar macrophage anti-fungal activity. J Biol Chem 286:28902-28913.

Movia, D., A. Prina-Mello, D. Bazou, Y. Volkov, and S. Giordani. 2011. Screening the cytotoxicity of single-walled carbon nanotubes using novel 3D tissue-mimetic models. ACS Nano. 5:9278-90.

Murray, P.J., and T.A. Wynn. 2011. Protective and pathogenic functions of macrophage subsets. Nat.Rev.Immunol. 11:723-737.

Mustafa, G.M., J.R. Petersen, H. Ju, L. Cicalese, N. Snyder, S.J. Haidacher, L. Denner, and C. Elferink. 2013. Biomarker Discovery for Early Detection of Hepatocellular Carcinoma (HCC)in Hepatitis C (HCV) Infected Patients. Mol. Cell.Proteomics.

Nazmi, A.R., O. Gabriel, P. Milena, J.P. Whitelegge, G. Volker, and L. Hartmut. 2012. N-terminal acetylation of annexin A2 is required for S100A10 binding. 393:1141.

Nel, A., T. Xia, H. Meng, X. Wang, S. Lin, Z. Ji, and H. Zhang. 2013. Nanomaterial toxicity testing in the 21st century: use of a predictive toxicological approach and high-throughput screening. Acc.Chem.Res. 46:607-621.

Nel, A.E., L. Madler, D. Velegol, T. Xia, E.M. Hoek, P. Somasundaran, F. Klaessig, V. Castranova, and M. Thompson. 2009. Understanding biophysicochemical interactions at the nano-bio interface. Nat.Mater. 8:543-57.

Nel, A., T. Xia, L. Mädler, and N. Li. 2006. Toxic Potential of Materials at the Nanolevel. Science. 311:622-627.

Nemmar, A., H. VanBilloen, M.F. Hoylaerts, P.H.M. Hoet, A. Verbruggen, and B. Nemery. 2001. Passage of Intratracheally Instilled Ultrafine Particles from the Lung into the Systemic Circulation in Hamster. Am.J.Respir.Crit.Care Med. 164:1665-1668.

Novoselov, K.S., A.K. Geim, S.V. Morozov, D. Jiang, Y. Zhang, S.V. Dubonos, I.V. Grigorieva, and A.A. Firsov. 2004. Electric field effect in atomically thin carbon films. Science. 306:666-669.

Oberdorster, G., E. Oberdorster, and J. Oberdorster. 2005. Nanotoxicology: an emerging discipline evolving from studies of ultrafine particles. Environ.Health Perspect. 113:823-839.

Ogata, H., S. Goto, K. Sato, W. Fujibuchi, H. Bono, and M. Kanehisa. 1999. KEGG: Kyoto Encyclopedia of Genes and Genomes. Nucleic Acids Res. 27:29-34.

Ong, S.E. 2012. The expanding field of SILAC. Anal.Bioanal Chem. 404:967-976.

Palomäki, J., P. Karisola, L. Pylkkänen, K. Savolainen, and H. Alenius. 2010. Engineered nanomaterials cause cytotoxicity and activation on mouse antigen presenting cells. Toxicology. 267:125-131.

Palomäki, J., E. Valimäki, J. Sund, M. Vippola, P.A. Clausen, K.A. Jensen, K. Savolainen, S. Matikainen, and H. Alenius. 2011. Long, needle-like carbon nanotubes and asbestos activate the NLRP3 inflammasome through a similar mechanism. ACS Nano. 5:6861-6870.

Park, E.J., J. Yi, K.H. Chung, D.Y. Ryu, J. Choi, and K. Park. 2008. Oxidative stress and apoptosis induced by titanium dioxide nanoparticles in cultured BEAS-2B cells. Toxicol.Lett. 180:222-229.

Park, H., and V.H. Grassian. 2010. Commercially manufactured engineered nanomaterials for environmental and health studies: important insights provided by independent characterization. Environ.Toxicol.Chem. 29:715-721.

Parmigiani, R.B., W.S. Xu, G. Venta-Perez, H. Erdjument-Bromage, M. Yaneva, P. Tempst, and P.A. Marks. 2008. HDAC6 is a specific deacetylase of peroxiredoxins and is involved in redox regulation. Proc.Natl.Acad.Sci.U.S.A. 105:9633-9638.

Pauluhn, J. 2010. Multi-walled carbon nanotubes (Baytubes): approach for derivation of occupational exposure limit. Regul.Toxicol.Pharmacol. 57:78-89.

Pehar, M., and L. Puglielli. 2013 Lysine acetylation in the lumen of the ER: A novel and essential function under the control of the UPR. Biochim.Biophys.Acta 1833:686-697.

Perkins, D.N., D.J. Pappin, D.M. Creasy, and J.S. Cottrell. 1999. Probability-based protein identification by searching sequence databases using mass spectrometry data. Electrophoresis. 20:3551-3567.

Pfaller, T., V. Puntes, E. Casals, A. Duschl, and G.J. Oostingh. 2009. *In vitro* investigation of immunomodulatory effects caused by engineered inorganic nanoparticles – the impact of experimental design and cell choice. Nanotoxicology. 3:46-59.

Phanstiel, D.H., J. Brumbaugh, C.D. Wenger, S. Tian, M.D. Probasco, D.J. Bailey, D.L. Swaney, M.A. Tervo, J.M. Bolin, V. Ruotti, R. Stewart, J.A. Thomson, and J.J. Coon. 2011. Proteomic and phosphoproteomic comparison of human ES and iPS cells. Nat.Methods. 8:821-827.

Poland, C.A., R. Duffin, I. Kinloch, A. Maynard, W.A. Wallace, A. Seaton, V. Stone, S. Brown, W. Macnee, and K. Donaldson. 2008. Carbon nanotubes introduced into the abdominal cavity of mice show asbestos-like pathogenicity in a pilot study. Nat.Nanotechnol. 3:423-428.

Qi, T.G., W. Zhang, Y. Luan, F. Kong, D.W. Xu, G.H. Cheng, and Y.S. Wang. 2013. Proteomic Profiling Identified Multiple Short-lived Members of the Central Proteome as the Direct Targets of the Addicted oncogenes in Cancer Cells. Mol. Cell.Proteomics.

Rabilloud, T., M. Heller, F. Gasnier, S. Luche, C. Rey, R. Aebersold, M. Benahmed, P. Louisot, and J. Lunardi. 2002. Proteomics analysis of cellular response to oxidative stress. Evidence for *in vivo* overoxidation of peroxiredoxins at their active site. J.Biol.Chem. 277:19396-19401.

Raghavan M, S.J. Wijeyesakere, L.R. Peters, and N. Del Cid. 2013. Calreticulin in the immune system: ins and outs. Trends Immunol 34:13-21.

Rakkola, R., S. Matikainen, and T.A. Nyman. 2007. Proteome analysis of human macrophages reveals the upregulation of manganese-containing superoxide dismutase after toll-like receptor activation. Proteomics. 7:378-384.

Rancan, F., Q. Gao, C. Graf, S. Troppens, S. Hadam, S. Hackbarth, C. Kembuan, U. Blume-Peytavi, E. Ruhl, J. Lademann, and A. Vogt. 2012. Skin penetration and cellular uptake of amorphous silica nanoparticles with variable size, surface functionalization, and colloidal stability. ACS Nano. 6:6829-6842.

R Core Team. 2013. R: A language and environment for statistical computing. R Foundation for Statistical Computing, Vienna, Austria. [Online] Available at: http://www.R-project.org/.

Reynolds, K.J., X. Yao, and C. Fenselau. 2002. Proteolytic 18O labeling for comparative proteomics: evaluation of endoprotease Glu-C as the catalytic agent. J.Proteome Res. 1:27-33.

Robichaud, C.O., A.E. Uyar, M.R. Darby, L.G. Zucker, and M.R. Wiesner. 2009. Estimates of Upper Bounds and Trends in Nano-TiO_2 Production As a Basis for Exposure Assessment. Environ.Sci.Technol. 43:4227-4233.

Rodriguez-Franco, E.J., Y.M. Cantres-Rosario, M. Plaud-Valentin, R. Romeu, Y. Rodriguez, R. Skolasky, V. Melendez, C.L. Cadilla, and L.M. Melendez. 2012. Dysregulation of macrophage-secreted cathepsin B contributes to HIV-1-linked neuronal apoptosis. PLoS One. 7:e36571.

Rogowska-Wrzesinska, A., M.C. Le Bihan, M. Thaysen-Andersen, and P. Roepstorff. 2013. 2D gels still have a niche in proteomics. J.Proteomics. 88:4-13.

Ross, P.L., Y.N. Huang, J.N. Marchese, B. Williamson, K. Parker, S. Hattan, N. Khainovski, S. Pillai, S. Dey, S. Daniels, S. Purkayastha, P. Juhasz, S. Martin, M. Bartlet-Jones, F. He, A. Jacobson, and D.J. Pappin. 2004. Multiplexed protein quantitation in Saccharomyces cerevisiae using amine-reactive isobaric tagging reagents. Mol.Cell.Proteomics. 3:1154-1169.

Rossi, E.M., L. Pylkkänen, A.J. Koivisto, H. Nykasenoja, H. Wolff, K. Savolainen, and H. Alenius. 2010a. Inhalation exposure to nanosized and fine TiO_2 particles inhibits features of allergic asthma in a murine model. Part.Fibre Toxicol. 7:35-8977-7-35.

Rossi, E.M., L. Pylkkänen, A.J. Koivisto, M. Vippola, K.A. Jensen, M. Miettinen, K. Sirola, H. Nykäsenoja, P. Karisola, T. Stjernvall, E. Vanhala, M. Kiilunen, P. Pasanen, M. Mäkinen, K. Hämeri, J. Joutsensaari, T. Tuomi, J. Jokiniemi, H. Wolff, K. Savolainen, S. Matikainen, and H. Alenius. 2010b. Airway exposure to silica-coated TiO_2 nanoparticles induces pulmonary neutrophilia in mice. Toxicol. Sci. 113:422-433.

Rostila, A., A. Puustinen, T. Toljamo, K. Vuopala, I. Lindström, T.A. Nyman, P. Oksa, T. Vehmas, and S.L. Anttila. 2012. Peroxiredoxins and tropomyosins as plasma biomarkers for lung cancer and asbestos exposure. Lung Cancer. 77:450-459.

Ryman-Rasmussen, J., M.F. Cesta, A.R. Brody, J. Shipley-Phillips, J.I. Everitt, E.W. Tewksbury, O.R. Moss, B.A. Wong, D.E. Dodd, M.E. Andersen, and J.C. Bonner. 2009. Inhaled carbon nanotubes reach the subpleural tissue in mice. Nat.Nano. 4:747-751.

Sadygov, R.G., D. Cociorva, and J.R. Yates 3rd. 2004. Large-scale database searching using tandem mass spectra: looking up the answer in the back of the book. Nat.Methods. 1:195-202.

Safi, M., J. Courtois, M. Seigneuret, H. Conjeaud, and J.F. Berret. 2011. The effects of aggregation and protein corona on the cellular internalization of iron oxide nanoparticles. Biomaterials. 32:9353-9363.

Sager, T.M., C. Kommineni, and V. Castranova. 2008. Pulmonary response to intratracheal instillation of ultrafine versus fine titanium dioxide: role of particle surface area. Part Fibre Toxicol. 5:17-8977-5-17.

Salari S, T. Seibert, Y.X. Chen, T. Hu, C. Shi, X. Zhao, C.M. Cuerrier, J.E. Raizman, and E.R. O'Brien. 2013. Extracellular HSP27 acts as a signaling molecule to activate NF-kappaB in macrophages. Cell Stress Chaperones 18:53-63.

Schleh, C., C. Muhlfeld, K. Pulskamp, A. Schmiedl, M. Nassimi, H.D. Lauenstein, A. Braun, N. Krug, V.J. Erpenbeck, and J.M. Hohlfeld. 2009. The effect of titanium dioxide nanoparticles on pulmonary surfactant function and ultrastructure. Respir.Res. 10:90-9921-10-90.

Schulze, W.X., and B. Usadel. 2010. Quantitation in mass-spectrometry-based proteomics. Annu.Rev.Plant.Biol. 61:491-516.

Schwanhäusser, B., D. Busse, N. Li, G. Dittmar, J. Schuchhardt, J. Wolf, W. Chen, and M. Selbach. 2011. Global quantification of mammalian gene expression control. Nature. 473:337-342.

Selvaraju, S., and Z.E. Rassi. 2012. Liquid-phase-based separation systems for depletion, prefractionation and enrichment of proteins in biological fluids and matrices for in-depth proteomics analysis--an update covering the period 2008-2011. Electrophoresis. 33:74-88.

Sharma, C.S., S. Sarkar, A. Periyakaruppan, J. Barr, K. Wise, R. Thomas, B.L. Wilson, and G.T. Ramesh. 2007. Single-walled carbon nanotubes induces oxidative stress in rat lung epithelial cells. J.Nanosci Nanotechnol. 7:2466-2472.

Sherry, B., N. Yarlett, A. Strupp, and A. Cerami. 1992. Identification of cyclophilin as a proinflammatory secretory product of lipopolysaccharide-activated macrophages. Proc.Natl.Acad.Sci.U.S.A. 89:3511-3515.

Shi, H., R. Magaye, V. Castranova, and J. Zhao. 2013. Titanium dioxide nanoparticles: a review of current toxicological data. Part.Fibre Toxicol. 10:15-8977-10-15.

Shi, X., A. von dem Bussche, R.H. Hurt, A.B. Kane, and H. Gao. 2011. Cell entry of one-dimensional nanomaterials occurs by tip recognition and rotation. Nat. Nanotechnol. 6:714-719.

Shvedova, A.A., E.R. Kisin, R. Mercer, A.R. Murray, V.J. Johnson, A.I. Potapovich, Y.Y. Tyurina, O. Gorelik, S. Arepalli, D. Schwegler-Berry, A.F. Hubbs, J. Antonini, D.E. Evans, B.K. Ku, D. Ramsey, A. Maynard, V.E. Kagan, V. Castranova, and P. Baron. 2005. Unusual inflammatory and fibrogenic pulmonary responses to single-walled carbon nanotubes in mice. Am.J.Physiol.Lung Cell.Mol.Physiol. 289:L698-708.

Shvedova, A.A., E.R. Kisin, A.R. Murray, O. Gorelik, S. Arepalli, V. Castranova, S.H. Young, F. Gao, Y.Y. Tyurina, T.D. Oury, and V.E. Kagan. 2007. Vitamin E deficiency enhances pulmonary inflammatory response and oxidative stress induced by single-walled carbon nanotubes in C57BL/6 mice. Toxicol.Appl. Pharmacol. 221:339-348.

Shvedova, A.A., N. Yanamala, E.R. Kisin, A.V. Tkach, A.R. Murray, A. Hubbs, M.M. Chirila, P. Keohavong, L.P. Sycheva, V.E. Kagan, and V. Castranova. 2013. Long-Term Effects of Carbon Containing Engineered Nanomaterials and Asbestos in the Lung: One Year Post Exposure Comparisons. Am.J.Physiol.Lung Cell.Mol. Physiol.

Shvedova, A.A., A. Pietroiusti, B. Fadeel, and V.E. Kagan. 2012. Mechanisms of carbon nanotube-induced toxicity: Focus on oxidative stress. Toxicol.Appl. Pharmacol. 261:121-133.

Simon-Deckers, A., B. Gouget, M. Mayne-L'Hermite, N. Herlin-Boime, C. Reynaud, and M. Carrière. 2008. *In vitro* investigation of oxide nanoparticle and carbon nanotube toxicity and intracellular accumulation in A549 human pneumocytes. Toxicology. 253:137-146.

Sjöstrand, M., R. Rylander, and R. Bergström. 1989. Lung cell reactions in guinea pigs after inhalation of asbestos (amosite). Toxicology. 57:1-14.

Smith, L.M., N.L. Kelleher, and Consortium for Top Down Proteomics. 2013. Proteoform: a single term describing protein complexity. Nat.Methods. 10:186-187.

Smyth G.K., M. Ritchie, and N. Thorne. 2012. limma: Linear Models for Microarray Data User' s Guide (Now Including RNA-Seq Data Analysis). Melbourne, VIC: Bioinformatics Division, The Walter and Eliza Hall Institute of Medical Research 1-123.

Som, C., B. Nowack, H.F. Krug, and P. Wick. 2012. Toward the Development of Decision Supporting Tools That Can Be Used for Safe Production and Use of Nanomaterials. Acc.Chem.Res. 46:863-872.

Strowig, T., J. Henao-Mejia, E. Elinav, and R. Flavell. 2012. Inflammasomes in health and disease. Nature. 481:278-86.

Su, C.L., T.T. Chen, C.C. Chang, K.J. Chuang, C.K. Wu, W.T. Liu, K.F. Ho, K.Y. Lee, S.C. Ho, H.E. Tseng, H.C. Chuang, T.J. Cheng, and Taiwan CardioPulmonary Research Group (T-CPR). 2013. Comparative proteomics of inhaled silver nanoparticles in healthy and allergen provoked mice. Int.J.Nanomedicine. 8:2783-2799.

Sue, G.R., Z.C. Ho, and K. Kim. 2005. Peroxiredoxins: A historical overview and speculative preview of novel mechanisms and emerging concepts in cell signaling. Free Rad.Biol.Med. 38:1543-1552.

Switzar, L., M. Giera, and W.M. Niessen. 2013. Protein digestion: an overview of the available techniques and recent developments. J.Proteome Res. 12:1067-1077.

Tahara, Y., M. Nakamura, M. Yang, M. Zhang, S. Iijima, and M. Yudasaka. 2012. Lysosomal membrane destabilization induced by high accumulation of single-walled carbon nanohorns in murine macrophage RAW 264.7. Biomaterials. 33:2762-2769.

Taira, M.F., K.F. Sasaki, S.F. Saitoh, T.F. Nezu, M.F. Sasaki, S.F. Kimura, K.F. Terasaki, K.F. Sera, T.F. Narushima, and Y. Araki. 0320. Accumulation of element Ti in macrophage-like RAW264 cells cultured in medium with 1 ppm Ti and effects on cell viability, SOD production and TNF-alpha secretion. Dent. Mater.J.25:726-732.

Takagi, A., A. Hirose, T. Nishimura, N. Fukumori, A. Ogata, N. Ohashi, S. Kitajima, and J. Kanno. 2008. Induction of mesothelioma in p53+/- mouse by intraperitoneal application of multi-wall carbon nanotube. J.Toxicol.Sci. 33:105-116.

Teeguarden, J.G., B.J. Webb-Robertson, K.M. Waters, A.R. Murray, E.R. Kisin, S.M. Varnum, J.M. Jacobs, J.G. Pounds, R.C. Zanger, and A.A. Shvedova. 2011. Comparative proteomics and pulmonary toxicity of instilled single-walled carbon nanotubes, crocidolite asbestos, and ultrafine carbon black in mice. Toxicol.Sci. 120:123-35.

Tenzer, S., D. Docter, S. Rosfa, A. Wlodarski, J. Kuharev, A. Rekik, S.K. Knauer, C. Bantz, T. Nawroth, C. Bier, J. Sirirattanapan, W. Mann, L. Treuel, R. Zellner, M. Maskos, H. Schild, and R.H. Stauber. 2011. Nanoparticle size is a critical physicochemical determinant of the human blood plasma corona: a comprehensive quantitative proteomic analysis. ACS Nano. 5:7155-7167.

Tenzer, S., D. Docter, J. Kuharev, A. Musyanovych, V. Fetz, R. Hecht, F. Schlenk, D. Fischer, K. Kiouptsi, C. Reinhardt, K. Landfester, H. Schild, M. Maskos, S.K. Knauer, and R.H. Stauber. 2013. Rapid formation of plasma protein corona critically affects nanoparticle pathophysiology. Nat Nano. advance online publication.

Than, N.G., R. Romero, A.L. Tarca, S. Draghici, O. Erez, T. Chaiworapongsa, Y. Mee Kim, S.K. Kim, E. Vaisbuch, and G. Tromp. 2009. Mitochondrial manganese superoxide dismutase mRNA expression in human chorioamniotic membranes and its association with labor, inflammation, and infection. J.Matern.Fetal Neonatal Med. 22:1000-1013.

Thimiri Govinda Raj, D.B., B. Ghesquiere, A.K. Tharkeshwar, K. Coen, R. Derua, D. Vanderschaeghe, E. Rysman, M. Bagadi, P. Baatsen, B. De Strooper, E. Waelkens, G. Borghs, N. Callewaert, J. Swinnen, K. Gevaert, and W. Annaert. 2011. A novel strategy for the comprehensive analysis of the biomolecular composition of isolated plasma membranes. Mol.Syst.Biol. 7:541.

Tilton, S.C., N.J. Karin, A. Tolic, Y. Xie, X. Lai, H.R. F. Jr, K.M. Waters, A. Holian, F.A. Witzmann, and G. Orr. 2013. Three human cell types respond to multi-walled carbon nanotubes and titanium dioxide nanobelts with cell-specific transcriptomic and proteomic expression patterns. Nanotoxicology.

Treuel, L., S. Brandholt, P. Maffre, S. Wiegele, L. Shang, and G.U. Nienhaus. 2014. Impact of protein modification on the protein corona on nanoparticles and nanoparticle-cell interactions. ACS Nano. 8:503-513.

Tung, J.J., and J. Kitajewski. 2010. Chloride intracellular channel 1 functions in endothelial cell growth and migration. J.Angiogenesis Res. 2:23.

Turk, V., and W. Bode. 1991. The cystatins: protein inhibitors of cysteine proteinases. FEBS Lett. 285:213-219.

Unfried, K., C. Albrecht, L. Klotz, A. Von Mikecz, S. Grether-Beck, and R.P.F. Schins. 2007. Cellular responses to nanoparticles: Target structures and mechanisms. Nanotoxicology. 1:52-71.

Van Duuren-Stuurman, B., S.R. Vink, K.J. Verbist, H.G. Heussen, D.H. Brouwer, D.E. Kroese, M.F. Van Niftrik, E. Tielemans, and W. Fransman. 2012. Stoffenmanager Nano version 1.0: a web-based tool for risk prioritization of airborne manufactured nano objects. Ann.Occup.Hyg. 56:525-541.

Van Oudenhove, L., and B. Devreese. 2013. A review on recent developments in mass spectrometry instrumentation and quantitative tools advancing bacterial proteomics. Appl.Microbiol.Biotechnol. 97:4749-4762.

Walkey, C.D., and W.C. Chan. 2012. Understanding and controlling the interaction of nanomaterials with proteins in a physiological environment. Chem.Soc.Rev. 41:2780-2799.

Walkey, C.D., J.B. Olsen, F. Song, R. Liu, H. Guo, D.W. Olsen, Y. Cohen, A. Emili, and W.C. Chan. 2014. Protein Corona Fingerprinting Predicts the Cellular Interaction of Gold and Silver Nanoparticles. ACS Nano.

Wallace, A.M., A. Hardigan, P. Geraghty, S. Salim, A. Gaffney, J. Thankachen, L. Arellanos, J.M. D'Armiento, and R.F. Foronjy. 2012. Protein phosphatase 2A regulates innate immune and proteolytic responses to cigarette smoke exposure in the lung. Toxicol.Sci. 126:589-599.

Wang, J., U.B. Jensen, G.V. Jensen, S. Shipovskov, V.S. Balakrishnan, D. Otzen, J.S. Pedersen, F. Besenbacher, and D.S. Sutherland. 2011. Soft interactions at nanoparticles alter protein function and conformation in a size dependent manner. Nano Lett. 11:4985-4991.

Wang, J., J.D. Gerlach, N. Savage, and G.P. Cobb. 2013. Necessity and approach to integrated nanomaterial legislation and governance. Sci.Total Environ. 442:56-62.

Wang, L., S. He, Y. Tu, P. Ji, J. Zong, J. Zhang, F. Feng, J. Zhao, Y. Zhang, and G. Gao. 2012a. Elevated expression of chloride intracellular channel 1 is correlated with poor prognosis in human gliomas. J.Exp.Clin.Cancer Res. 31:44-9966-31-44.

Wang, P., C. Zhang, P. Yu, B. Tang, T. Liu, H. Cui, and J. Xu. 2012b. Regulation of colon cancer cell migration and invasion by CLIC1-mediated RVD. Mol.Cell. Biochem. 365:313-321.

Weir, A., P. Westerhoff, L. Fabricius, K. Hristovski, and N. von Goetz. 2012. Titanium dioxide nanoparticles in food and personal care products. Environ.Sci. Technol. 46:2242-2250.

Wilson, R. 2013. Sensitivity and specificity: twin goals of proteomics assays. Can they be combined? Expert Rev.Proteomics. 10:135-149.

Xia, T., R.F. Hamilton, J.C. Bonner, E.D. Crandall, A. Elder, F. Fazlollahi, T.A. Girtsman, K. Kim, S. Mitra, S.A. Ntim, G. Orr, M. Tagmount, A.J. Taylor, D. Telesca, A. Tolic, C.D. Vulpe, A.J. Walker, X. Wang, F.A. Witzmann, N. Wu, Y. Xie, J.I. Zink, A. Nel, and A. Holian. 2013. Interlaboratory evaluation of *in vitro* cytotoxicity and inflammatory responses to engineered nanomaterials: the NIEHS Nano GO Consortium. Environ.Health Perspect. 121:683-690.

Xiong, Y., and K.L. Guan. 2012. Mechanistic insights into the regulation of metabolic enzymes by acetylation. J.Cell Biol. 198:155-164.

Xu, W., Y. Li, C. Liu, and S. Zhao. 2013. Protein lysine acetylation guards metabolic homeostasis to fight against cancer. Oncogene.

Yamashita, M. and J.B. Fenn. 1984. Electrospray ion source. Another variation on the free-jet theme. J.Phys.Chem. 88:4451-4459.

Yates, J.R., C.I. Ruse, and A. Nakorchevsky. 2009. Proteomics by mass spectrometry: approaches, advances, and applications. Annu.Rev.Biomed.Eng. 11:49-79.

Yazdi, A.S., G. Guarda, N. Riteau, S.K. Drexler, A. Tardivel, I. Couillin, and J. Tschopp. 2010. Nanoparticles activate the NLR pyrin domain containing 3 (Nlrp3) inflammasome and cause pulmonary inflammation through release of IL-1alpha and IL-1beta. Proc.Natl.Acad.Sci.U.S.A. 107:19449-19454.

Yin, Z.F., L. Wu, H.G. Yang, and Y.H. Su. 2013. Recent progress in biomedical applications of titanium dioxide. Phys.Chem.Chem.Phys. 15:4844-4858.

Yu, Y.Q., J. Fournier, M. Gilar, and J.C. Gebler. 2009. Phosphopeptide enrichment using microscale titanium dioxide solid phase extraction. J.Sep.Sci. 32:1189-1199.

Yuan, J., H. Gao, J. Sui, W.N. Chen, and C.B. Ching. 2011. Cytotoxicity of single-walled carbon nanotubes on human hepatoma HepG2 cells: an iTRAQ-coupled 2D LC-MS/MS proteome analysis. Toxicol.in.Vitro. 25:1820-1827.

Ünlü, M., M.E. Morgan, and J.S. Minden. 1997. Difference gel electrophoresis: A single gel method for detecting changes in protein extracts. Electrophoresis. 18:2071-2077.

Zaidi, N., A. Maurer, S. Nieke, and H. Kalbacher. 2008. Cathepsin D: A cellular roadmap. Biochem.Biophys.Res.Commun. 376:5-9.

Zhang, B., Y. Wang, and Y. Su. 2009. Peroxiredoxins, a novel target in cancer radiotherapy. Cancer Lett. 286:154-160.

Zhang, Y., B.R. Fonslow, B. Shan, M.C. Baek, and J.R. Yates 3rd. 2013. Protein analysis by shotgun/bottom-up proteomics. Chem.Rev. 113:2343-2394.

Zuin, S., C. Micheletti, A. Critto, G. Pojana, H. Johnston, V. Stone, L. Tran, and A. Marcomini. 2011. Weight of evidence approach for the relative hazard ranking of nanomaterials. Nanotoxicology. 5:445-458.

Öhman, T., N. Lietzen, E. Välimäki, J. Melchjorsen, S. Matikainen, and T.A. Nyman. 2010. Cytosolic RNA recognition pathway activates 14-3-3 protein mediated signaling and caspase-dependent disruption of cytokeratin network in human keratinocytes. J.Proteome Res. 9:1549-1564.